

I give permission for public access to my thesis and for copying to be done at the discretion of the archives' librarian and/or the College library.

Signature

Date

* * * * *

Immunomodulation in the Murine AIDS Model

by

Lindsay Sceats

A Paper Presented to the

Faculty of Mount Holyoke College in

Partial Fulfillment of the Requirements for

the Degree of Bachelors of Arts with

Honor

Department of Biological Sciences

South Hadley, MA 01075

May 2011

This paper was prepared
under the direction of
Professor Sharon Stranford
for eight credits.

* * * * *

ACKNOWLEDGMENTS

Many special thanks are owed to those who have helped to see me through this senior thesis project.

This work was supported with funding from the Mount Holyoke College Biology Department, as well as an NIH Grant awarded to Dr. Sharon Stranford (NIH:2R15A1051674-03). Many thanks.

I wish to recognize Professor Sharon Stranford for your guidance and assistance during my time in your laboratory. You have ignited in me a deep-seated love for immunology – the struggle between the ‘good guys’ of the immune system and the ‘bad guy’ viruses – that will never leave me. For that, my deepest thanks.

To Dr. Sonia Bakkour, an immense thank you for your patient teaching in both the classroom and lab. The calmness and humor you unfailingly show has brightened my day on countless occasions. Despite my inevitable panic when things went wrong, you taught me that nearly all mistakes are, in fact, recoverable – a good life lesson for both in and out of the lab.

A special thank you to Dr. Janice Gifford for your tolerance in explaining basic statistics over and over again, despite your own busy schedule – your assistance showed me the palpable thrill that comes with finding statistical significance.

To my Stranford labmates, especially Macy Akalu, Courtney Caminiti, Caitlin Pacheco, and Barret Zimmerman. I will forever appreciate your camaraderie and friendship.

Special thanks to my mom and dad for their unconditional support and love, and for giving me the chance to attend Mount Holyoke. I promise that someday, approximately 7 to 10 years from now, I will actually stop attending school and make it into the working world.

Thanks and love to Brian and my MHC Equestrian family. Without your support my life would be a far worse place indeed. I love you guys more than you will ever know.

Timshel – go get ‘em.

TABLE OF CONTENTS

	Page
List of Figures	viii
List of Tables	xi
Abstract	xii
Introduction	1
Organs of the Immune System.....	2
Immune System Basics – Characteristics of Innate Immunity.....	3
Immune System Basics – Characteristics of Adaptive Immunity.....	6
Th1- versus Th2-mediated Adaptive Immune Responses.....	7
Turning off an Immune Response.....	9
Human Immunodeficiency Virus (HIV) and Acquired Immunodeficiency Syndrome (AIDS).....	16
Murine Leukemia Virus (MuLV) and Murine Acquired Immunodeficiency Syndrome (MAIDS).....	19
AIDS versus MAIDS.....	23
Previous Work – Type I Interferons in Murine Retroviral Models.....	24
Previous Work – IDO in Murine Retroviral Models.....	26
Previous Work – IL-10 in Murine Retroviral Models.....	28
Proposed Studies.....	30
Materials and Methods	33
Animals.....	33

RNA Concentration and Quality.....	33
DNase Treatment of RNA.....	34
cDNA Synthesis.....	35
Primer Design.....	36
Conventional Polymerase Chain Reaction.....	39
Primer Optimization.....	41
Primer Efficiency Testing.....	46
Quantitative PCR.....	49
Quantitative PCR Data Analysis.....	50
Preparation of ELISA Supernatants.....	51
Bradford Assay to Determine Total Protein Concentration.....	52
ELISA.....	53
IL-10 ELISA.....	55
IFN- α ELISA.....	56
ELISA DATA Analysis.....	57
Results.....	58
Interferon- β Expression by conventional PCR and qPCR.....	58
Interferon- α Expression by qPCR.....	63
Interferon- α Expression by ELISA.....	69
IDO Expression by Conventional PCR and qPCR.....	75
Interleukin-10 Expression by ELISA.....	85
Discussion.....	91

Type I interferon expression does not differ between BALB/c and C57BL/6 mice.....	97
IL-10 protein is differentially expressed by BALB/c and C57BL/6 mice.....	101
IDO mRNA is differentially expressed by BALB/c and C57BL/6 mice.....	106
Sources of Error.....	111
Future Studies.....	114
Conclusions.....	118
Appendix.....	121
Bradford Assay Results.....	121
Statistical Analysis.....	124
References.....	129

LIST OF FIGURES

	Page
Figure 1.	Diagram of Treg suppression mechanisms in vivo.....11
Figure 2.	Kynurenine pathway of tryptophan degradation.....15
Figure 3.	Diagram of the HIV replication cycle.....18
Figure 4.	Genome of the murine leukemia virus and the replication-defective virus causing MAIDS.....21
Figure 5.	Quantitative PCR primer optimization plate set-up.....44
Figure 6.	Sample dissociation curve for IDO at 500 nM forward primer : 500 nM reverse primer.....45
Figure 7.	Sample standard curve plot generated for primer efficiency experiments.....48
Figure 8.	Sample sandwich ELISA procedure.....54
Figure 9.	Ethidium bromide-stained agarose gel of conventional PCR products generated using IFN- β primers and 8 hour post-MuLV-infection BALB/c Spleen cDNA template.....60
Figure 10.	Amplification plot of cycle number versus Delta Rn (level of fluorescence) for trial qPCR experiment for IFN- β as compared to the housekeeping gene TBP.....62
Figure 11.	Efficiency experiment showing the standard curves and amplification efficiencies calculated for TBP and IFN- α primers.....64

Figure 12.	IFN- α mRNA fold expression does not differ significantly between MuLV-infected BALB/c and BL/6 mice.....	66
Figure 13.	Test standard curve for IFN- α ELISA plate.....	70
Figure 14.	IFN- α protein expression does not differ between strains in naïve and MuLV-infected BALB/c and BL/6 mice at three time points post-infection.....	72
Figure 15.	Time course showing IFN- α protein expression in the spleens of naïve and MuLV-infected BALB/c and BL/6 mice.....	73
Figure 16.	Ethidium bromide-stained agarose gel of PCR products generated using IDO primers and 24 hour post-MuLV infection BALB/c lymph node cDNA template.....	76
Figure 17.	Dissociation curves of IDO Primer Pair #1 at concentrations of 500 nM forward primer: 500 nM reverse primer.....	78
Figure 18.	Efficiency experiment showing the standard curves and amplification efficiencies calculated for TBP and IDO primers.....	80
Figure 19.	IDO mRNA expression differs significantly between strains in the lymph nodes of naïve and MuLV-infected BALB/c and BL/6 mice.....	83
Figure 20.	IDO mRNA fold expression changes significantly across time in naïve and MuLV-infected BALB/c and BL/6 mice.....	84
Figure 21.	Example standard curve for IL-10 ELISA plate.....	86

Figure 22.	IL-10 protein expression differs significantly between strains in the spleens of naïve and MuLV-infected BALB/c and BL/6 mice.....	88
Figure 23.	Natural log of IL-10 protein expression differs significantly across time in the spleens of naïve and MuLV-infected BALB/c and BL/6 mice.....	89
Figure 24.	BM5 <i>Def</i> viral load as compared to IDO mRNA fold expression.....	104
Figure 25.	BM5 <i>Def</i> viral load as compared to IL-10 protein expression.....	109
Figure 26.	Standard curves for Bradford assays used to calculate total protein concentration ($\mu\text{g}/\text{mL}$) in spleen supernatants used for ELISA.....	122

LIST OF TABLES

	Page
Table 1. IFN- α mRNA fold expression varies widely within conditions between individual MuLV-infected mice 24 hours and 7days post-infection.....	67
Table 2. IFN- α Protein Expression (pg/mg of protein) in the spleens of individual naïve and MuLV-infected mice.....	71
Table 3. IDO mRNA fold expression by qPCR in the lymph nodes of individual naïve and MuLV-infected mice, 24 hours, 3 days, and 7 days post-infection.....	82
Table 4. IL-10 Protein Expression (pg/mg of protein) in the spleens of individual naïve and MuLV-infected mice.....	87
Table 5. Spleen supernatant protein concentrations (μ g/mL) obtained via Bradford Assay.....	123
Table 6. Means, Standard Deviations, and Univariate ANOVA Tables from SPSS.....	125

ABSTRACT

Murine acquired immunodeficiency syndrome (MAIDS) is a model of immunodeficiency useful for studying human AIDS. Murine leukemia virus (MuLV) produces a fatal disease course in some strains of mice with symptoms mimicking AIDS. BALB/c mice exhibit natural MAIDS resistance and suppress viral replication, while C57BL/6 mice cannot control viral replication and develop MAIDS. Identifying genes and proteins differentially expressed between strains may aid in defining a 'successful' immune response against MuLV.

Candidate molecules for study include natural immunosuppressors that protect against strong, unnecessary immune responses. Overexpression of immunosuppressors may turn down immune responses necessary for eliminating viruses. Two natural immunosuppressors are indoleamine 2,3-dioxygenase (IDO) and interleukin-10 (IL-10). Immune activators including Type I (α/β) interferons may also be differentially expressed. This study compared the balance in immunosuppressive (IDO and IL-10) versus immune activating (IFN- α/β) molecules between BALB/c and C57BL/6 mice to elucidate relative levels of natural immunosuppression in MAIDS.

Techniques used included RNA-based and protein-based assays. No significant differences were seen between strains in IFN- α/β expression, either at the mRNA or protein level. In contrast, results showed significant upregulation of IDO and IL-10 by disease-susceptible mice in the first week of infection. Immunosuppressor upregulation in MAIDS-susceptible mice may prevent effective T cell responses, predisposing susceptible mice towards developing MAIDS. Further study may delineate potential roles for IDO and IL-10 in human development of AIDS.

INTRODUCTION

The human immunodeficiency virus (HIV) has threatened millions of lives since breaching the species barrier between non-human primates and humans in the early 20th century. As a member of a group of retroviruses known as the lentiviruses, HIV is known to induce the onset of acquired immune deficiency syndrome (AIDS) in humans. As of 2009, around 33.3 million adults and 2.5 million children were living with HIV around the globe (WHO 2010). The pandemic is disproportionately prevalent in impoverished regions of the world. Malnutrition, limited access to basic health care, and inadequate distribution of antiretroviral therapies predispose areas like sub-Saharan Africa and South Asia to a widespread HIV crisis. In countries such as Botswana, nearly 25% of the adult population is HIV-infected – a number that threatens to debilitate economies and orphan tens of thousands of children (USAID 2010). In contrast, only 0.5% of U.S. adults are HIV-infected and nearly all of these individuals receive antiretroviral therapy (UNAIDS 2010).

Recent data suggests that the past decade's preventative and educational efforts, along with increased availability of antiretroviral therapies, has begun to halt the spread of the epidemic. Today, the number of new infections is 19% lower than 1999, the year estimated as the peak of the HIV epidemic (UNAIDS 2010). Despite this encouraging progress, extensive social and research efforts remain necessary to reach the ultimate goal of zero new HIV-infections and zero AIDS-related deaths. Attainment of this goal will prove a crucial step in

improving global quality of life and increasing economic freedom around the world.

Organs of the Immune System

Immune cells can be found circulating in blood and lymphatic vessels as well as in specialized lymphoid tissues. Lymphoid organs are divided into two types – the primary (central) lymphoid tissues, where immune cells develop and mature, and the secondary (peripheral) lymphoid tissues, where mature immune cells become activated to respond to invading pathogens (Parham, 2009). Primary lymphoid tissues include bone marrow and the thymus. Immune cells originate from lymphoid precursors in the bone marrow, and can complete their maturation in either the bone marrow or thymus.

The more specific arm of immunity known as adaptive immunity is initiated in the secondary lymphoid tissues. Secondary lymphoid tissues include the spleen, lymph nodes, adenoids, tonsils, appendix, and Peyer's patches in the gut. The spleen serves as the lymphoid organ responsible for filtering blood. Damaged red blood cells are removed in the spleen's 'red pulp', while immune cells gather in the spleen's 'white pulp' to defend against blood-borne pathogens (Parham, 2009). In contrast, lymph nodes serve as meeting points for lymph-borne pathogens draining from nearby infected tissues and blood-borne immune cells. Lymph nodes lie at the junctions of the lymphatic vessel network, which originates in connective tissues to collect leaking extracellular fluid. Finally, gut-

associated lymphoid tissue (GALT) includes the tonsils, adenoids, appendix, and Peyer's patches. The extensive mucosal surfaces of respiratory and gastrointestinal tissues makes these regions of the body particularly vulnerable to food- and air-borne pathogens, and necessarily requires large numbers of immune cells waiting to fight potential invaders.

Immune System Basics – Characteristics of Innate Immunity

The immune system represents the body's primary defense against invading pathogens such as bacteria and viruses. By distinguishing between foreign and self cells, the immune system can enact appropriate defense mechanisms and destroy attackers. The primary players in immune responses are the leukocytes, more commonly known as white blood cells. Types of leukocytes include the granulocytes (basophils, eosinophils, and neutrophils), lymphocytes (B cells, T cells, and natural killer cells), and dendritic cells, monocytes, and macrophages (Parham, 2009). Many subsets within each category exist; each particular subset often has its own specialized function.

The body's first passive line of defense against pathogens is comprised of physical barriers such as skin and mucosal linings. Should a pathogen surpass these physical barriers, the pathogen may stimulate an active immune response. An immune response can be divided into two arms – a fast, early-acting nonspecific response known as innate immunity, as well as a later immune response targeted specifically towards the respective pathogen. This later phase is

referred to as adaptive immunity. In many cases, an innate response is all that is necessary to contain a potential source of infection.

A primary role of innate immunity is differentiating between foreign antigens and self cells. Innate immune cells recognize pathogens via a limited number of germline-encoded pattern-recognition receptors (PRRs). PRRs identify basic microbial structures known as pathogen-associated molecular patterns (PAMPs). PAMPs are usually essential to the life of the pathogen and are therefore difficult to alter (Akira *et al.*, 2006). Examples of PAMPs include bacterial motifs such as lipopolysaccharides and flagellin, or viral structures such as double-stranded RNA and unmethylated CpG motifs. Examples of PRRs include Toll-like receptors (TLRs), nucleotide-binding oligomerization domain – ligand recognition receptor (NOD-LRR) proteins, and retinoic-acid-inducible (RIG-I) proteins (Akira *et al.*, 2006).

Upon recognizing a pathogen as foreign, innate immune cells initiate a variety of nonspecific defense mechanisms. Tissue-resident dendritic cells and macrophages become activated upon recognizing a foreign pathogen, causing the release of inflammatory cytokines that attract additional immune cells to the site of attack. Cytokines are small peptides secreted by immune cells used to mediate intercellular signaling. Cytokines exert their effects by binding to cell surface receptors and initiating signal transduction within the cell, leading to transcription of certain genes (Sharon, 1998). Recognition of a foreign pathogen can also activate a cascade of proteins known as complement to mark and lyse

extracellular pathogens. Phagocytic cells such as neutrophils and macrophages then engulf and degrade complement-marked antigens.

The class of cytokines called interferons represents another defense mechanism offered by innate immunity against potential viral invaders. Interferons are further subdivided into Type I (including IFN- α , IFN- β , and IFN- ω), Type II (IFN- γ), and Type III. Of the Type I interferons, IFN- β is represented by a single intronless member; in contrast, twenty different IFN- α genes encode thirteen functional polypeptides (Theofilopoulos *et al.*, 2005). While all cells are capable of producing Type I interferons, plasmacytoid dendritic cells (pDCs) are the most potent producers, producing up to 1000-fold more IFN- α/β than other cell types (Theofilopoulos *et al.*, 2005). IFN- γ is secreted primarily by T cells and natural killer (NK) cells (Boehm *et al.*, 1997). In a viral infection, infected cells secrete interferons that inhibit viral replication, cause apoptosis of infected cells, and establish an antiviral state in neighboring cells (Sharon, 1998). Inhibition of viral replication is conducted in part by activation of a ribonuclease known as RNaseL. RNaseL degrades single-stranded viral and cellular RNAs, thereby inhibiting protein synthesis and viral growth (Boehm *et al.*, 1997).

A major effect of the interferons is their ability to induce cell-surface upregulation of Class I and II MHC molecules in neighboring cells (Pestka and Langer, 1987). Increased MHC expression allows for more presentation of antigenic peptides to adaptive immune cells, aiding in the transition between an innate and adaptive immune response. Deficiencies in interferon expression have

serious consequences in host viability. Fatal infections overpowering the adaptive immune system can result from failure to contain viral infections at early stages.

Immune System Basics – Characteristics of Adaptive Immunity

While the ability to rapidly activate innate immune responses allows for quick vanquishing of invading pathogens, nonspecific mechanisms of defense are at times not enough to stop an infection. In these cases, the adaptive arm of the immune system must be activated. Although adaptive leukocytes use many of the same effector mechanisms as innate cells, the two arms differ in adaptive immunity's ability to specifically identify individual pathogens and make a focused and forceful response (Parham, 2009). B and T cells are the primary cells of adaptive immunity. Each has a cell-surface receptor of one molecular type used to recognize pathogens, known as B-cell receptors (BCR) and T-cell receptors (TCR). During the process of lymphocyte differentiation, these receptors can be mutated to generate an almost infinite number of ligand binding sites, allowing for the recognition of an immense variety of pathogens. Only those adaptive lymphocytes with receptors that can bind to components of the invading pathogen are selected to divide, proliferate, and differentiate into effector lymphocytes, allowing the immune system to channel its resources into fighting only the current crisis (Parham, 2009).

Should an infection require further containment after an innate immune response, antigen-presenting innate immune cells (APCs) initiate adaptive

immunity by capturing the offending antigen and migrating to the meeting points of the immune system – the lymph nodes. Upon arrival, APCs present the foreign antigen to waiting B and T cells in hopes of finding adaptive immune cells exactly specific to the antigen. Once the appropriate B and T cell clones are selected, the clones activate and multiply, giving rise to millions of specific clones. These clones may then enact a strong immune response expressly targeting the individual pathogen.

An adaptive immune response primarily mediated by B cells and their production of antibodies (soluble BCRs) is referred to as a humoral immune response. B cell-produced antibodies recognize a unique antigen, allowing them to neutralize it and mark it for phagocytosis. A humoral response is utilized when the antigen is large or extracellular. In contrast, intracellular pathogens such as viruses require the initiation of an immune response mediated by cytotoxic T cells. A cytotoxic T cell response results in the direct apoptosis of pathogen-infected cells (Parham, 2009).

Th1 versus Th2-mediated Adaptive Immune Responses

Different cytokine environments can drive the differentiation of CD4⁺ T cells to acquire different functions, promoting either a humoral or cytotoxic adaptive response. The two main subsets of CD4⁺ T helper cells are referred to as Type I helper T (Th1) cells and Type II helper T (Th2) cells. Other CD4⁺ T cells that have recently gained recognition include T helper 17 (Th17) and regulatory T

(Treg) cells. Interferon- γ (IFN- γ) and interleukin-12 (IL-12) are thought to be the major cytokines necessary for promoting Th1 differentiation (Constant and Bottomly, 1997). These cytokines induce changes in the gene expression of a transcription factor known as T-bet, which turns on IFN- γ expression in a T cell. Increasing prevalence of IFN- γ in the environment facilitates further differentiation of activated CD4⁺ T cells along the Th1 pathway. Principal effector functions of Th1 cells include macrophage activation at the site of infection, induction of T cell proliferation, and recruiting of phagocytes such as macrophages and neutrophils to sites of infection (Parham, 2009). In contrast, Th2 cells are primarily influenced by the presence of interleukin-4 (IL-4) in their immediate environment (Constant and Bottomly, 1997). IL-4 induces expression of the transcription factor GATA-3, which turns on expression of IL-4 and other genes characteristic of Th2 cells (Parham, 2009). An increasing presence of IL-4 creates a local environment that facilitates further differentiation of CD4⁺ T cells along the Th2 pathway. Principal effector functions for Th2 cells include the promotion of B cell proliferation and clonal expansion and further differentiation of B cells into plasma cells (Parham, 2009).

Th1 cells produce IL-2, IFN- γ and lymphotoxin (LT), while Th2 cells produce IL-4, IL-5, IL-6, IL-9, IL-10 and IL-13 (Mosmann and Sad, 1996). The cytokine products of Th1 and Th2 cells are mutually inhibitory for the reciprocal phenotype. Thus, IFN- γ selectively inhibits proliferation of Th2 cells, and IL-10 inhibits cytokine synthesis by Th1 cells (Mosmann and Sad, 1996). The functions

of Th1 and Th2 cells correlate well with their distinctive cytokines. Th1 cells are involved in cell-mediated inflammatory reactions: several Th1 cytokines lead to macrophage activation, inflammation, and the production of opsonizing antibodies that enhance pathogen phagocytosis (Parham, 2009). Some B-cell activation help can be provided by Th1 cells, but as Th1 cell numbers increase this aid turns to B cell suppression. Th2 cytokines encourage antibody production and enhance eosinophil proliferation and function. Accordingly, Th2 cytokines are commonly found in association with strong antibody and allergic responses.

Infection by certain pathogens may result in strong biases towards Th1 or Th2 responses during murine or human infection. In several cases, altering these patterns by cytokine or anti-cytokine reagents reverses host resistance or susceptibility to infection. Thus, ample evidence supports the idea that Th1 versus Th2 cytokine patterns are important in mediating resistance to certain infectious agents.

Turning Off an Immune Response

A successful immune response not only elicits an active pathogen-fighting response, but also balances activation and suppression throughout the immune response, appropriately stops the response at the conclusion of an infection, and generates immunological memory. Immune responses that continue after a pathogen has been cleared may cause substantial unnecessary damage to the host; accordingly, limiting an immune response is as important as activating the

response. Upon resolution of an infection, the antigen signals stimulating the adaptive response are removed. Loss of these signals result in ‘death by neglect’ for most antigen-specific B and T cells, who remove themselves by apoptosis (Parham, 2009). Decreased production of the cytokine IL-2 as a result of lower antigen levels also assists in decreasing the number of activated T cells (Paul, 2003). Regulatory T cells (Tregs) have also been implicated in ending T cell immune responses by both cell-contact dependent mechanisms and production of immunomodulatory cytokines (Fehérvári and Sakaguchi, 2004). Cell-contact dependent mechanisms include Treg-expression of the inhibitory T cell surface glycoprotein CTLA-4, while the immunomodulatory cytokines produced include IL-10 and TGF- β . Active immune suppression by Tregs, and perhaps other leukocytes, helps to minimize unnecessary collateral damage to the host caused by antigen-specific immune cells which may cross-react with host cells (O’Garra *et al.* 2004). This active immune suppression aids in maintaining homeostasis, avoiding outcomes such as autoimmunity. Please refer to Figure 1 for a visual description of possible Treg suppressive mechanisms.

CTLA-4 (Cytotoxic T-Lymphocyte Antigen 4) is an immunoglobulin superfamily member that plays an important role in immune system control. CTLA-4 aids in slowing an immune response by delivering a negative costimulatory signal to T cells via binding to the B7-1 and B7-2 molecules on antigen presenting cells (APCs), effectively dampening an immune response (Krummel and Allison, 1995).

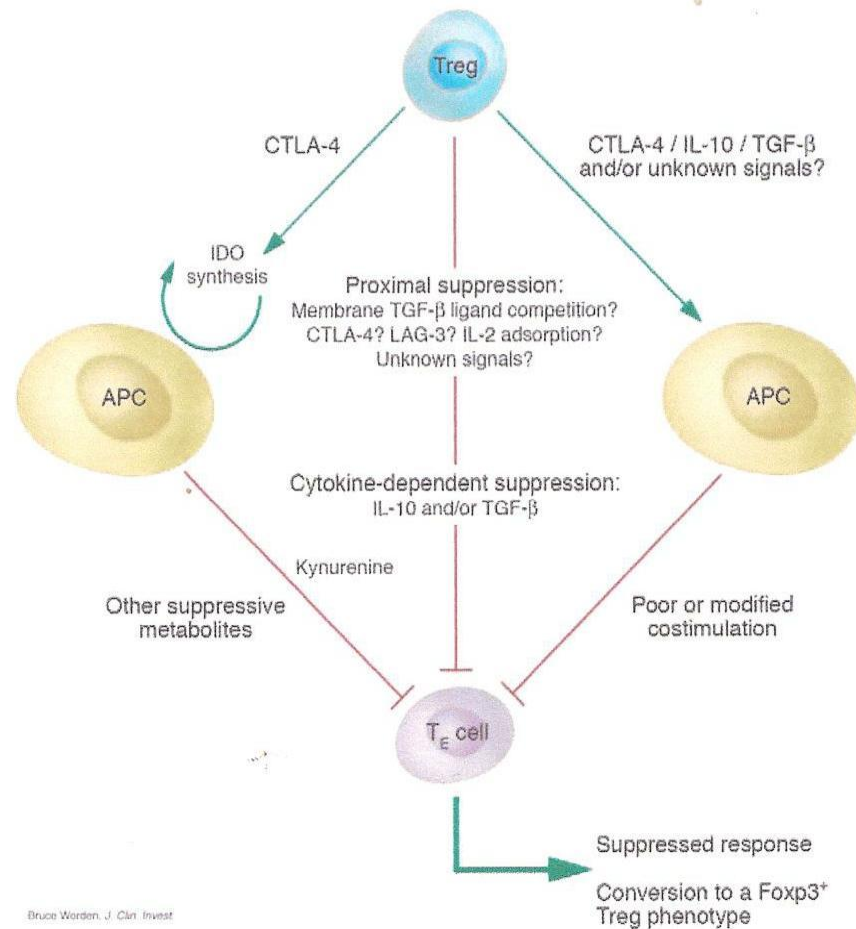


Figure 1. Diagram of Treg suppression mechanisms in vivo. Tregs may act in a cell contact-dependent manner to negatively bind stimulatory ligands on the antigen-presenting cell (APC), act as a cytokine ‘sink’ for cytokines such as IL-2 necessary for maintenance of effector T cells, or secrete long-range suppressive cytokines such as IL-10 and TGF-β. Through CTLA-4, Tregs may directly mediate suppression. CTLA-4 expressed on Tregs can trigger induction of the enzyme indoleamine 2,3-dioxygenase (IDO) in dendritic cells (DCs) by interacting with DC-expressed molecules CD80 and CD86, resulting in the generation of immunosuppressive metabolites. More than one Treg activity may operate in tandem. (Fehérvari and Sakaguchi, 2004).

CTLA-4 is upregulated on activated T cells as well as Tregs, ensuring that the immune system begins to check its response even in the midst of battling an infection to prevent devastating overactivation.

Interleukin-10 (IL-10) represents a long-range tolerogenic mechanism used by Tregs at the end of an immune response. It is an anti-inflammatory cytokine produced by Tregs and many other immune cells. IL-10 acts by inhibiting monocyte and macrophage expression of MHC class II and costimulatory molecule B7-1/B7-2 necessary for T cell activation. By directly limiting T cell activation and differentiation, IL-10 restricts the production of proinflammatory cytokines and chemokines (Couper *et al.*, 2008). The cytokine also limits the activity of Th1 cells, NK cells, and macrophages. This leads to decreased pathogen control as well as reduced immunopathology. IL-10 is also notable for its ability to induce apoptosis in plasmacytoid dendritic cells, known for their prolific production of IFN- α (Moore *et al.*, 2001). While IL-10 is adept at curbing Th1-biased responses, the cytokine actually enhances the survival of B cells and serves as a potent inducer for differentiation of B cell precursors (Moore *et al.*, 2001). By improving the B cell-focused response, IL-10 pushes an immune response from cellular to humoral (e.g. from Th1 to Th2). As a T-cell mediated immune response continuing inappropriately is at special risk of severely damaging self tissues, IL-10 provides a control mechanism to 'brake' an immune response in favor of preventing injury to self.

Despite the obvious benefits offered by its regulation of the immune system, an inappropriate IL-10 response can be as dangerous as a complete lack of regulation. Excessive or ill-timed IL-10 production can inhibit an inflammatory response to the extent that pathogens escape immune control, resulting in either rapidly fatal or chronic non-healing infections. In infections marked by high levels of IL-10 production and poor pathogen control, including *Leishmania* spp., *Listeria monocytogenes*, and *T. cruzi*, knock-down of IL-10 or inhibition of IL-10 signaling restores pathogen control and reduces the severity of disease (Couper *et al.*, 2008). This indicates a direct correlation between inappropriate IL-10 production and increased disease severity.

While early inflammation helps to prevent or limit infection, an uncontrolled response may eventually oppose disease eradication (Zelante *et al.*, 2009). In addition to anti-inflammatory cytokines, some cells may attempt to control or end a local immune response by limiting neighboring immune cells' access to crucial nutrients such as amino acids. Indoleamine 2,3-dioxygenase (IDO) is an enzyme catalyzing the first step of L-tryptophan degradation to kynurenines that has been found to have powerful immunomodulatory effects (Mellor and Munn, 1999). While IDO is detectable at low levels in many tissues from healthy animals, its expression is markedly elevated in animals harboring pathogens (Mellor and Munn, 1999). IDO is expressed by many cells, such as macrophages, neutrophils, epithelial cells, and plasmacytoid dendritic cells (Zelante *et al.*, 2008). Production of inflammatory cytokines, particularly

interferon- γ , induces increased IDO expression. Figure 2 depicts the tryptophan degradation pathway in which IDO functions.

IDO activity reduces extracellular tryptophan concentrations, preventing propagation of nearby microbes as well as the proliferation and activation of adjacent T cells (Mellor and Munn, 1999). Several theories exist as to how the catabolic enzyme enacts its apoptotic effects on T cells. A simple model suggests that T cells cannot proliferate in the presence of IDO because of the tryptophan-sensitive G1 cell cycle checkpoint in T cells, preventing clonal expansion (Munn and Mellor, 2004). Other research shows that IDO produces various downstream metabolites, some of which are toxic to T cells in vitro (Munn and Mellor, 2004). IDO activity has also been found to induce the expansion of suppressive T regulatory cells by way of kynurenine accumulation, further encouraging an immunosuppressive environment. (Zelante *et al.*, 2008).

IDO may have inadvertent consequences in instances of chronic infection. Some pathogens may exploit the immune system's attempt at natural immunoregulation to their own benefit, taking advantage of decreased T cell proliferation to fortify pathogen numbers (Mellor and Munn, 1999). It has been established that patients infected with HIV have chronically reduced levels of plasma tryptophan and increased levels of kynurenine, consistent with widespread IDO activation (Schröcksnadel *et al.*, 2005). Studies have shown IDO expression levels to be markedly increased in the tonsils of untreated HIV+ patients as compared to patients undergoing antiretroviral therapy (Andersson *et al.*, 2005).

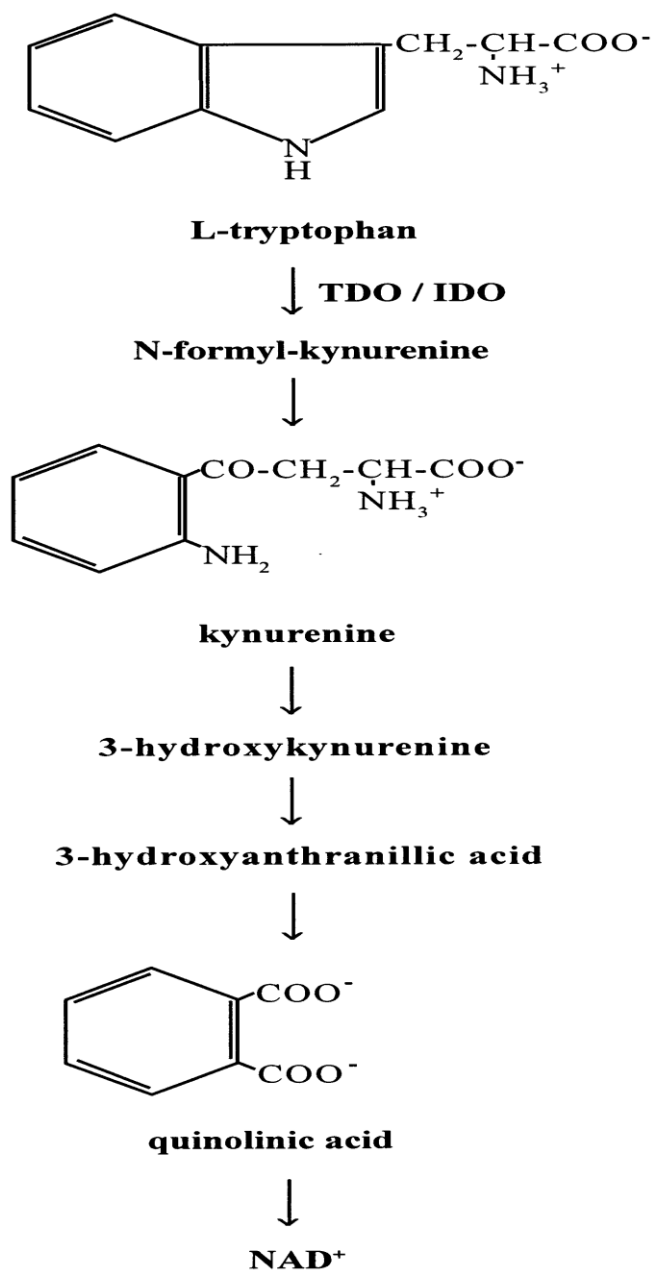


Figure 2. Kynurenine pathway of tryptophan degradation.

Indoleamine 2,3-dioxygenase (IDO) is the first and the rate-limiting enzyme in the generation of quinolinic acid from tryptophan via the kynurenine pathway. (Espey and Namboodiri, 2000).

Human Immunodeficiency Virus (HIV) and Acquired Immunodeficiency Syndrome (AIDS)

Acquired immune deficiency syndrome (AIDS) was first described in humans in the early 1980s. By 1983, the virus causing the strange new epidemic was isolated and identified as the human immunodeficiency virus (HIV) (Gallo *et al.*, 1983). HIV is a member of the genus *Lentivirus* in the family *Retroviridae*; the Latin-derived 'lenti' refers to the slow disease course caused by these viruses. Two types of HIV exist (HIV-1 and HIV-2), with many different clades within each type. HIV's two copies of its single-stranded RNA genome encode the classical retroviral proteins (*gag*, *pol*, and *env*), as well as several accessory proteins (*nef*, *rev*, *tat*, *vif*, *vpr*, and *vpu*) (Norkin, 2010). While *gag* encodes the viral nucleocapsid, *pol* encodes the viral reverse transcriptase, protease, ribonuclease, and integrase enzymes (Hutchison, 2001). *Env* encodes several proteins of the viral envelope, including gp120 and gp41 (Hutchison, 2001). The other accessory proteins conduct a variety of functions, ranging from regulation to promoting virus survival within host cells. HIV infects a cell by binding to the cell surface receptor CD4 as well as one of two coreceptors - either CCR5 or CXCR4 (Parham, 2009). The virus then copies its RNA genome into complementary DNA (cDNA) by reverse transcription. Once copied, cDNA is integrated into the host genome. Host cell machinery is then commandeered to produce viral proteins and RNA genomes, allowing assembly of new virions (Parham, 2009). New viral particles may then bud from the infected cell to

uninfected CD4 cells, directly transferring the infection (Norkin, 2010). The HIV life cycle is shown in Figure 3.

HIV infection typically occurs after transfer of body fluids such as blood, semen, vaginal fluids, or milk from an infected person to an uninfected recipient. Immune cells expressing CD4, such as macrophages, CD4+ helper T cells, and dendritic cells are the targets for HIV infection. Immediately after infection, a person may be asymptomatic or experience a flu-like illness marked by nonspecific symptoms such as fever, sore throat, rash, and muscle and joint pain (Fauci *et al.*, 1996). This acute infection is typically followed by activation of an HIV-specific adaptive immune response, leading to production of anti-HIV antibodies and seroconversion (Parham, 2009). Following the initial infection, an individual will experience a period of clinical latency often lasting up to ten years or more. In this time the virus infects and replicates in CD4+ cells, causing a slow decrease in CD4+ T cell numbers and gradually weakening the immune system. When CD4+ T cell numbers fall below 500 cells/ μ L, opportunistic infections and other symptoms become possible (Parham, 2009). The disease is then said to have entered the symptomatic phase. When CD4+ T cell numbers fall below 200 cells/ μ L, the patient is described as having AIDS (Parham, 2009). In this stage individuals become susceptible to a variety of cancers and opportunistic infections; it is these illnesses that eventually result in the patient's death.

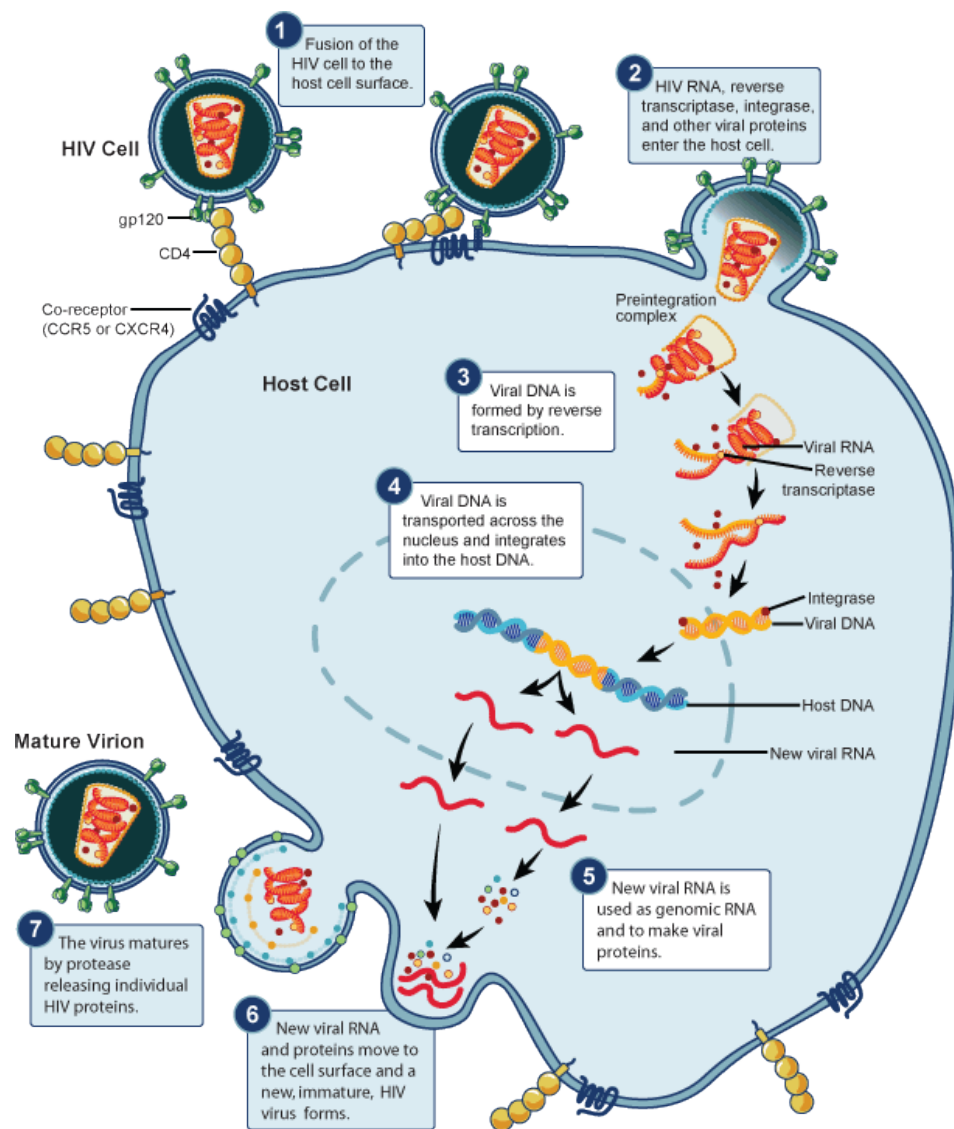


Figure 3. Diagram of the HIV replication cycle. HIV first fuses to the host cell surface, allowing HIV's RNA genome and viral proteins to enter the host cell. Next, viral DNA is formed by reverse transcription. Viral DNA is then transported across the nucleus and integrated into host DNA. It is then transcribed to form new viral mRNA, from which new viral proteins can be translated. New viral RNA and proteins next move to the cell surface to form a new, immature, HIV virus. The virus may mature when proteases release individual HIV proteins (NIAID, 2010).

Study of the AIDS epidemic has yielded a population of HIV-exposed people who never progress to AIDS. These individuals are referred to as long-term nonprogressors. This group exhibits normal CD4+ counts, low levels of viremia, and no symptoms of AIDS despite clear exposure to the virus. Another population known as exposed seronegative individuals remains completely uninfected despite repeated exposure to HIV. Much speculation has surrounded factors that allow long-term nonprogressors and exposed seronegative individuals to resist progression to widespread viremia and AIDS. It is hoped that study of the genetic backgrounds and immunological profiles of these individuals will generate ideas leading to the treatment or prevention of HIV.

Murine Leukemia Virus (MuLV) and Murine Acquired Immunodeficiency Syndrome (MAIDS)

The AIDS epidemic has prompted the creation of small animal models useful for studying retrovirus-mediated immunodeficiency. One such model is the murine AIDS (MAIDS) model induced by the LP-BM5 murine leukemia virus mixture in susceptible mouse strains post-infection (Liang *et al.*, 1996). While the effects of HIV and MuLV infection are not perfectly parallel, a striking number of similarities exist between murine and human AIDS. These similarities, along with the attractively well-characterized murine immune system, low biohazard risk, and relative economy as compared to primate models, make the MAIDS system extraordinarily useful in smaller research laboratories.

The murine leukemia virus is a type-C retrovirus marked by a central core with small spikes protruding from the viral capsid (Mosier, 1996; Norkin, 2010). The most common viral mixture causing MAIDS, called LP-BM5, includes: (1) a 4.8 kbp replication-defective BM5d, (2) a B-tropic mink cell focus-inducing virus (MCFV), and (3) a replication-competent B-tropic ectopic virus (BEV) (Liang *et al.*, 1996). The replication-defective virus encodes the ubiquitous retroviral *gag* gene, but the *pol* and *env* genes are largely deleted. This results in an unusual *gag*-encoded polyprotein (Jolicoeur, 1991). The altered murine leukemia virus genome causing MAIDS may be seen in Figure 4. While BM5d has been identified as the etiological agent responsible for causing MAIDS, it cannot replicate without help from MCFV and BEV. These helper viruses facilitate the transmission of BM5d within mouse tissue by providing the necessary protein machinery for viral replication (Chattopadhyay *et al.*, 1989).

Genetically-inbred mouse strains are differentially susceptible to developing MAIDS. Some strains (such as C57BL/6, C57BL/10, and 1/St) are highly susceptible to the disease, while others (such as BALB/c, A/J, and FVB) demonstrate total resistance (Jolicoeur, 1991). Susceptible strains mount a widely activated - yet ineffective - response that leads to further dysregulation and eventual overrun of the immune system. In contrast, resistant strains are not impervious to MuLV infection, but instead manage to eradicate or destroy the virus before developing a devastating immunodeficiency.

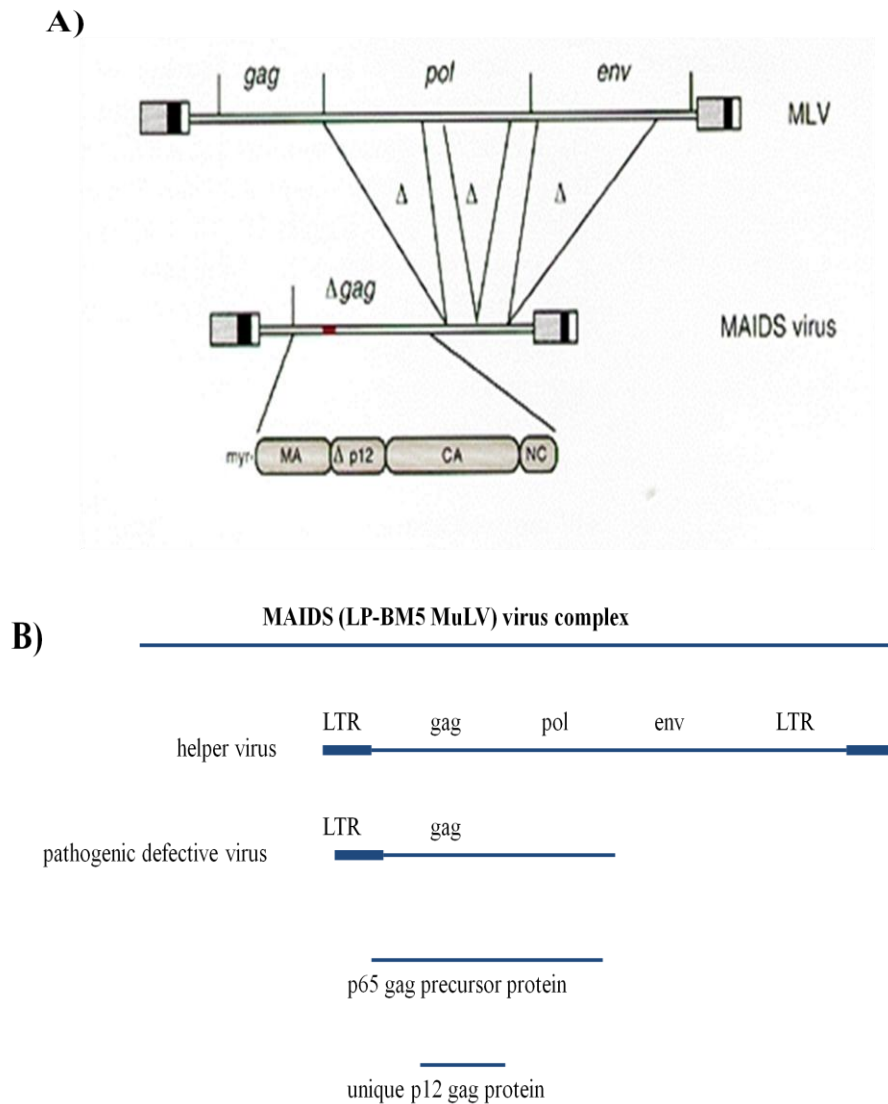


Figure 4. Genome of the murine leukemia virus and the replication-defective virus causing MAIDS. A) Triangles represent large deletions found within MuLV. The replication-defective virus expresses an altered *gag* gene product known as Pr60 Gag. Pr60 Gag also contains substitutions in the carboxy-terminal region of the MA protein and several changes within the p12 region. The *pol* and *env* genes are largely deleted. (Coffin *et al.*, 1997). B) Genome of the helper and replication-defective components of the MAIDS-inducing LP-BM5 virus complex (Mosier, 1996).

Symptoms induced by MuLV infection in susceptible mice include hypergammaglobulinemia, splenomegaly, lymphadenopathy, T cell functional deficiency, B cell dysfunction, neurological symptoms including paralysis, and opportunistic infections (Liang *et al.*, 1996). These are notable for their similarity to symptoms experienced by AIDS patients. On a cellular level, infection with LP-BM5 induces an early phase of B-cell hyperactivity and clonal activation (Liang *et al.*, 1996). Yet this prolific expansion of B cells and subsequent antibody production is not well-adapted to a controlled immune response – activated B cells are not antigen-specific, and therefore do not lead to virus removal. MuLV infection is also marked by CD4⁺ and CD8⁺ T cell unresponsiveness, as well as increased T cell activation followed by increased apoptosis (Liang *et al.*, 1996).

Cytokine dysregulation appears to be a crucial problem associated with both human and murine AIDS. Researchers have noted that a switch from a Th1 to a Th2-biased cytokine response can promote the development of MAIDS (Liang *et al.*, 1996). Th2 cytokines have been found in abnormally high levels in mice with MAIDS. Switching from an inflammatory Th1 response with high CD8⁺ T cell-mediated cytotoxicity to an antibody-mediated Th2 response with immunosuppressive potential may contribute to the poor response and prognosis of MAIDS-susceptible mice.

AIDS versus MAIDS

Despite the multitude of similarities between AIDS and MAIDS, crucial differences do exist that prevent MAIDS from serving as an ideal model system for human AIDS. One critical difference between MuLV and HIV are the cell targets. While the MAIDS-inducing viral mixture is primarily tropic for B cells and macrophages, HIV instead infects CD4+ T cells and macrophages using CD4 as a receptor (Mosier, 1996). MuLV and HIV are also different types of retrovirus. HIV belongs to a category of retroviruses known as the lentiviruses, while MuLV is identified only as a type-C retrovirus.

Even with these dissimilarities, the overall symptoms of the two diseases are easily comparable. MuLV infection induces a clinical spectrum of disease similar to HIV, including lymphomas and opportunistic infection (Mosier, 1996). Even though CD4+ cells are not the primary targets for MuLV infection, their presence is required for successful development of MAIDS, as is true with HIV and AIDS (Li and Green, 2006). Both MAIDS and AIDS show inflammation in secondary lymphoid organs, known as lymphadenopathy and splenomegaly (Liang *et al.*, 1996). Both MuLV and HIV infection induce CD4+ and CD8+ T cell anergy, limiting the ability of T cells to appropriately respond to viral infection (Mosier, 1996). Finally, activated B cells increase secretion of IgG in both syndromes (Li and Green, 2006). These similarities, along with the relative convenience offered by the MAIDS system, make it a worthwhile model for

generating new research ideas pertaining to AIDS, immunodeficiency, and retroviral infection.

Previous Work – Type I Interferons in Murine Retroviral Models

Type I interferons play a crucial role in the innate immune system's defenses against viral infection. IFN- α/β signaling upregulates IFN- γ production, and favors induction and maintenance of Type I helper T (Th1) cells. Th1-biased responses are associated with intracellular pathogens, while Th2-biased responses are dominated by antibody-mediated effector mechanisms and target extracellular pathogens (Boehm *et al.*, 1997). In turn, IFN- γ stimulates innate cell-mediated immunity through NK cell activation, adaptive cytotoxic immunity through MHC upregulation, and enhances phagocytosis of infected cells through macrophage activation (Boehm *et al.*, 1997). The interferon family can also promote humoral immunity by inducing increased expression of B cell survival factors (Theofilopoulos *et al.*, 2005). Because of the importance of Type I interferons in regulating immune responses to viruses, previous work has explored their effects within murine AIDS models.

In early research, the LP-BM5 retrovirus was found to inhibit IFN- α/β production in MAIDS-susceptible mice. Pitha *et al.* found that transcripts of IFN- α/β genes were undetectable in spleen cells of C57BL/10J (B10) susceptible mice at any time after LP-BM5 infection (Pitha *et al.*, 1988). In contrast, the group saw rapid induction of IFN- α/β genes after infection with Newcastle disease virus (a

paramyxovirus). The group concluded that these results suggested that normal contributions of IFN- α/β to controlling microbial spread, immune surveillance, and lymphoid interactions were disrupted by infection with LP-BM5 MuLV.

Heng *et al.* published a later paper linking the IFN- α/β response to increased strain-specific resistance to MAIDS (Heng *et al.*, 1996). The group demonstrated that resistant mice exhibited stronger IFN- α/β mRNA responses to LP-BM5 infection than did C57BL/6 and B6.CH-28c susceptible mice. They also showed that administration of IFN- α/β to susceptible mice significantly slowed the development of MAIDS. Heng and colleagues hypothesized that a difference in the kinetics or magnitude of the IFN- α/β response to LP-BM5 may help suppress the development of disease in resistant mice. The group was unable to detect the presence of IFN- α/β by bioassay, but did find evidence of a differential response when using RT-PCR. The group detected faint bands representing IFN- α/β mRNA on EtBr-stained agarose gels for MAIDS-resistant LP-BM5-infected mice at 3, 6, and 9 hours in the spleen and liver. The bands were faint enough to require the use of Southern dot blot hybridization to amplify the signal observed. In contrast to the resistant mice, IFN- α/β was not detected by RT-PCR amplification of spleen or liver samples from the MAIDS-susceptible strains at 3, 6, or 9 hours post infection. Heng's finding - that relative differential expression of IFN- α/β genes may be seen as early as three hours - indicates that varying success in very early innate responses may play an immense role in the final outcome of a viral infection.

Other groups have studied the impact of IFN- α/β on early differential immune responses in rodent HIV model systems. Gerlach *et al.* used the Friend virus model to determine the activity of type I interferons against a murine retrovirus (Gerlach *et al.*, 2006). The group demonstrated a peak in IFN- β expression at 18 hours post-infection (p.i.) using ELISA, but noted that IFN- α levels were twice as high as IFN- β levels. In studies using knockout mice, they found that resistant IFN- β $-/-$ mice had up to 10-fold-higher spleen viral loads than normal resistant mice. Gerlach *et al.* concluded that both IFN- α and IFN- β play a significant role in the innate immune defense against retroviral infection, but that IFN- α and IFN- β have different potentials for antiviral activity.

Taken together, the body of previous work indicates that differential levels of IFN- α/β can be seen between MAIDS-resistant and –susceptible mouse models, but cautions that low levels of Type I interferon expression can make quantification difficult using certain assays.

Previous Work – IDO in Murine Retroviral Models

IDO's role in immunoregulatory function is a relatively novel area of research; accordingly, scientists have only recently begun to define its role in chronic infection in animal retroviral models.

Very recent research has studied the relationship between IDO and Type I interferons in a murine model of LP-BM5 retroviral infection (Hoshi *et al.*, 2010). Both IDO $-/-$ mice and IDO inhibitor- administrated mice clearly suppressed LP-

BM5 viral replication. Furthermore, the group linked the absence of IDO to increased Type I interferon production, demonstrating upregulation of Type I interferons in IDO $-/-$ mice following LP-BM5 infection. Upregulated IFN- α/β resulted in an increased survival rate post-infection with LP-BM5. The group hypothesized that the absence of IDO allows the clearance of murine retroviral infection via increased interferon expression. The study concludes that inhibition of IDO is critical for the suppression of murine retroviral infection and that long-term activation of IDO might result in suppression of T-cell responses and immune exhaustion. Hoshi *et al.* provide convincing evidence that host expression of immunomodulatory compounds like IDO may at times be inappropriate, actually preventing the host from responding with anti-pathogenic factors necessary for a successful immune response.

Another group examined the role of IDO in a murine model of HIV-induced encephalitis (Potula *et al.*, 2005). They hypothesized that HIV-induced IDO activity in the brain may participate not only in local neurotoxicity by the generation of quinolinic acid and other toxins, but also in the failure of the immune system to clear HIV from this reservoir. Specifically, they pondered whether IDO-expressing antigen presenting cells (especially HIV-1-infected macrophages) might help to create a protected reservoir for HIV-1 persistence in the brain. Potula *et al.* used severe combined immunodeficient mice reconstituted with human peripheral-blood lymphocytes (hu-PBL-NOD/SCID) and intracranially injected them with HIV-1-infected macrophages to induce viral

encephalitis. This served to recapitulate the cellular immune responses against HIV-1–infected brain macrophages that occur in humans during progressive disease. The group demonstrated that inhibition of IDO activity during HIV-1 CNS infection significantly enhances CD8⁺ T cell-mediated clearance of virus-infected macrophages in brain. Attenuation of the immunosuppressive and neurotoxic IDO activities led to enhanced adaptive immune clearance of virus-infected cells. Because IDO was up-regulated in HIV-1–infected macrophages, Potula *et al.* hypothesized that the *in vivo* immunosuppressive properties of IDO may confer an advantage to HIV-1 by allowing the virus to escape T cell-mediated clearance.

IDO-focused research within murine retroviral model systems has indicated that IDO may inappropriately suppress effective innate and adaptive immune responses. These authors' data indicate that inhibition of IDO may serve as an additional and previously unsuspected target for HIV-1 therapy.

Previous Work – IL-10 in Murine Retroviral Models

Long recognized as an immunosuppressive cytokine, significant research has been conducted examining IL-10's role in inhibiting immune responses and general anergy in murine retroviral systems. Early work by Gazzinelli and colleagues showed a robust transition from Th1 to Th2 cytokines – including IL-10 – in MAIDS-susceptible mice, while resistant mice showed only transient expression of Th2 cytokines (Gazzinelli *et al.*, 1992). Th2 cytokines tend to

enhance B cell-mediated responses while suppressing T cell-mediated immunity. Resistant mice showed detectable levels of IL-10 only at one week, after which no expression was detected. In contrast, susceptible BL.6 mice expressed progressively higher levels of IL-10 between one and thirteen weeks post-LP-BM5 infection. The group hypothesized that repeated stimulation of cells through the T cell receptor without concomitant costimulation by antigen presenting cells would yield a cytokine pattern of high IFN- γ , IL-4, and -10 expression and scant expression of IL-2, resulting in T cell anergy. It is possible that increased IL-10 expression indicates stimulation of the 'wrong' type of immune response by disease-susceptible mice, preferentially aiding B cell activation over T cell activation. As B cells fight pathogens through antibody-mediated responses, the results of Gazzinelli *et al.* indicate that successful suppression of LP-BM5 retroviral infection relies primarily on T-cell mediated defenses instead of B cell-produced neutralizing antibodies.

While inappropriate immunosuppression of necessary immune responses is a potential effect of immunomodulators like IDO and IL-10, it is important to remember that a strong, uncontrolled immune response can be as damaging to the host as an uncontrolled infection. Accordingly, some researchers have studied IL-10's positive effects in limiting disease pathogenesis.

Green *et al.* have reported that BL6.IL-10 knockout mice are substantially more susceptible to LP-BM5-induced disease than wild-type BL6 mice (Green *et al.*, 2008). IL-10 knockouts showed exaggerated disease pathogenesis including

splenomegaly, hyper-Ig, and mitogen responsiveness as indicators of immunodeficiency. Further results suggested that Programmed Death Receptor-1/Programmed Death Receptor –Ligand (an immunosuppressive interaction) ligation might be the basis for IL-10 production, which then limits the extent of disease in infected BL/6 mice. Significantly, the group found no evidence for any consistent differences in viral load among wild type BL/6 versus IL-10 knockout strains. The results of Green *et al.* indicate that immunomodulation by IL-10 is important in suppressing exuberant immune responses causing harmful pathology, but does not significantly affect host ability to combat retroviral infection. This contrasts IDO's purported role in effectively inhibiting appropriate immune responses.

Proposed Studies

This research project will attempt to address the question of immune dysregulation and inappropriate immunosuppression in the MAIDS model system. Balance within an immune response is a fundamental concern. An immune response must obviously be strong enough to serve its ultimate goal of thwarting invading pathogens. However, it must not inadvertently harm the host it seeks to defend by provoking an overactive inflammatory response harmful to both self and pathogen. An immune response must also discern whether a particular pathogen is best targeted by T cell-mediated cytotoxicity or B cell-produced neutralizing antibodies. Once humoral or T cell-mediated immunity has

been chosen as the most effective type of response, the other arm of immunity must be suppressed to conserve immune efforts for the most constructive direction. Failure to do so will result in an overactive, improperly targeted response that cannot contain an infection without causing substantial pathology in the host. Others have hypothesized that MAIDS-susceptible mice may inappropriately suppress a well-directed Th1 response, instead utilizing a Th2 response that allows for widespread viremia and eventual progression to MAIDS. MAIDS-resistant mice may respond to retroviral infection with a directed, controlled Th1 immune response that allows for rapid viral control and no further immune disruption.

I will focus on comparing the expression levels of three immune molecules between resistant and susceptible strains of mice: the antiviral Type I interferons, the immunosuppressive tryptophan catabolic enzyme IDO, and the anti-inflammatory cytokine IL-10. Some have linked increased expression of inflammatory Th1 cytokines like Type I interferons with resistance to MAIDS, while others have noted higher expression of immunosuppressive Th2 cytokines like IL-10 in MAIDS-susceptible mice. Still other researchers have linked lowered levels of immunomodulators such as IDO with increased inflammatory cytokine levels, leading to more robust disease resistance.

The majority of previous MAIDS work has been completed at time points late in the MAIDS disease time course, long after susceptible animals have begun showing symptoms of disease. My research will instead focus on time points

within the first week following infection. IFN- α/β , IL-10, and IDO can act as part of the nonspecific innate immune response occurring immediately after pathogenic infection. I seek to discern whether inherent early differences in innate immunity—occurring even within hours after infection - send MAIDS-resistant and –susceptible mice down different paths before they may even mount a specific adaptive immune response. I also hope to characterize the balance between inflammation and immunosuppression at selected time points by comparing the levels of immunomodulatory IDO and IL-10 with the presence of pro-inflammatory Type I interferons. A relationship between the amount of immunosuppressors present compared to the presence of inflammatory molecules may suggest the immune balance required for successful resistance.

A significant finding characterizing the relationship between the selected immunomodulatory and inflammatory molecules may shed light on the importance of balancing immune system activation and control during a murine retroviral infection. This may be relevant to factors inducing vulnerability to the human retrovirus that induces AIDS.

MATERIALS AND METHODS

Animals

BALB/c and C57BL/6 mice were housed in the Mount Holyoke College Animal Facility according to the National Institute of Health's Guidelines for the Care and Use of Laboratory Animals. Six to ten week old female BALB/c and BL/6 mice were injected intraperitoneally with 1mL of MuLV virus stock (3×10^3 PFU). Mice were sacrificed at a variety of time points post-infection using carbon dioxide inhalation. Time points included 8 hours, 18 hours, 24 hours, 3 days, and 7 days. For quantitative PCR work, inguinal, brachial, axillary, and mesenteric lymph nodes were harvested as well as spleens. Mesenteric lymph nodes were not harvested during preparation of ELISA supernatants because of recent evidence showing strong differences in mesenteric lymph node gene and cytokine expression as compared to other lymph nodes.

RNA Concentration and Quality

RNA samples harvested from lymph nodes and spleens were previously collected in 2005 from both BALB/c and BL/6 naïve and MuLV-infected animals and stored at $-80\text{ }^{\circ}\text{C}$ (refer to Smita Gopinath (2006) and Suprawee Tepsuporn's (2005) theses). Organs were removed, placed in Trizol, and homogenized using the Polytron probe. Chloroform was added and the solution was centrifuged in a phase-lock gel tube. The upper aqueous phase containing RNA was subsequently transferred to a fresh tube to which isopropyl alcohol was added. The solution was

again centrifuged to obtain an RNA pellet. The RNA pellet was washed using 75% ethanol, and RNA was resuspended in RNase-free water. All RNA samples were analyzed using the Agilent 2100 Bioanalyzer to determine the RIN (RNA Integrity Number). The protocol in the Agilent Chip handbook was followed when preparing and assessing RNA samples for the Bioanalyzer. Values for the RIN range from 0-10; 0 represents complete RNA degradation. As per Smita Gopinath's thesis, RNA samples were considered degraded if the RIN value was less than 6. The majority of our viable RNA samples had an average RIN of 8. Degradation of RNA as well as DNA contamination could be visually determined using the histogram and gel electrophoresis images produced by the electropherogram of the Bioanalyzer. Viable RNA is indicated by the presence of two sharp peaks representing 18S and 28S ribosomal RNA. The presence of many smaller peaks indicates degradation of the sample. The Nanodrop 3.1 spectrophotometer machine was used to calculate RNA concentration levels as well as to detect protein contamination using the 260/280nm ratio. An ideal absorbance ratio of 2 indicates no protein contamination. A significant amount of protein contamination will lower the 260/280 absorbance ratio to less than 2.

DNase Treatment of RNA

Analysis of genes where the primers are contained within one exon required DNase treatment of RNA to prevent contamination with genomic DNA. The Qiagen Mini RNEasy kit in combination with DNase I (Qiagen) was used to

DNase-treat samples. 32 μL of DNA-contaminated RNA at varying concentrations was mixed with 10 μL Qiagen Buffer RDD, 2.5 μL DNase I stock solution, and 55.5 μL water and incubated on the benchtop for 10 minutes. 350 μL of Qiagen Buffer RLT and 250 μL 100% ethanol were added and mixed thoroughly. The solution was centrifuged at 8,000 g for 15 seconds and the flow-through was discarded. 500 μL of Qiagen Buffer RPE was added to the spin column, the tube was again centrifuged at 8,000 g for 15 seconds, and the flow-through was discarded. 500 μL of 80% ethanol was added to the spin column to dry the silica gel membrane, followed by centrifugation for 2 minutes at 8,000 g and discarding of flow-through. The spin column cap was opened and the tube was centrifuged at full speed for 5 minutes to ensure membrane drying. Finally, RNA was eluted by adding an appropriate volume of RNase-free water and centrifuging at full speed for 1 minute.

cDNA Synthesis

RNA samples stored at $-80\text{ }^{\circ}\text{C}$ were thawed and diluted to a concentration of 125 ng/ μL with nuclease-free water. 8 μL of RNA at 125 ng/ μL were added to 1 μL of 0.5 $\mu\text{g}/\mu\text{L}$ Random Primers (Promega) and 1 μL of 0.5 $\mu\text{g}/\mu\text{L}$ Oligod(T) primers (Promega). The solution was vortexed and incubated in a heat bath at $75\text{ }^{\circ}\text{C}$ for 5 minutes, after which it was placed on ice. Random primers and Oligod(T) primers act to build the cDNA template simultaneously. Oligod(T) primers add nucleotides to the leading mRNA strand's poly-A tail, while random primers add

six nucleotide fragments randomly to the template. Next, 10 μL of the appropriate master mix was added to the tube. The cDNA master mix contained 4 μL of 5x First Strand Buffer (GibcoBRL), 2 μL of 0.1 M dTT (Invitrogen), 1 μL of 10 mM dNTPs, 2 μL of nuclease-free water, and 1 μL of ImProm-II Reverse Transcriptase. Master mixes made for the control No-RT wells omitted the ImProm-II Reverse Transcriptase, including instead an extra 1 μL of nuclease-free water. After adding the master mix, the solution was incubated on the benchtop for 5 minutes, followed by incubation at 42 °C for one hour. At the conclusion of the 42 °C incubation stage, the reverse transcriptase enzyme was inactivated by heating the solution to 95 °C for 5 minutes. cDNA samples were then stored at -20 °C.

Primer Design

Primer sets were designed for selected genes to amplify selected regions of DNA within the chromosomes of *mus Musculus*. Guidelines established by Dr. Sonia Bakkour (personal communication) were used when designing primers. Each primer set was designed to amplify a product between 50-150 nt. Optimum primer length was set at 20 nt, with an allowable range between 15-25 nt. Primers were designed with an optimal G/C content of 50%, with an allowable range between 30-80%. Primer annealing temperature was targeted at 60 °C. First, the mRNA transcript sequence and genomic DNA sequence for the gene of interest were identified using the National Center for Biotechnology Information website

(<http://www.ncbi.nlm.nih.gov/>). By evaluating relative positions of introns and exons, exons were chosen in which to design primers. Ideally, forward and reverse primers were designed to lie within different exons separated by at least one intron with a minimum size of 400 bp. This qualification ensured easy identification of genomic DNA contamination during conventional PCR experiments. Some genes of interest contained only one exon, making this criterion impossible to achieve and necessitating DNase treatment of RNA. After identifying potential exons in which to design primers, a variety of software programs were used to design primers. These programs included Primer Quest from IDT (<http://www.idtdna.com/Scitools/Applications/Primerquest/>), Primer Express from Applied Biosystems (commercial software available on the Stranford Lab computer), and Primer-Blast from NCBI (<http://www.ncbi.nlm.nih.gov/tools/primer-blast/primertool.cgi>). The Harvard/MGH/CCIB PrimerBank was also utilized when designing primers for IDO (<http://pga.mgh.harvard.edu/primerbank/>).

Primers designed within one program were crosschecked in other programs to ensure high specificity for the intended target sequence and limited potential secondary structure. If it was impossible to fully avoid primer dimers, primers with deltaG values no more negative than -10 kcal/mol were chosen. IDT's mFold program (<http://www.idtdna.com/Scitools/Applications/mFold>) was used to determine deltaG values for primers. Two sets of primers were

designed for each gene. Results from conventional PCR and primer optimization experiments were used to select the primer pair used for real time PCR.

TBP Primer Sequence #1: 80 nt amplicon, Exon 2-3 (designed by Dr. Bakkour)

Forward Primer: 5' CAA CAG CCT TCC ACC TTA TGC 3' (21 nt)

T_m = 58°C G/C Content: 52%

Reverse Primer: 5' GAT GGG AAT TCC AGG AGT CAT G 3' (22 nt)

T_m = 59°C G/C Content: 50%

IFN-β Primer Sequence #1: 107 nt amplicon, Exon 1

Forward Primer: 5' CGT GGG AGA TGT CCT CAA CTG CT 3' (23 nt)

T_m = 58°C G/C Content: 56%

Reverse Primer: 5' TCG GAC CAC CAT CCA GGC GT 3' (20 nt)

T_m = 60°C G/C Content: 65%

IFN-β Primer Sequence #2: 125 nt amplicon, Exon 1 (Linenklaus *et al.* 2009)

Forward Primer: 5' CTG GCT TCC ATC ATG AAC AA 3' (20 nt)

T_m = 53°C G/C Content: 45%

Reverse Primer: 5' CAT TTC CGA ATG TTCGTC CT 3' (20 nt)

T_m = 52.9°C G/C Content: 45%

IFN-α Primer Sequence #1: 145 nt amplicon, Exon 1 (designed by Dr. Bakkour)

Forward Primer Sequence: 5' CTA GAC TCA TTC TGC AAT G 3' (19 nt)

T_m = 45°C G/C Content: 42°C

Reverse Primer Sequence: 5' ACA CAG TGA TCC TGT CGA A 3' (19 nt)

T_m = 50°C G/C Content: 47%

IDO Primer Sequence #1: 120 nt amplicon, Exon 3-4 (Harvard PrimerBank)

Forward Primer Sequence: 5' TGG CGT ATG TGT GGA ACC G (19 nt)

T_m = 62.3°C G/C Content: 58%

Reverse Primer Sequence: 5'CTG CAT AAG ACA GAA TAG GAC GC 3' (23)

T_m = 60.2°C G/C Content: 48%

IDO Primer Sequence #2: 150 nt amplicon, Exon 1-2

Forward Primer Sequence: 5' GGG GTC AGT GGA GTA GAC AGC A 3' (22 nt)

T_m = 60.5°C G/C Content: 59%

Reverse Primer Sequence: 5' CAG GGG CTG TAT GCG TCG GG 3' (23 nt)

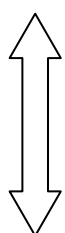
T_m = 63.1°C G/C Content: 70%

Conventional Polymerase Chain Reaction

Conventional Polymerase Chain Reaction (PCR) experiments were used to assess the quality of cDNA samples as well as to ensure efficiency of primers designed for genes of interest. Conventional PCR amplifies a specific region of DNA using thermal cycling through three discrete temperatures. An initial denaturation stage melts the double stranded DNA template by disrupting hydrogen bonds. It is followed immediately by an annealing stage in which forward and reverse primers bind to the newly single-stranded template. Finally, an elongation stage allows the DNA polymerase to synthesize a new DNA strand complementary to the template strand. Assuming 100% efficiency, the amount of

DNA target is doubled with each elongation stage, resulting in exponential amplification of DNA.

Three tubes were prepared for each target sequence: (1) cDNA prepared as previously described, (2) No reverse transcriptase enzyme included, and (3) No RNA included in the PCR mix. PCR master mixes included 10 μL of 5x Green GoTaq Buffer, 1 μL of 10 mM dNTPs (Promega), 2 μL of 25 mM MgCl_2 , 0.25 μL of 5 unit/ μL GoTaq Polymerase, and 32.75 μL of nuclease-free water. 1.5 μL of the appropriate forward and reverse primers at 10 μM was then added to 46 μL of master mix. Finally, 1 μL of the appropriate template at 12.5 ng/ μL was added and the solution was then vortexed thoroughly. The PCR reactions were run at 35 cycles at the temperatures listed below:

<u>Temperature</u>	<u>Time</u>	<u>Step</u>	
95°C	2 min		
95°C	30 seconds	Denaturation	
55°C	30 seconds	Annealing	
72°C	30 seconds	Extension	
72°C	5 minutes		
4°C	Hold		

Conventional PCR products were then analyzed by agarose gel electrophoresis. 2% agarose gels were made using 1 g agarose, 50 mL TAE buffer, and 5 μL of 10 $\mu\text{g}/\text{mL}$ ethidium bromide (EtBr). Ethidium bromide serves as a fluorescent intercalating agent that intertwines in double-stranded DNA,

allowing for visualization of DNA bands under UV light. Agarose gels were allowed to polymerize for at least 30 minutes, before suspending the gel in additional TAE buffer and loading samples. 25 μ L of each sample was loaded into wells 2-9, while 15 μ L of 50 bp mini ladder (Promega) was loaded into well 1. Gels were run for approximately 1 hour at 96 V. An image was then taken using the FujiFilm LAS-3000 Intelligent Darkbox machine with ImageReader LAS-3000 software. Primer amplification of the intended target was confirmed by comparing the position of the DNA band in cDNA template wells to the base pair ladder.

Primer Optimization

Primer concentrations were optimized for quantitative PCR work using PerfeCTa SYBR Green Supermix (Quanta Biosciences) on an ABI 7300 Real Time PCR Machine. Optimization of primer concentration maximizes amplification of target DNA finding primer concentrations that avoid primer-dimers while providing enough primers to anneal to the target. Both forward and reverse primers were optimized using combinations of each primer in concentrations of 100 nM, 300 nM, and 500 nM. Optimum primer concentrations were determined based on cycle threshold (Ct) values and melting curves for each pair. Ct values indicate the cycle at which the amount of fluorescence exceeds the level of background fluorescence, meaning that the target DNA is being amplified exponentially in that cycle. Therefore, a low Ct value indicates a higher initial

amount of double stranded DNA being amplified that allows for earlier detection of fluorescence. In contrast, melting or dissociation curves aid in discerning the homogeneity of double stranded DNA that was amplified. Quantitative PCR machines may be programmed to incrementally raise the plate temperature after a run and simultaneously measure the change in fluorescence. The two strands of DNA will separate at the melting point, causing the fluorescence to rapidly decrease. ABI 7300 software can then plot the rate of change of fluorescence with time on the Y-axis versus the temperature on the X-axis, showing a peak at the melting temperature. A single large peak with a T_m of approximately 82 °C indicates amplification of a single cDNA target size of the expected amplicon. The specific melting temperature of the amplicon peak also represents the temperature at which half of the DNA helical structure is lost. Additional peaks may indicate presence of larger sequences of contaminating genomic DNA, unintended cDNA target sequences, or smaller primer dimers. Primer pairs were chosen based on the lowest Ct value in combination with a large specific amplicon peak seen in the melting curve.

Master mixes for qPCR primer optimization were created that included 12.5 μL of SYBR Green Master Mix, 6.7 μL of nuclease-free water, and 0.8 μL of cDNA or No RT template at 12.5 ng/ μL per well. In addition to 20 μL of this master mix, 2.5 μL of both forward and reverse primer at the appropriate concentration were added to each well and mixed thoroughly. Each sample was run in duplicate, and No RT control wells were run for each primer pair to assess

formation of primer dimers. After loading samples into wells, the plate was sealed with a plastic coverslip, and bubbles were removed by gently tapping the plate on the benchtop. Finally, the plate was centrifuged at 1,200 g for 3 minutes at room temperature prior to commencing the reaction in the ABI 7300 machine. All qPCR reactions were run on cycles as shown below:

<u>Temperature</u>	<u>Time</u>	<u>Step</u>	
95°C	2:00		
95°C	0:30	Denaturation	
55°C	0:30	Annealing	40 cycles
72°C	0:30	Extension	*Data Collection*
95°C	0:15		
60°C	1:00	Dissociation stage	
95°C	0:15		



Please refer to Figure 5 for a sample primer optimization plate set up, and to Figure 6 for a sample melting curve showing specific amplification of a cDNA target.

	1	2	3	4	5	6	7	8	9
A	500nM F 500nM R	500nM F 500nM R	500nM F 300nM R	500nM F 300nM R	500nM F 100nM R	500nM F 100nM R	x	x	x
B	300nM F 500nM R	300nM F 500nM R	300nM F 300nM R	300nM F 300nM R	300nM F 100nM R	300nM F 100nM R	x	x	x
C	100nM F 500nM R	100nM F 500nM R	100nM F 300nM R	100nM F 300nM R	100nM F 100nM R	100nM F 100nM R	x	x	x
D	500:500 No RT	500:300 No RT	500:100 No RT	300:50 0 No RT	300:30 0 No RT	300:10 0 No RT	100:50 0 No RT	100:30 0 No RT	100:10 0 No RT

Figure 5. Quantitative PCR primer optimization plate set-up. Various concentrations of forward (F) and reverse (R) primers (100 nM, 300 nM, and 500 nM) were tested in duplicate wells using qPCR. Each primer combination was run with a corresponding negative control (No RT) sample.

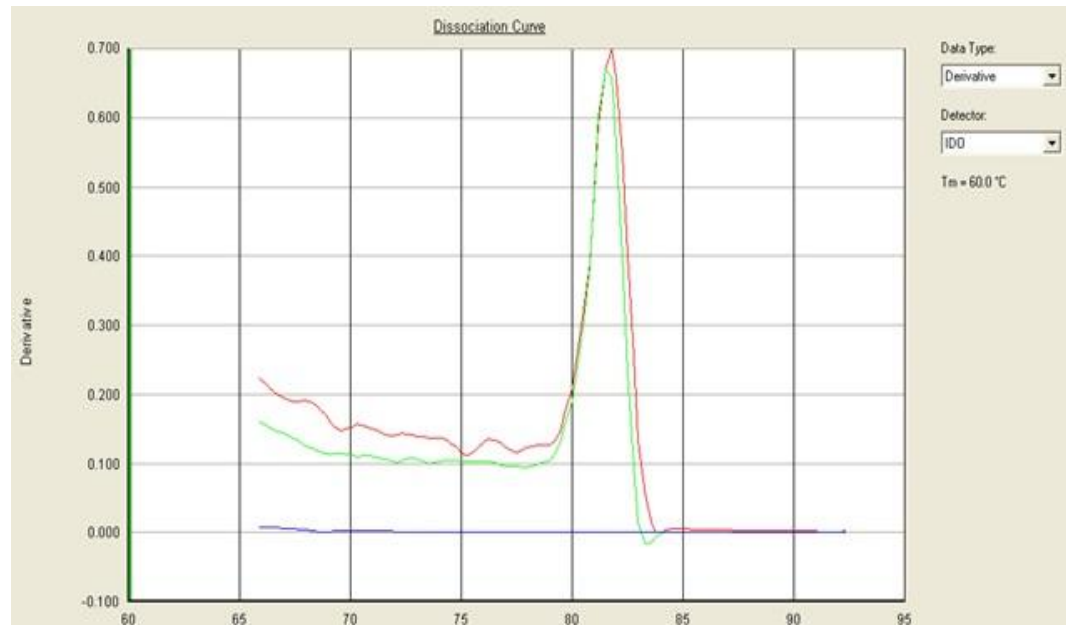


Figure 6. Sample dissociation curve for IDO at 500 nM forward primer: 500 nM reverse primer. The plot shows the derivative of fluorescent intensity as a function of temperature in degrees Celsius. The single red and green peaks representing two wells indicate amplification of a single target cDNA sequence in both 500:500 reaction wells on the plate, with no genomic and non-specific DNA binding or primer dimer presence. The flat blue line indicates no DNA amplification in the corresponding 500:500 No RT control well, demonstrating no reagent contamination or primer dimer formation in the absence of template.

Primer Efficiency Testing

The next step in qPCR optimization was primer efficiency testing on the ABI 7300 Real Time PCR Machine. Different primer pairs amplify DNA at different rates. In an ideal PCR reaction, the quantity of DNA will double with each cycle during the linear phase of amplification. This constitutes 100% efficiency. However, some primers are defined as overefficient (>100% efficient), and produce more than double the amount of DNA with each cycle. Others are underefficient (<100% efficient) and produce less than double the amount of DNA with each cycle. Efficiencies of each primer pair were determined by creating a standard curve from serial dilutions of a single cDNA template. Concentrations of cDNA template used included 200 ng, 20 ng, 2 ng, 0.2 ng, and 0.02 ng per reaction well. Standard curve wells were run in duplicate to ensure accuracy. Primer efficiency can be found from the equation of each standard curve by inserting the slope of the standard curve into the efficiency equation shown below:

$$\text{Efficiency} = [10^{(-1/\text{slope})}] - 1$$

A slope value of -3.33 represents 100% efficiency and an exponential amplification value of 2, while slope values above -3.33 mean overefficient primers and slope values more negative than -3.33 represent underefficient primers.

When using relative quantification as the method of data analysis, primer efficiencies between the housekeeping (endogenous control) gene and gene of

interest must be compared to choose between ddCt quantification versus standard curve quantification. Should the housekeeping gene and gene of interest have efficiencies between 90-110% and within 5% of each other, the appropriate assumptions are met to compare gene expression using the ddCt method. Efficiencies outside of that range, or more different than 5%, necessitate running a standard curve on every experimental plate. All primer pairs tested in these experiments later required use of a standard curve. Please refer to Figure 7 for a sample primer efficiency standard curve plot.

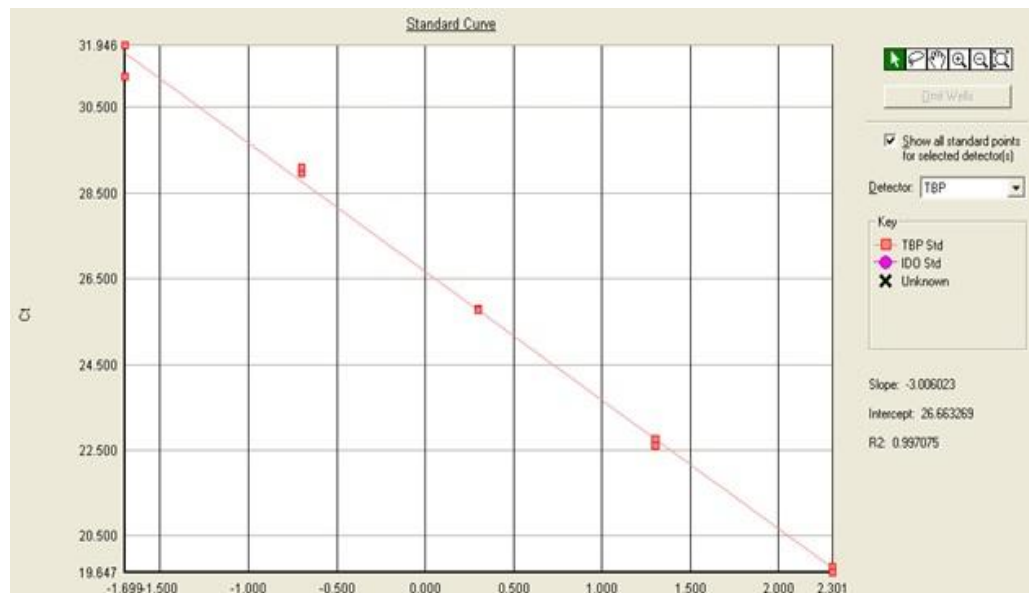


Figure 7. Sample standard curve plot generated for primer efficiency experiments. Transcription factor IID TATA-Box binding protein (TBP) primers were run using cDNA template from a 24 hour MuLV-infected BALB/c lymph node. The x-axis represents the log concentration of TBP for each serial dilution of the standard curve, while the y-axis represents the threshold Ct value for each sample. The equation of the standard curve is $y = -3.006023x + 26.663269$, and the R^2 value is 0.997075. From this equation, TBP primer efficiency is calculated to be 115% efficient (overefficient primers).

Quantitative PCR

After completing optimization of each primer set, experimental quantitative PCR (qPCR) was completed using the ABI 7300 Real Time PCR Machine. Plates were designed to quantify relative mRNA expression of both a housekeeping gene and one gene of interest using the relative standard curve method (see Data Analysis for further explanation). Plates were run on ABI's 'Absolute Quantification' plate setting to enable use of a standard curve. Both BALB/c and BL/6 in combination with both the housekeeping and gene of interest primers were run on the same plate, with each sample run in triplicate wells. Biological replicates were run on separate plates. All conditions for both strains were run on the same plate (naïve and MuLV-infected).

qPCR master mixes for each primer pair were made to reduce variation between individual reaction wells. Each reaction contained 12.5 μ L PerfeCTa SYBR Green Master Mix (Quanta Biosciences), 2.5 μ L of forward and reverse primers at an optimized concentration (1 μ M, 3 μ M, or 5 μ M), and 3.5 μ L of nuclease-free water to a total volume of 21 μ L. 4 μ L of the appropriate cDNA or No RT template was then added to each well and mixed thoroughly by pipetting up and down. Standard curves for each gene were run on each plate, using the same RNA sample for every plate within a group of experiments (#25 for IFN- α , #32 for IDO). The plate was sealed with plastic film and centrifuged at 1,200 g for 2 minutes at room temperature prior to placing it in the ABI Machine.

Quantitative PCR Data Analysis

Data generated from qPCR experiments was analyzed using relative quantification with a standard curve. While absolute quantification makes use of an external standard curve made from a single pure species such as plasmid DNA of the sequence of interest, standard curve relative quantification uses any cDNA sample expressing both a gene of interest and an endogenous control gene to create the standard curve. Use of a standard curve enables accurate measurement of reaction fluorescence and quantification of gene expression. After completing an experimental run, the selected endogenous gene is used to normalize expression values for a gene of interest. This is done by dividing the average gene of interest expression level by the average housekeeping gene expression level. A housekeeping (endogenous) gene is a gene expressed at similar levels in all mice and in all cell types. Normalization to an internal reference helps to minimize random fluctuation or background 'noise' in changing gene of interest expression levels.

The housekeeping gene TBP (Transcription factor IID TATA-Box binding protein) was used to normalize selected genes in these qPCR experiments. TBP has been shown to be stably expressed across a variety of tissues and cell types (Vandesompele *et al.*, 2002). Standard curves for both TBP and the gene of interest were run on each RT-PCR plate with serial dilutions of cDNA template. The standard curve template concentrations ranged from 0.02 ng/ μ L to 200 ng/ μ L. The same template (#25 for IFN- α , #32 for IDO) was used on all plates

within a set of experiments. mRNA expression associated with each template was quantified based on quantity values derived by ABI software from Ct values.

After normalizing the data with the housekeeping gene TBP, samples were calibrated against the template used to generate the standard curve. This calibration served to generate relative fold expression levels to allow for appropriate comparison within groups. mRNA expression values of each strain and condition were averaged with three biological replicates per condition. An ANOVA statistical analysis of variance on the SPSS statistical computer program was used to calculate p-values to determine statistical significance. Fold expression values were transformed using the natural log prior to conducting univariate ANOVA analysis, in order to meet the assumption of equal variances.

Preparation of ELISA Supernatants

ELISA supernatants were prepared using a protocol adapted by Oana Ursu from Borovikova *et al.* for rat liver homogenization (Borovikova *et al.*, 2000). Spleens and axillary, brachial, and inguinal lymph nodes were harvested from naïve and MuLV infected mice. Each spleen was cut into longitudinal halves. Immediately upon harvesting, organs were placed in a chilled lysis buffer and homogenized by polytron. Spleen halves were placed in 1 mL of lysis buffer, while lymph nodes were placed in 500 µL of lysis buffer. The lysis buffer was composed of 1x Protease Inhibitor Cocktail (BD BaculoGold, containing: 800 µg/mL benzamidine HCl, 500 µg/mL phenanthroline, 500 µg/mL aproptonin, 500

$\mu\text{g/mL}$ leupeptin A, and 50 mM PMSF), 0.5% Triton X-100, and sterile PBS at a pH of 7.2. Following polytron homogenization, samples were centrifuged at 12,000 g for 15 minutes at 4 °C. Supernatants were collected away from cell debris, aliquoted, and stored at -80 °C.

Bradford Assay to Determine Total Protein Concentration

Protein concentration in ELISA supernatants was measured using the Coomassie (Bradford) Protein Assay Kit. The kit uses a Coomassie-binding colorimetric method for protein concentration. Diluted albumin (BSA) standards were prepared as directed by the Pierce Company manual. Standards were then diluted 1:10 in sterile PBS, mixed thoroughly with Coomassie Reagent, and read on the Beckman DU Series 600 spectrophotometer at 595 nm to create a standard curve ranging from 12.5 $\mu\text{g/mL}$ to 75 $\mu\text{g/mL}$. After obtaining an accurate standard curve, lysed spleen and lymph node samples were diluted in Coomassie Reagent, mixed thoroughly by tapping, and their absorbance was measured at 595 nm. Dilutions ranged between 1:60 to 1:300 to give readings within the boundaries of the standard curve. Samples were incubated on the benchtop for a few minutes after adding Coomassie Reagent to ensure all protein was bound. Bradford reagent was kept on ice until absolutely necessary to improve consistency between 'blank' readings. Absorbance readings were used to find a total protein concentration that enabled more precise quantification of final IFN- α and IL-10 concentrations.

ELISA

The protein assay known as the sandwich ELISA was used to quantify the differential expression of IFN- α and IL-10 in MuLV-infected BALB/c and BL/6 mice. Sandwich ELISAs use a capture antibody bound to a microtiter plate to capture an antigen of interest. After capturing the antigen, a secondary enzyme-conjugated detection antibody is added that also binds to the antigen of interest. Upon addition of a chromogenic substrate, a color change will develop in wells containing the captured antigen that can be quantified using a spectrophotometer (Stranford Immunology class protocol). The sandwich ELISA procedure is outlined in Figure 8 shown below.

A BD OptEIA Set was used for IL-10 experiments following the BD protocol. A VeriKine Mouse Interferon Alpha ELISA Kit purchased from R & D System was utilized to study IFN- α expression following the recommended VeriKine protocol. Both ELISA kits were first tested using standard chemokine concentrations until good standard curves were obtained to ensure assay viability before testing samples. Protein concentrations obtained using the Bradford assay were used to estimate initial dilutions for sample supernatants. Dilutions of 1:10 (IL-10) and 1:2 (IFN- α) were ultimately found to produce detectable amounts of protein that fell within the standard curve of both assays. Samples for IFN- α were diluted in the Sample Buffer included in the IFN- α kit, while IL-10 samples were diluted within PBS with 10% fetal bovine serum (FBS).

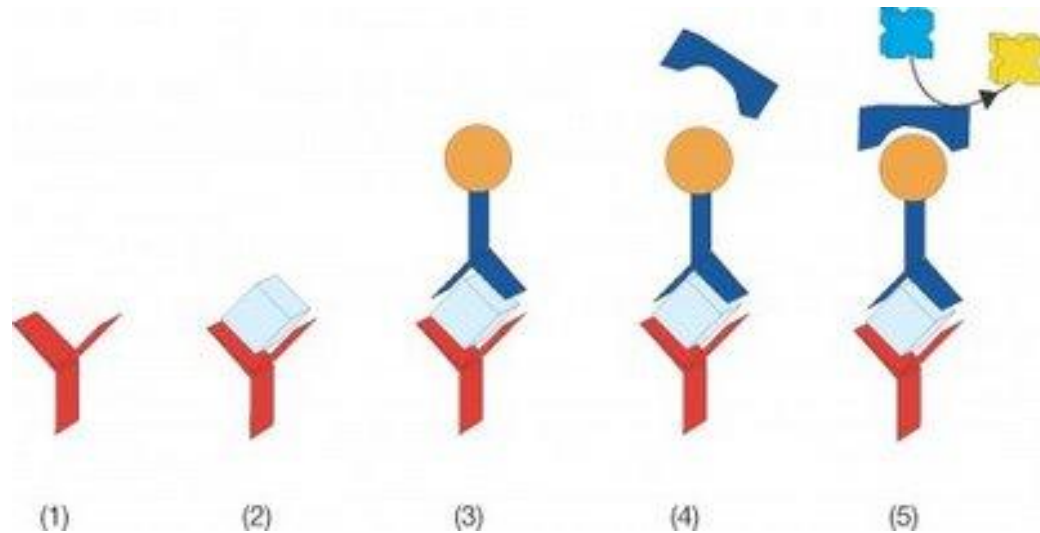


Figure 8. Sample sandwich ELISA procedure. (1) A microtiter plate is coated with capture antibody specific to the antigen of interest. (2) Samples to be tested are added to the plate, allowing the antigen of interest to bind to the capture antibody. (3) An enzyme-conjugated secondary antibody specific to another epitope on the antigen of interest is added and binds to captured antigen. (4) A chromogenic substrate such as 3,3', 5,5'-tetramethylbenzidine (TMB) is added to the plate. (5) The enzyme conjugated to the secondary antibody reacts with the chromogenic substance in a manner producing an observable color change in wells containing the bound antigen. Color change may then be quantified using a spectrophotometer. Photo courtesy of <veryviciousviruses.blogspot.com>).

IL-10 ELISA

An IL-10 ELISA kit (catalogue number #555252) was purchased from BD Biosciences and used in combination with BD Falcon ELISA plates (catalogue number #353279). Plates were coated with 100 μ L of capture antibody at a 1:250 dilution in coating buffer overnight at 4 $^{\circ}$ C. Coating buffer contained 12.49 g Na_2HPO_4 and 15.47 g NaH_2PO_4 per 1 L, with a pH of 6.5. Plates were then washed five times with wash buffer (sterile PBS with 0.05% Tween) and blocked with 200 μ L of PBS with 10% FBS for 3-4 hours at room temperature. Plates were again washed five times. Following washing, 100 μ L of sample or standard diluted at 1:5 and 1:10 in PBS with 10% FBS were added to the appropriate wells and incubated for two hours at room temperature. Standards were made in PBS with 10% FBS by creating seven 2-fold serial dilutions from the IL-10 standard provided, ranging from 31.25 to 1000 pg/mL. All standard and sample wells were tested in duplicate to control for well-to-well variation. Wells were washed five times after the samples' incubation period. Next, 100 μ L of Working Detector (Biotinylated Anti-mouse IL-10 detection antibody and streptavidin-horseradish peroxidase, both at 1:250 dilutions in Reagent Diluent) was added to wells and incubated for one hour at room temperature. Wells were then washed ten times with 30 second soaks. Following washing, 100 μ L of freshly prepared substrate solution (a 1:1 ratio of 3,3',5,5'-tetramethylbenzidine (TMB) and H_2O_2) was added to each well, and the plate was incubated for 30 minutes at room temperature in the dark. The reaction was then stopped by adding 50 μ L of stop solution (2 N

H₃PO₄). The plate was swirled gently to ensure complete mixing, and the plate was then read within 5 minutes on the ELISA Plate Reader (VersaMaxPLUS ROM) at 450 nm with a 570 nm correction.

IFN- α ELISA

A VeriKine Mouse Interferon Alpha ELISA KIT (catalogue number #42120-1) was purchased from R&D Systems in the form of a pre-coated microtiter plate. 100 μ L of samples and standards diluted in 1x of the included Sample Buffer (sample dilutions at 1:2) and 50 μ L of Antibody Solution were added to the plate and incubated sealed at room temperature with shaking for one hour. Standards were prepared by creating six 2-fold dilutions of the provided Mouse IFN- α standard in Sample Buffer, with concentrations ranging from 12.5 to 400 pg/mL. After one hour, the plate was incubated overnight at 4 °C without shaking. Next, the plate was washed 4 times with diluted Wash Solution provided with the kit. Following washing, 100 μ L of HRP Solution was added to each well and incubated sealed for 2 hours at room temperature with shaking. After two hours, the plate was again washed 4 times. 100 μ L of TMB Substrate Solution was added and the plate was incubated unsealed for 15 minutes in the dark. 100 μ L of the Stop Solution included in the kit was added, and the plate was swirled gently. The plate was then read within 5 minutes on the ELISA Plate Reader (VersaMaxPLUS ROM) at 450 nm with a 570 nm correction.

ELISA Data Analysis

Both IL-10 and IFN- α ELISA plates were read using the colorimetric ELISA Plate Reader (VersaMaxPLUS ROM) with SoftMax Pro Software at 450 nm with a 570 nm correction for any remaining blue color. Concentration values for unknown samples were generated from the standard curve. The final concentrations for IL-10 and IFN- α were computed using the following equation:

$$IL-10/IFN-\alpha \text{ Concentration (in pg/mg protein)} = OD \text{ reading} \times \text{dilution of the sample} / \text{total protein concentration}$$

Statistical significance was assessed using an ANOVA statistical analysis of variance to generate p-values between different strains and conditions, conducted using IBM's SPSS software. IL-10/IFN- α concentrations in pg/mg total protein were transformed using the natural log prior to conducting univariate ANOVA analysis, in order to meet the assumption of equal variances.

RESULTS

Interferon- β Expression by conventional PCR and qPCR

The overall goal of this group of experiments was to begin to find time points and organs in which detectable levels of Type I interferon mRNA such as IFN- β may be expressed. The level of IFN- β mRNA was analyzed in different organs at a variety of time points, using conventional PCR with ethidium bromide-stained agarose gel electrophoresis as well as by qPCR. A significant amount of time was initially devoted to finding an appropriate time point and organ for testing Type I interferon levels, based on conditions used in previously published literature. Conditions tested included:

Naïve BL/6 Thymus

8 hour MuLV-infected BALB/c Spleen

8 hour MuLV-infected BALB/c Liver

18 hour MuLV-infected BALB/c Spleen

24 hour MuLV-infected BALB/c Spleen (run with both IFN- β primer pairs)

3 day Mock-infected BL/6 Spleen

3 day MuLV-infected BALB/c Spleen

Following regular PCR, no bands were seen at the expected IFN- β band size for any conditions except for 8 hour and 18 hour MuLV-infected BALB/c Spleen.

This was initially thought to be the fault of the IFN- β primer pair that was designed, so another pair of primers was ordered as discussed in the methods section. IFN- β primer pair #2 did not amplify more IFN- β but exhibited slightly fewer primer-dimers than IFN- β primer pair #1, so pair #2 was used for all later

experiments. In the 8 hour and 18 hour MuLV-infected BALB/c Spleen conditions, an extremely faint band appeared at the correct band size in the IFN- β cDNA lanes. To test if this was a mere shadow or contamination within the gel, these gels were run again using an increased amount of cDNA template (10 μ L instead of 1 μ L, with the appropriate amount of water removed from the reaction). The same band appeared, only slightly stronger. This indicates that the primers indeed worked and IFN- β is present, albeit at extremely low levels. Please refer to Figure 9 for a representative gel photograph showing the extremely low level of IFN- β expression seen by conventional PCR.

Because conventional PCR is less sensitive and less quantitative than qPCR, a trial qPCR experiment was completed to see if IFN- β was more easily detectable using this assay. cDNA made from 18 hour-infected MuLV BALB/c spleen (one of the few time points and conditions where IFN- β was seen using conventional PCR) was used along with a 'No Reverse Transcriptase' (No RT) template control made from the same animal in qPCR reactions with TBP and IFN- β primers. The experiment was used to answer two questions – if the chosen cDNA contained enough IFN- β mRNA to generate a measurable level of fluorescence, and if these fluorescent levels were above the 'background IFN- β signal' seen in No RT samples. Ct values that described when the level of fluorescence crossed a set threshold were used to roughly compare the amount of TBP and IFN- β . TBP cDNA was found to cross the fluorescence threshold after

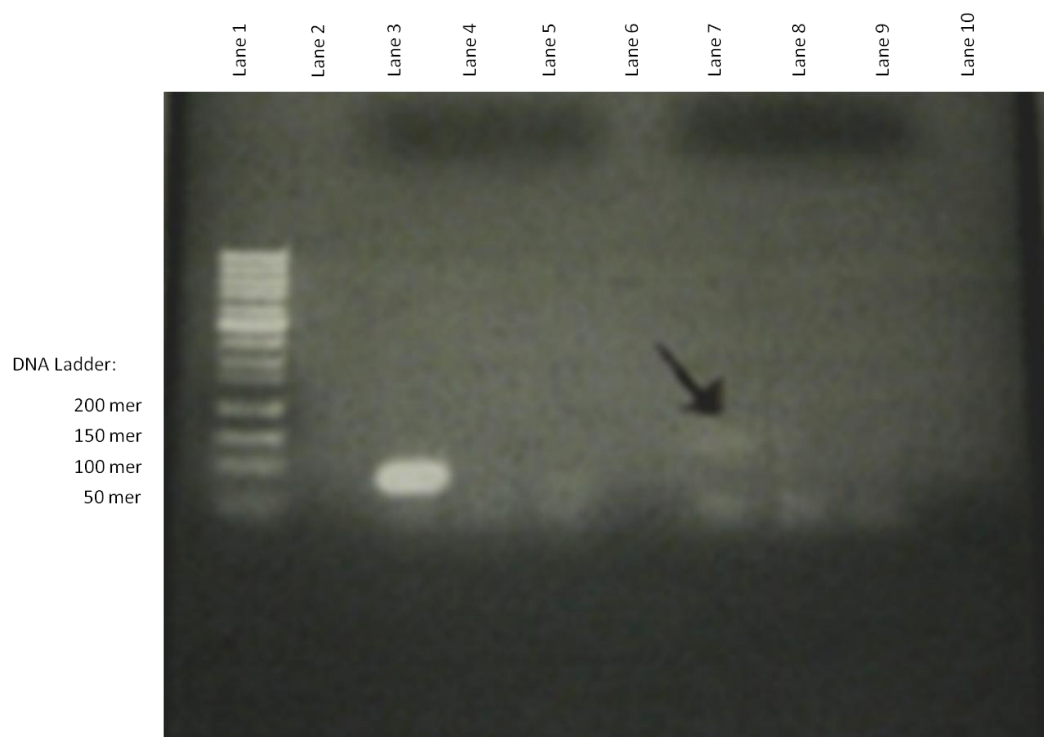


Figure 9. Ethidium bromide-stained agarose gel of conventional PCR products generated using IFN- β primers and 8 hour post-MuLV-infection BALB/c Spleen cDNA template. The TBP housekeeping gene amplified normally (Lane 3). A very faint band can be seen in the IFN- β cDNA lane correlating with low levels of IFN- β expression, as demarcated by the arrow (Lane 7). The size of the TBP band is 88 mer, while the size of the IFN- β band is 125 mer. Lane 1:50 mer ladder. Lane 2: X. Lane 3:TBP cDNA. Lane 4: TBP No RT. Lane 5: TBP No RNA. Lane 6: X. Lane 7: IFN- β cDNA. Lane 8: IFN- β No RT. Lane 9: IFN- β No RNA. Lane 10: X.

22.2 cycles, while TBP No RT template crossed the fluorescence threshold after 31.4 cycles. This large difference in timing of fluorescence detection indicates that, as expected, significant TBP mRNA is present in the cDNA template that generates fluorescence well above a background signal seen in the No RT wells. This indicated a successful experiment and lack of reagent contamination. However, IFN- β cDNA crossed the threshold only after 34.6511 cycles, while IFN- β No RT template never generated a detectable level of fluorescence. A plot of fluorescence level versus cycle number for this experiment may be seen in Figure 10.

IFN- β cDNA template can generate a detectable level of fluorescence and IFN- β No RT template cannot, indicating that the fluorescence seen is indicative of actual IFN- β mRNA signal. However, the extremely high cycle number at which it becomes detectable suggests a very limited presence of IFN- β mRNA. It was thought that such low IFN- β amplification could not be sufficiently improved by further primer optimization to later generate reliable standard curves and comparable quantitative fluorescence levels. Since both conventional PCR and qPCR indicated very limited quantities of IFN- β mRNA, future work with IFN- β using RT-PCR was discarded in favor of testing other Type I interferons with potentially higher levels of expression.

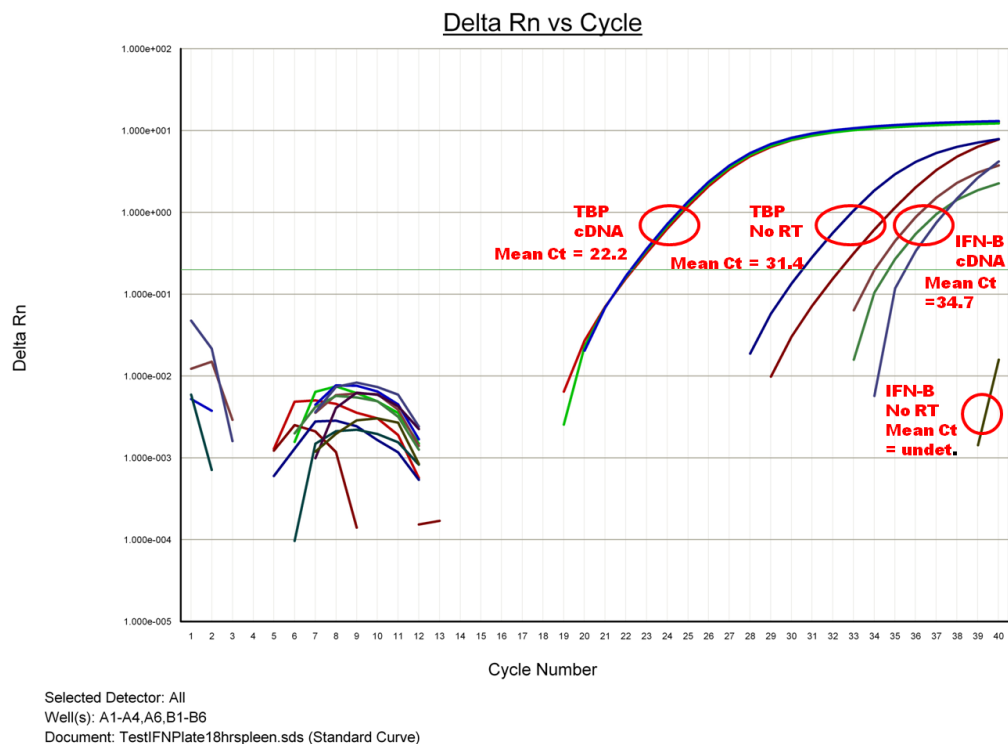


Figure 10. Amplification plot of cycle number versus Delta Rn (level of fluorescence) for trial qPCR experiment for IFN- β as compared to the housekeeping gene TBP. 18 hour MuLV-infected BALB/c spleen cDNA and No RT templates were used. Reactions were run in triplicate; one outlier well from the TBP No RT samples was discarded prior to averaging cycle numbers. On average, fluorescence in the TBP cDNA template crossed the threshold after 22.2138 cycles, while TBP No RT template fluorescence became detectable after 31.3514 cycles. Fluorescence with the IFN- β cDNA template crossed the threshold only after 34.6511 cycles. Fluorescence with the IFN- β No RT template never crossed the set threshold.

Interferon- α Expression by qPCR

The overall goal for this group of experiments was to continue Dr. Bakkour's work analyzing IFN- α mRNA expression in the spleens of naïve and MuLV-infected mice, with the hope that qPCR expression of IFN- α proved easier to detect than expression of IFN- β , both Type I interferons. Primers for IFN- α were designed, tested by conventional PCR, and optimized for concentration by Dr. Bakkour. Dr. Bakkour determined the primers were most effective at a 500 nM F: 500 nM R concentration. The first experiment completed by this researcher analyzed primer efficiency. The slopes from the standard curves in the efficiency experiment were used to calculate primer efficiencies as shown below:

$$\begin{aligned} \text{IFN-}\alpha \text{ primer efficiency} &= 10^{(-1/-3.7392)} - 1 \\ &= 1.8511 - 1 \\ &= 0.85 = 85\% \text{ efficient} \end{aligned}$$

$$\begin{aligned} \text{TBP primer efficiency} &= 10^{(-1/-3.3915)} - 1 \\ &= 1.9718 - 1 \\ &= 0.97 = 97\% \text{ efficient} \end{aligned}$$

The IFN- α primers were determined to be 85% efficient, or slightly under-efficient. Because the efficiency value did not fall between 90-110% and the housekeeping gene primer efficiency was more than 5% different (TBP primers gave an efficiency of 97%), the ddCt method of analysis could not be used for qPCR data. Accordingly, a standard curve was run on every experimental plate. Please refer to Figure 11 for a plot showing the standard curves (cDNA range tested = 0.02 ng to 200 ng) and amplification efficiencies for IFN- α as compared to TBP primers.

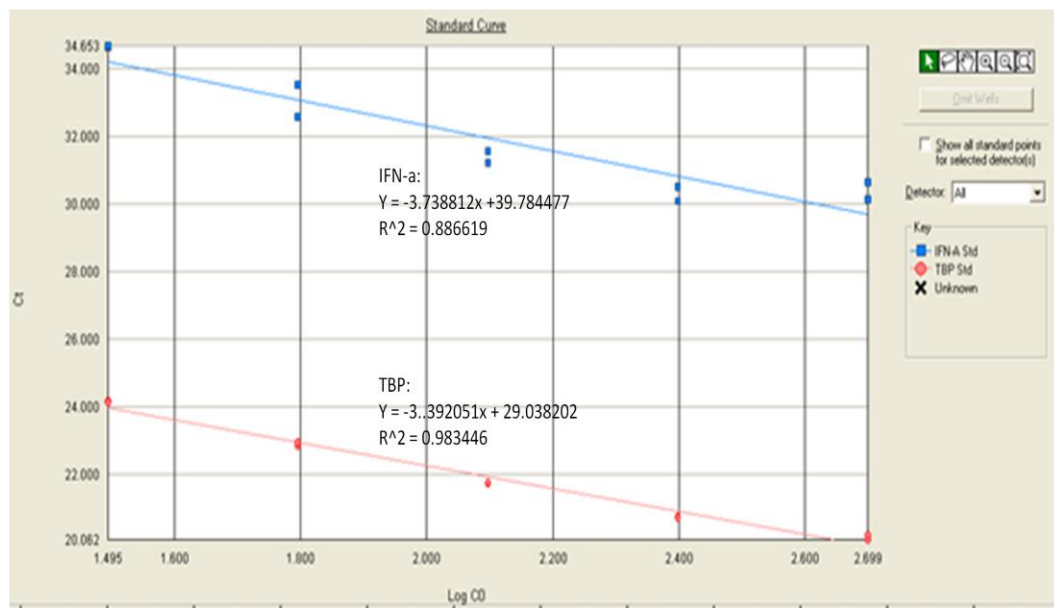


Figure 11. Efficiency experiment showing the standard curves and amplification efficiencies calculated for TBP and IFN- α primers. The values of the template concentration are labeled on the x-axis and the Ct values for each data point are listed on the y-axis. Animal samples used in the primer efficiency experiment were BALB spleens, 24 hours post-MuLV infection. The exponential amplification values for TBP and IFN- α were 1.9718 and 1.8511, respectively. This suggests TBP and IFN- α primers were 97% and 85% efficient, respectively.

Following primer efficiency testing, experiments were completed analyzing IFN- α mRNA expression at two time points post-infection in the spleens of BALB/c and BL/6 mice. As Type I interferons are part of the innate immune response, an early time point (24 hours) was compared to a later time point (7 days) to assess strain-specific differences in expression. Three animals were analyzed per condition. Ct values for No RT controls served as endpoint values for 'real' amplification. Due to the low levels of IFN- α seen using PCR, 200 ng of cDNA template was added per well instead of the lab standard of 50 ng. Even with the extra initial cDNA, low levels of IFN- α were seen, often not crossing the threshold of detectable fluorescence until 29-30 cycles (considered a high Ct value). This indicates very low levels of IFN- α mRNA expression in the spleen at the time points tested.

Based on qPCR data, the average normalized IFN- α expression in the spleens of BALB/c and BL/6 mice is shown using a bar graph (refer to Figure 12); normalized IFN- α expression values for individual animals are shown in Table 1. Large levels of animal-to-animal variation existed within each condition, generating considerable standard deviation values that called into question the importance of the small strain-specific differences seen. One animal in each of the 24 hour BL/6, 7 day BALB/c, and 7 day BL/6 MuLV-infected triplicates expressed approximately twice as much IFN- α as the other two animals in the group. No further experiments were pursued after testing three animals per strain at the 24 hour and 7 day time points due to this sizeable amount of animal-to-

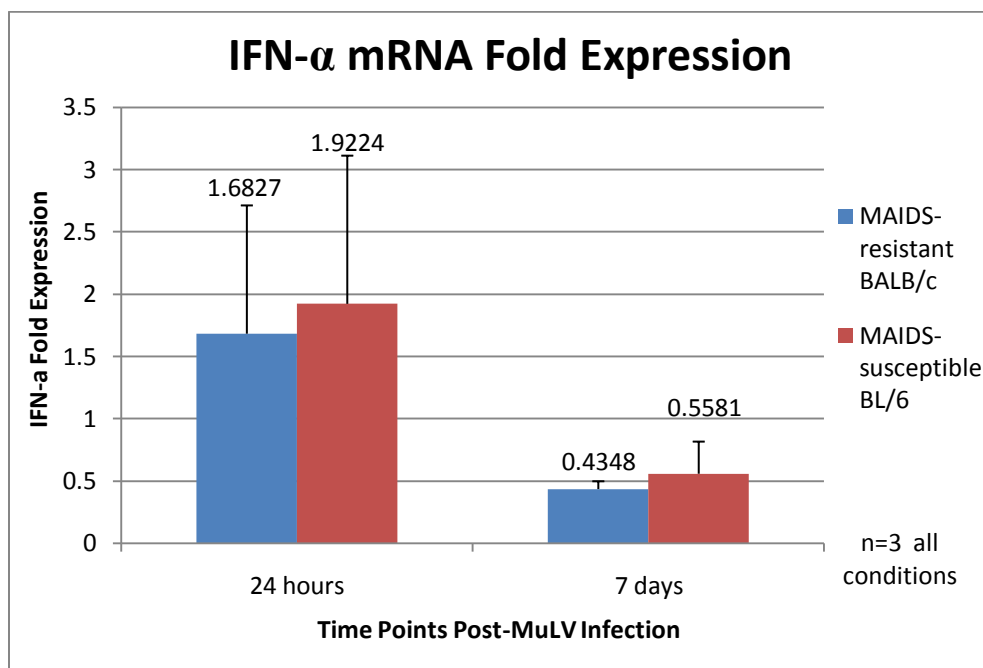


Figure 12. IFN- α mRNA fold expression does not differ significantly between MuLV-infected BALB/c and BL/6 mice. The x-axis shows the condition of the animals; the y-axis shows IFN- α fold expression normalized by TBP and calibrated against the one of the 24 hour post-MuLV infection BALB/c animals (#25, used to create the standard curve). Three animals compose each averaged group (n=3). The standard deviation within each group is indicated by the error bars; significantly larger standard deviations are seen at the 24 hour time point where more IFN- α is also expressed by both strains. P-values were calculated by univariate ANOVA following transformation of the data to natural logs. There is no significant difference in IFN- α mRNA expression between strain ($p = 0.563$) but a highly significant difference is seen across time in both strains ($p = 0.002$).

Table 1. IFN- α mRNA fold expression varies widely within conditions between individual MuLV-infected mice 24 hours and 7 days post-infection. IFN- α expression values found using qPCR were first normalized by dividing these values by the TBP expression value for the same animal. Then, these values were calibrated against the template used to create all standard curves (24 hour post-MuLV infection BALB/c spleen) to give the IFN- α mRNA fold expression values shown below.

IFN-α Fold Expression		
Infection Time Point	BALB/c (Resistant)	BL/6 (Susceptible)
24 hour – #1	1	1.134079245
#2	2.873053168	3.293227
#3	1.175015252	1.340067
<i>Average \pm std. dev</i>	1.683 \pm 1.035	1.922 \pm 1.192
7 day – #1	0.466085351	0.85351295
#2	0.362587404	0.378021
#3	0.475650514	0.442875
<i>Average \pm std. dev</i>	0.4348 \pm 0.0627	0.5581 \pm 0.2579

-animal variability and relatively modest differences observed between strains.

Data was analyzed using a univariate ANOVA test to assess the significance of differences in IFN- α expression between strains and over time. IFN- α mRNA fold expression values were transformed using the natural log prior to conducting univariate ANOVA analysis, in order to meet the assumption of equal variances. No significant difference was found in IFN- α expression between BALB/c and BL/6 mice ($p = 0.563$). As might be expected for a molecule related to innate immunity, a highly significant difference in IFN- α expression exists between 24 hours and 7 days post-infection ($p = 0.002$), with far more IFN- α expressed at 24 hours than at 7 days.

Interferon- α Expression by ELISA

As mRNA expression is not always indicative of the amount of protein present, IFN- α ELISA experiments were conducted to compare protein expression in the spleens of naïve and MuLV-infected BALB/c and BL/6 mice following completion of IFN- α qPCR experiments. MuLV-infected mice were assessed at 24 hours, 3 days, and 7 days post-infection. A working standard curve was obtained prior to examining any unknown samples to ensure that the assay system was working; this test standard curve can be seen in Figure 13. Next, dilutions of spleen lysates from three animals per strain and condition were examined on an ELISA plate pre-coated with capture antibody. OD readings of unknowns, in combination with the standard curve obtained on the same plate, were used to generate a value for pg IFN- α /mL expression for each individual. This value was then multiplied by two to account for the 1:2 dilution used. Finally, individual values for pg IFN- α /mL expression were divided by the individual lysates' total protein concentration in mg protein/mL. This resulted in a value for pg IFN- α /mg of total protein tested for each animal. Individual values may be seen in Table 2. Average expression values per group may be seen in Figure 14, while a plot showing a time course of expression for each strain can be seen in Figure 15.

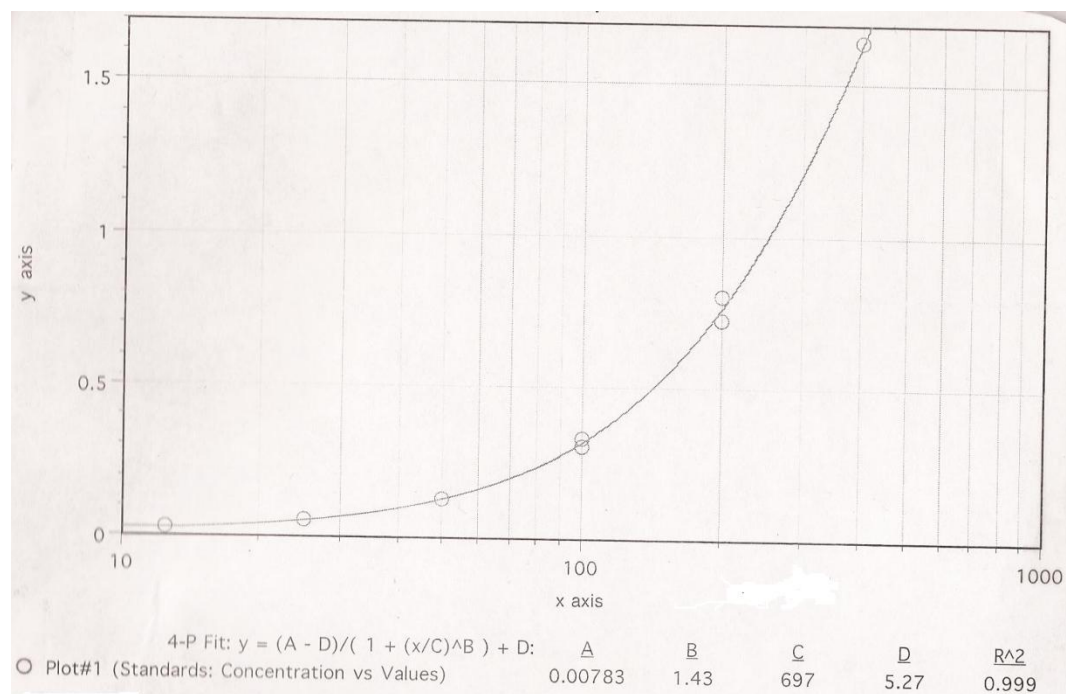


Figure 13. Test standard curve for IFN- α ELISA plate. Shown on the x-axis is concentration of IFN- α (in pg IFN- α /mL); shown on the y-axis is the optical density (OD) reading. Six 2-fold serial dilutions were made from a concentrated IFN- α standard diluted in sample buffer, beginning with a concentration of 1000 pg/mL. Each standard concentration was tested in duplicate wells. The curve generated was fitted with a four-parameter line of best fit as suggested by the kit protocol. The standard curve equation was determined to be $y = (0.00783 - 5.27)/(1 + (x/697)^{1.43}) + 5.27$, with an r^2 value of 0.999.

Table 2. IFN- α Protein Expression (pg/mg of protein) in the spleens of individual naïve and MuLV-infected mice. IFN- α protein values in pg/mL found using ELISA were divided by the total protein concentration for each homogenate in mg/mL determined by Bradford assay to give the value shown below in pg IFN- α /mg total protein tested.

IFN-α Protein Expression (pg/mg protein)				
	Time Point Post-Infection			
	Naïve (Uninfected)	24 hour	3 day	7 day
BALB/c (Resistant)				
#1	1.1895	2.0106	0.6409	0.8029
#2	2.8996	4.5471	---	2.1378
#3	2.3968	2.2943	1.6221	0.7966
<i>Average \pm std. dev.</i>	2.1620 \pm 0.8789	2.9507 \pm 1.3898	1.1315 \pm 0.6938	1.2458 \pm 0.7726
BL/6 (Susceptible)				
#1	2.3052	1.7366	2.4802	2.0627
#2	3.0024	2.1488	2.1117	2.8492
#3	2.5676	1.6539	1.8574	1.5826
<i>Average \pm std. dev.</i>	2.6251 \pm 0.3522	1.8464 \pm 0.2651	2.1498 \pm 0.3131	1.8315 \pm 0.2406

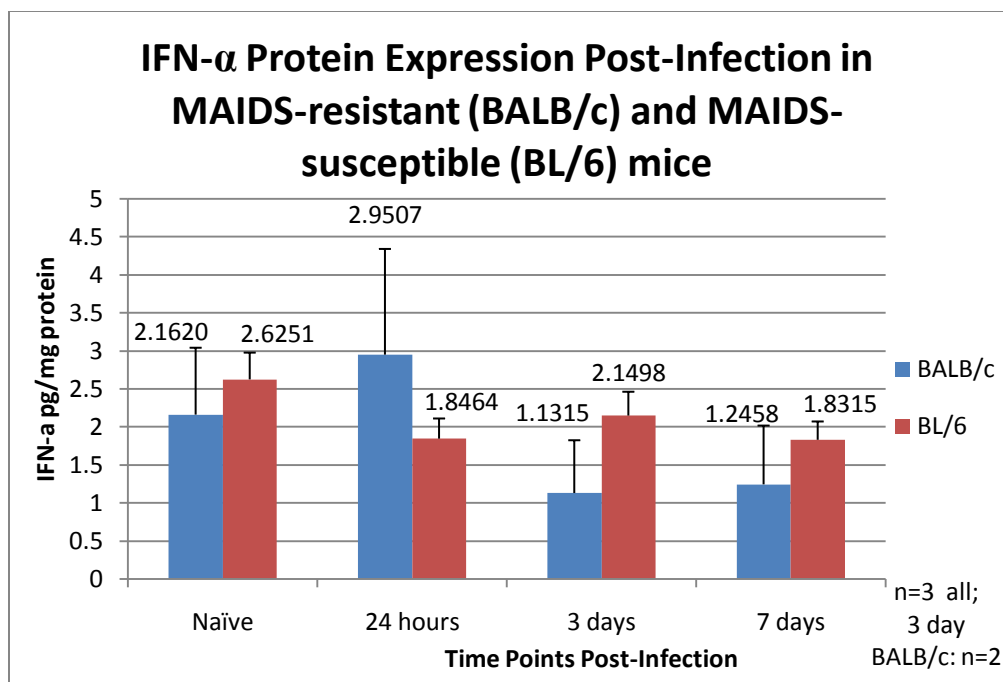


Figure 14. IFN- α protein expression does not differ between strains in naïve and MuLV-infected BALB/c and BL/6 mice at three time points post-infection. The x-axis shows the condition of the animals; the y-axis shows the average IFN- α protein expression in pg/mg protein tested. Three animals compose each averaged group (n=3), except for the 3 day BALB/c group where n=2 (one major outlier was discarded). The standard deviation within each group is indicated by the error bars. In general, very low levels of IFN- α expression are seen, with no individual animal expressing more than 4.5 pg IFN- α /mg total protein. Data was transformed via natural log transformation prior to statistical analysis by ANOVA test. No significant difference was found between strains ($p = 0.103$) or across time ($p = 0.072$).

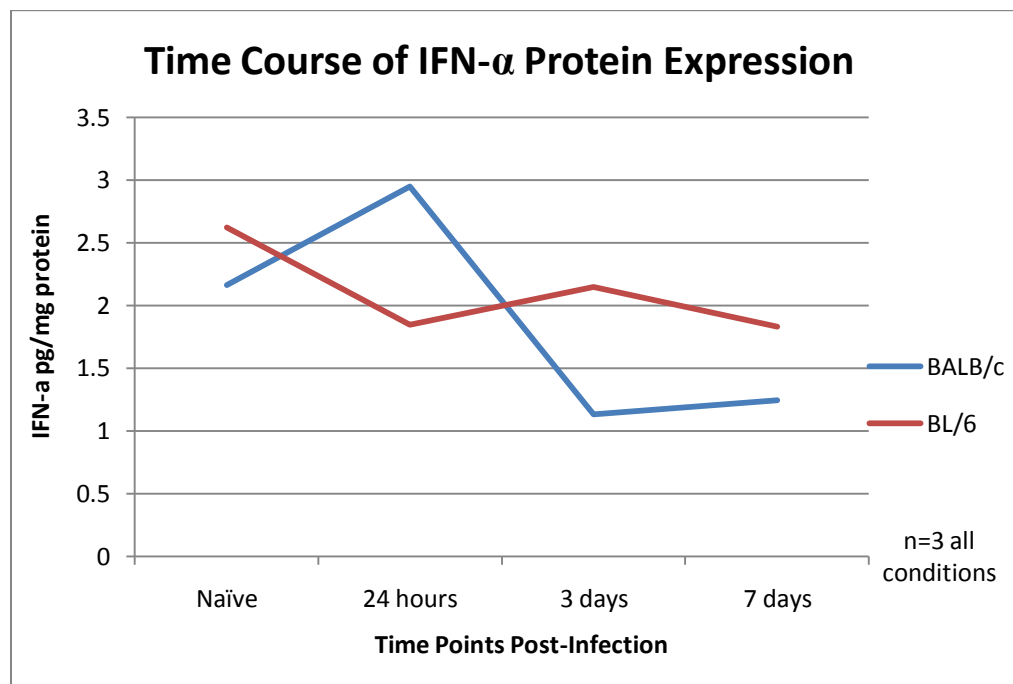


Figure 15. Time course showing IFN- α protein expression in the spleens of naïve and MuLV-infected BALB/c and BL/6 mice. Naïve and 24 hour post-infection BALB/c mice express slightly more IFN- α than do their BL/6 cohorts. The trend reverses at the later 3 day and 7 day time points where BL/6 mice express slightly more IFN- α . Naïve (uninfected) mice express a relatively high level of IFN- α , a cytokine usually induced in the early hours of an innate immune response. BALB/c mice express more IFN- α at 24 hours than at 7 days, a trend matching the results from qPCR. Very little IFN- α is seen at any time point or condition, with a maximum average of IFN- α protein expression of 2.95 pg IFN- α /mg total protein.

Several notable observations may be made from the IFN- α ELISA results. Very low levels of IFN- α protein were seen in all samples, with the highest individual measurement of IFN- α expression hovering near 4.55 pg IFN- α / mg total protein in MAIDS-resistant (BALB/c) mice at 24 hours post-MuLV infection. This approached the bottom limit of the standard curve, with some samples requiring extrapolation of the standard curve to attain concentration readings. These results match those of previous qPCR experiments, where very little IFN- α / β mRNA could be detected. Naïve mice express relatively similar levels of IFN- α when compared to animals actually mounting an immune response to MuLV— one expects physiologically relevant IFN- α expression only after an innate immune response has been induced. BALB/c mice seem to experience a small spike in IFN- α protein expression at 24 hours post-infection (p.i.), a result supported by the qPCR data, where the highest level of IFN- α mRNA expression was also seen in the spleens of BALB/c mice 24 hours p.i. BL/6 mice express a relatively consistent level of IFN- α , with naïve mice oddly expressing slightly more IFN- α than any post-infection time points.

IFN- α ELISA data was analyzed for statistical significance using a univariate ANOVA test, following transformation of the data via natural log in order to meet the assumption of equal variances. No significant difference in IFN- α protein expression was found between BALB/c and BL/6 ($p = 0.103$) or across time points ($p = 0.072$).

IDO Expression by Conventional PCR and qPCR

The overall goal of this group of experiments was to determine the relative levels of IDO expression in the lymph nodes of naïve and MuLV-infected BALB/c and BL/6 mice at several time points post-infection. The first step following primer design was testing general primer efficacy using regular PCR to ensure that the primers amplified the correct target without amplifying genomic DNA or forming excessive primer-dimers. Conventional PCR products were analyzed using agarose gel electrophoresis (Figure 16). Both primer pairs amplified the correct product size (IDO primer pair #1 – 120 mer, IDO primer pair #2 – 150 mer) with no additional bands to indicate genomic DNA or primer-dimer amplification. IDO primer pair #2 generated a slightly stronger band, suggesting better amplification of the desired target.

Following determination of general primer efficacy using conventional PCR experiments, qPCR experiments were initiated to optimize the working primer concentrations for both IDO primer pairs. Both cycle threshold (Ct) values and dissociation curves were compared for varying concentrations (100 nM, 300 nM, and 500 nM) of forward and reverse primer to find a combination that yielded a low Ct value as well as a defined singular peak in the dissociation curve. Satisfying the requirement for low Ct value amplification indicates high sensitivity for mRNA quantification, while a single dissociation peak indicates no primer-dimer or nonspecific amplification.

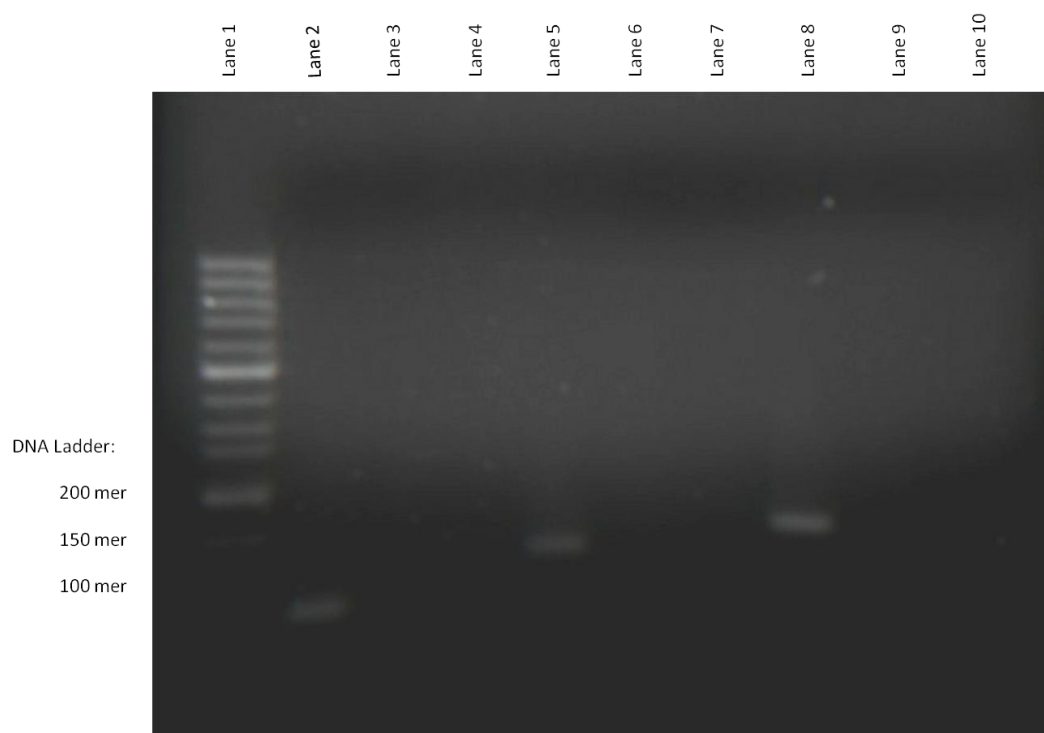


Figure 16. Ethidium bromide-stained agarose gel of PCR products generated using IDO primers and 24 hour post-MuLV infection BALB/c lymph node cDNA template. The TBP housekeeping gene amplified normally (lane 2 = 88 mer). Distinct bands can be seen in both the IDO Primers #1 and IDO Primers #2 cDNA lane correlating with detectable levels of IDO expression (lanes 5 and 8). The size of the IDO #1 band is 120 mer, and the size of the IDO #2 band is 150 mer. Lane 1: 50 mer ladder. Lane 2: TBP cDNA. Lane 3: TBP No RT. Lane 4: TBP No RNA. Lane 5: IDO #1 cDNA. Lane 6: IDO #1 No RT. Lane 7: IDO #1 No RNA. Lane 8: IDO #2 cDNA. Lane 9: IDO #2 No RT. Lane 10: IDO #2 No RNA.

The primer optimization experiment for the second IDO primer pair – which showed a stronger band of amplification when the conventional PCR products were analyzed by gel electrophoresis – yielded a melting curve with two distinct peaks at all primer pair concentrations, indicating nonspecific amplification. This primer pair may amplify several isoforms of IDO mRNA that differ only by a few base pairs, resulting in a slightly different melting temperature but appearing as one ‘stronger’ band when analyzed by gel electrophoresis. In contrast, the first IDO primer pair showed a distinct single peak, with no primer-dimer peaks appearing in the No RT sample, even at the highest primer concentrations. Dissociation curves for the IDO primer pair #1 can be seen in Figure 17. As the most concentrated primer pair (500 nM F: 500 nM R) amplified at the lowest Ct value without generating primer-dimer in the dissociation curve, all subsequent IDO experimental work was completed with IDO primer pair #1 at these concentrations.

Next, primer efficiency for IDO primer pair #1 was compared to the efficiency of the TBP housekeeping gene primers to be used for normalization in later experimental work. Efficiencies were determined by preparing a standard curve of 10-fold serial dilutions (range: 0.02 ng to 200 ng) and testing using the standard curve absolute quantification setting on the qPCR machine. Reaction efficiencies between 90-110% and within 5% of each other allow one to use the ddCt method of quantification, avoiding the need for a standard curve on every experimental plate.

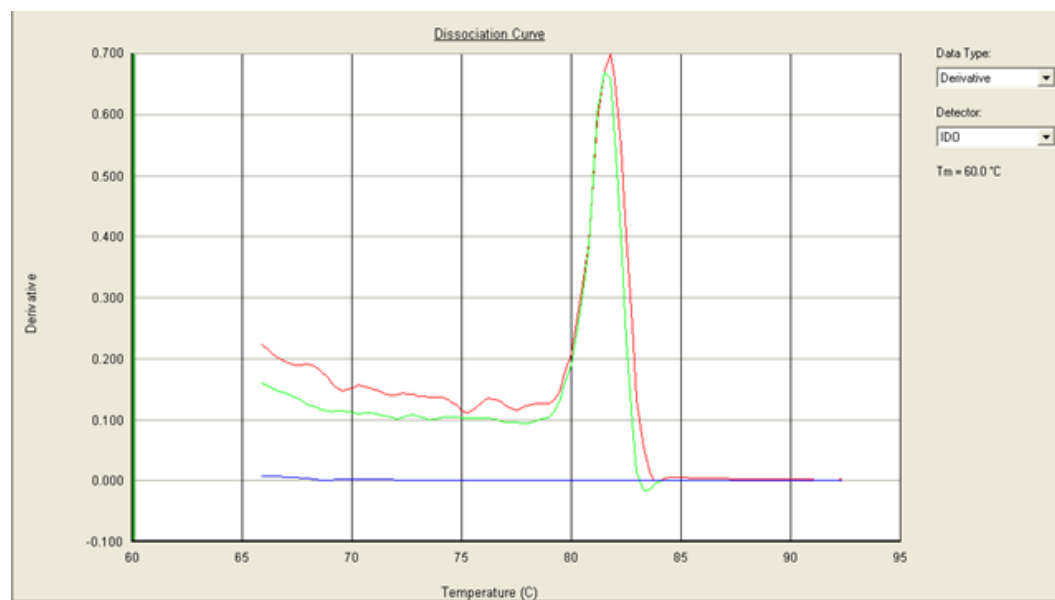


Figure 17. Dissociation curves of IDO Primer Pair #1 at concentrations of 500 nM forward primer: 500 nM reverse primer. The red and green lines represent wells containing cDNA from a BALB/c mouse lymph node 24 hours post-infection; the blue line at the bottom represents a well containing a No RT control. The singular peaks seen in the cDNA samples indicate no primer-dimer formation or nonspecific amplification. The flat dissociation curve from the No RT sample indicates no primer-dimer formation in the absence of template, even in the most concentrated primer pair tested (500 nM F: 500 nM R). The Ct value associated with this primer pair was 28.5 cycles.

Using cDNA made from BALB/c mouse lymph node 24 hours post MuLV-infection, TBP and IDO primer pair #1 efficiencies were determined to be incompatible for use with the ddCt method. Primer efficiencies are calculated from the slope of the standard curves obtained as shown below:

$$\begin{aligned} \text{IDO primer efficiency} &= 10^{(-1/-2.9192)} - 1 \\ &= 2.2007 - 1 \\ &= 1.20 = 120\% \text{ efficient} \end{aligned}$$

$$\begin{aligned} \text{TBP primer efficiency} &= 10^{(-1/-3.0060)} - 1 \\ &= 2.1511 - 1 \\ &= 1.15 = 115\% \text{ efficient} \end{aligned}$$

IDO primer efficiency was calculated to be 120% (overefficient primers), while TBP primer efficiency was determined to be 115% (also overefficient). While the primers are indeed within 5% of each other, both exceed the 90-110% range recommended for ddCt quantification. Accordingly, all future experimental IDO quantification was completed using a standard curve on every plate. Please refer to Figure 18 for a plot of IDO and TBP reaction efficiencies.

Following IDO primer efficiency testing, qPCR experiments analyzing IDO expression in the lymph nodes of naïve and MuLV-infected BALB/c and C57BL/6 mice were completed. Values obtained for IDO were normalized against values obtained for the TBP housekeeping gene; these normalized values were then calibrated against the sample used to create the standard curves on all IDO plates (24 hours post-MuLV infection BALB/c lymph node). Time points examined in MuLV-infected mice included 24 hours, 3 days, and 7 days post-infection. Five animals were analyzed per condition.

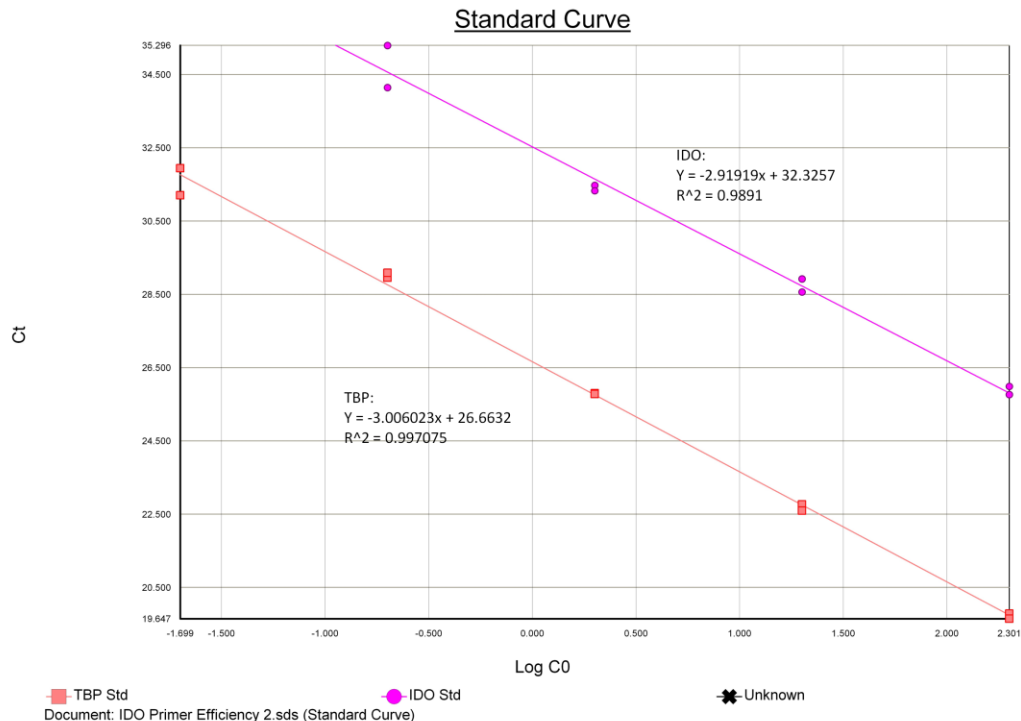


Figure 18. Efficiency experiment showing the standard curves and amplification efficiencies calculated for TBP and IDO primers. The values of the template concentration are labeled on the x-axis and the Ct values for each data point are listed on the y-axis. Animal samples used in the primer efficiency experiment were BALB/c lymph nodes, 24 hours post-MuLV infection. The exponential amplification values for TBP and IDO were 2.1511 and 2.2007 respectively. This suggests TBP and IDO primers were 120% and 115% efficient, respectively. These values were incompatible with future ddCt quantification, requiring the use of standard curves on every experimental plate.

Ct values for No RT controls served as endpoints values for ‘real’ amplification. IDO mRNA fold expression values for individual animals are shown in Table 3. The average IDO mRNA fold expression values in the lymph nodes of BALB/c and C57BL/6 mice are shown using a bar graph (refer to Figure 19); a time course showing IDO mRNA fold expression for each strain may be seen in Figure 20.

IDO mRNA fold expression values were transformed using the natural log prior to conducting univariate ANOVA analysis, in order to meet the assumption of equal variances. Differential IDO mRNA expression between BALB/c and BL/6 mice was shown to be highly significant across all time points ($p < 0.001$). BL/6 mice expressed more IDO mRNA at every time point tested. IDO mRNA expression also significantly differed across time for both strains ($p = 0.006$). BALB/c and BL/6 mice showed slightly different expression patterns for IDO. Both strains experienced a decrease in IDO expression between control conditions (uninfected mice) and mice sacrificed 24 hours post infection; however, BL/6 mice had more than recovered this decrease by 3 days while BALB/c expression continued to decline. Both BALB/c and BL/6 mice expressed more IDO at 7 days post-infection than in naïve mice.

Table 3. IDO mRNA fold expression by qPCR in the lymph nodes of individual naïve and MuLV-infected mice, 24 hours, 3 days, and 7 days post-infection. IDO expression values found using qPCR were normalized by dividing IDO values by TBP expression values for the same animal. Next, normalized values were calibrated against the sample used in the standard curves run on all IDO plates (24 hours post-MuLV infection BALB/c lymph node).

IDO mRNA Fold Expression				
	Time Points Post-MuLV Infection			
	Naïve (Uninfected)	24 hour	3 day	7 day
BALB/c (Resistant) #1	1.0181	1.0000	0.8236	1.4223
#2	2.1437	1.5336	1.0144	4.2790
#3	1.8039	1.6674	0.9282	3.0277
#4	1.2761	1.2320	1.2787	1.4137
#5	0.9646	1.1915	0.9504	1.9129
<i>Avg ± std. dev.</i>	1.4413 ± 0.5144	1.3249 ± 0.2706	0.9991 ± 0.1707	2.4111 ± 1.2339
BL/6 (Susceptible) #1	1.6400	2.0462	1.7436	2.0910
#2	3.3828	2.3774	2.6435	3.5676
#3	2.2025	2.4342	4.0005	6.0412
#4	2.1204	1.4199	1.3317	2.4910
#5	2.3473	1.6092	1.7265	1.9155
<i>Avg ± std. dev.</i>	2.3386 ± 0.6412	1.9774 ± 0.4527	2.2892 ± 1.0706	3.2213 ± 1.7021

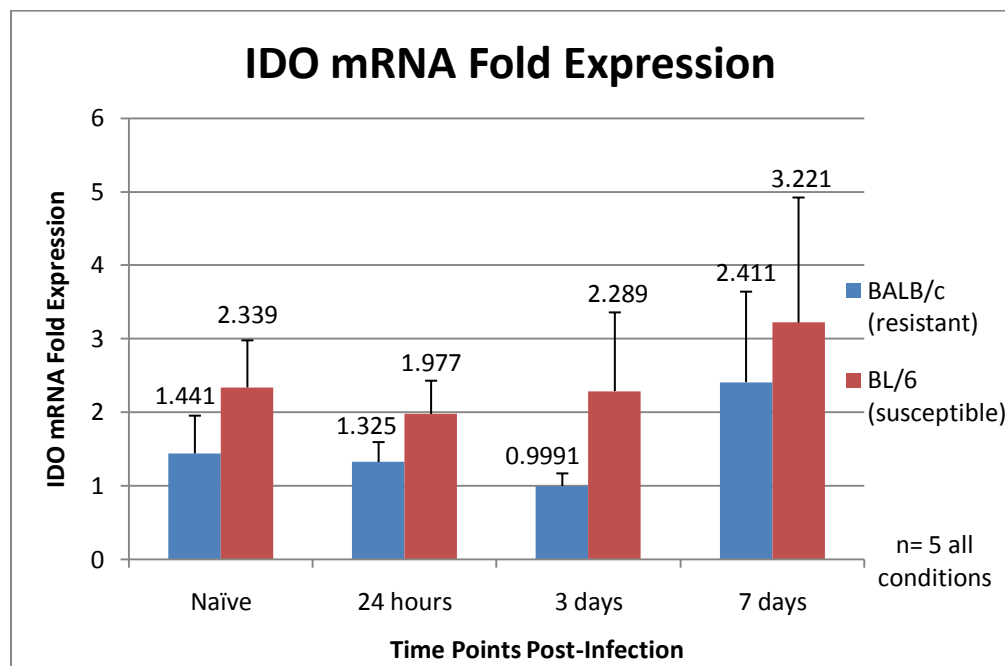


Figure 19. IDO mRNA expression differs significantly between strains in the lymph nodes of naïve and MuLV-infected BALB/c and BL/6 mice. The x-axis shows the condition of the animals; the y-axis shows the relative IDO expression normalized by TBP and calibrated against the sample used for the standard curve of IDO plates (24 hour MuLV-infected BALB/c lymph nodes). Five animals compose each averaged group (n=5). The standard deviation within each group is indicated by the error bars; larger standard deviations are seen in conditions with larger expression values. More IDO is expressed by BL/6 strains at all time points. Based on p-values calculated by ANOVA, there is a significant difference in IDO expression in both strains across time ($p = 0.006$) and a highly significant difference between strains ($p < 0.001$).

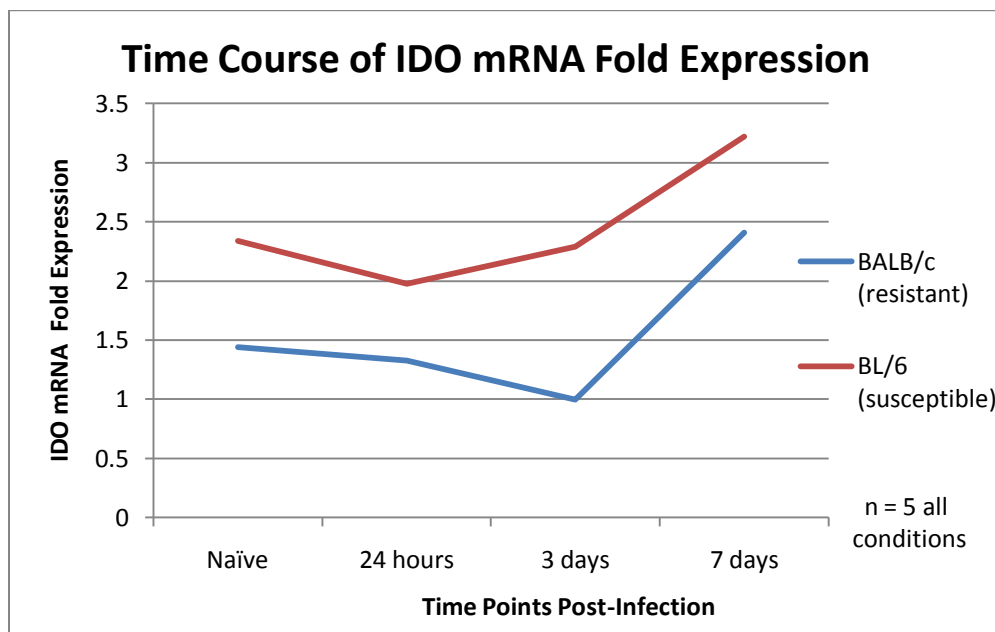


Figure 20. IDO mRNA fold expression changes significantly across time in naïve and MuLV-infected BALB/c and BL/6 mice.

BL/6 mice express more IDO mRNA at all time points than do BALB/c mice ($p < 0.001$). BL/6 and BALB/c mice express IDO mRNA in slightly different patterns. BL/6 mice show a slight decrease in IDO expression between naïve mice and 24 hours, followed by recovery and then upregulation at 3 days and 7 days. BALB/c mice show a very slight decrease in IDO expression from naïve mice to 24 hours post-infection, followed by a further drop in expression at 3 days. Recovery and IDO upregulation is again seen in BALB/c mice by 7 days. IDO mRNA expression in both strains is significantly affected by time post-infection ($p = 0.006$).

Interleukin-10 Expression by ELISA

The main goal of the IL-10 ELISA experiments was to analyze expression of this immunosuppressive cytokine in the spleens of naïve and MuLV-infected BALB/c and BL/6 mice. MuLV-infected mice were assessed at 24 hours, 3 days, and 7 days post-infection. A working standard curve was obtained prior to examining unknown samples; an example of this standard curve can be seen in Figure 21. Next, lysates from three animals per strain and condition were examined on an ELISA plates prepared using a BD IL-10 ELISA kit; please refer to materials and methods for further details. OD readings, in combination with the standard curve obtained on the same plate, were used to generate a value for pg/mL IL-10 expression for each individual. OD readings defined by the standard curve as representative of ‘negative’ IL-10 expression were defined as containing 0 pg IL-10/ mg protein. The pg IL-10/ mL value was multiplied by ten to account for the 1:10 dilution used on the plate. Finally, individual values for pg/mL IL-10 expression were divided by the individual lysates’ total protein concentration in mg protein/mL. This resulted in a pg IL-10/mg total protein value for each animal. Individual values may be seen in Table 4. Average expression values per group may be seen in Figure 22, while a plot showing a time course of expression (transformed by natural log) for each strain can be seen in Figure 23.

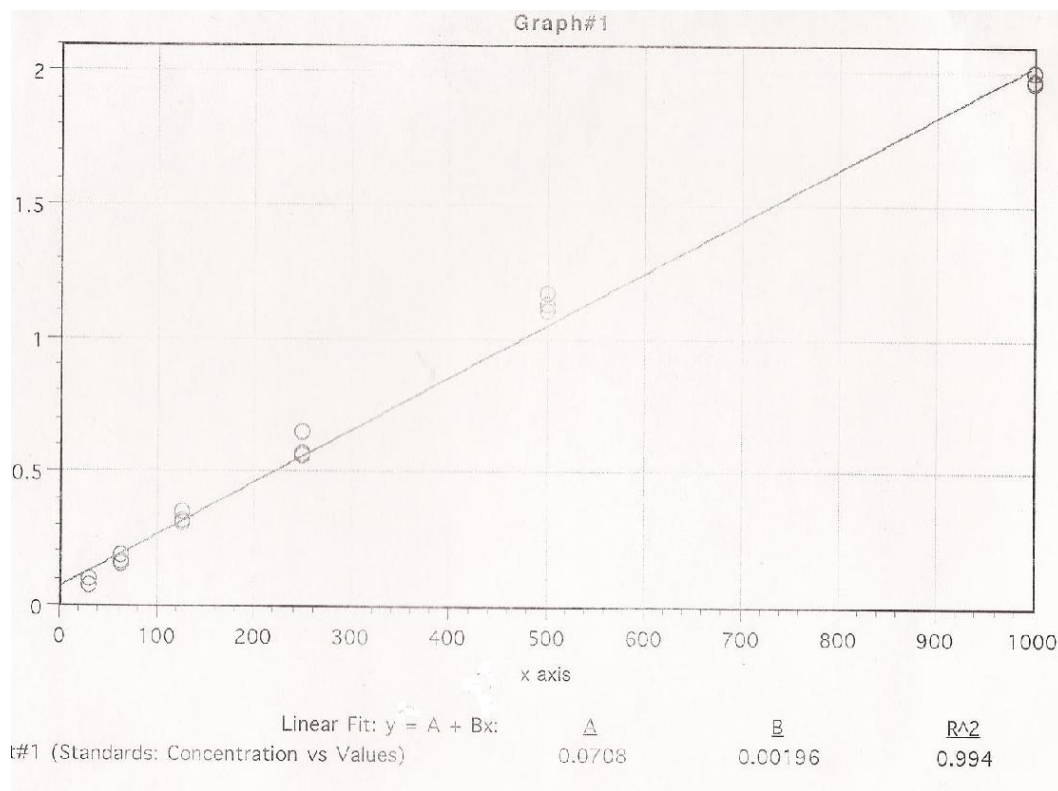


Figure 21. Example standard curve for IL-10 ELISA plate. Shown on the x-axis is concentration of IL-10 (in pg IL-10/mL); shown on the y-axis is the optical density (OD) reading. Six 2-fold serial dilutions were made from a concentrated IL-10 standard diluted in reagent diluent, beginning with a concentration of 1000 pg/mL. Each standard concentration was tested in duplicate wells. The curve generated was fitted with a linear line of best fit as suggested by the kit protocol. The standard curve equation was determined to be $y = 0.00196x + 0.0708$, with an r^2 value of 0.994.

Table 4. IL-10 Protein Expression (pg/mg of protein) in the spleens of individual naïve and MuLV-infected mice. IL-10 protein values in pg/mL found using ELISA were divided by the total protein concentration for each homogenate in mg/mL found by Bradford assay to give the value shown below in pg/mg protein. Individuals with OD readings represented by the standard curve as 'negative' IL-10 expressors were defined as having 0 pg IL-10/ mg total protein.

IL-10 pg/ mg of protein tested				
	Time Point Post-Infection			
	Naïve (uninfected)	24 hour	3 day	7 day
BALB/c (resistant)				
#1	26.4235	0	0	0
#2	33.0099	0	0	0.0892
#3	71.5540	0	0	2.2913
<i>Average ± std. dev.</i>	43.6625 ± 24.3782	0	0	0.7935 ± 2.9589
BL/6 (susceptible)				
#1	79.4367	7.1343	0	25.9490
#2	227.2829	6.0017	4.3803	170.7434
#3	137.3552	13.4780	42.6142	83.5994
<i>Average ± std. dev.</i>	148.0249 ± 74.4984	8.8713 ± 4.0295	15.6648 ± 24.2698	93.4306 ± 72.8961

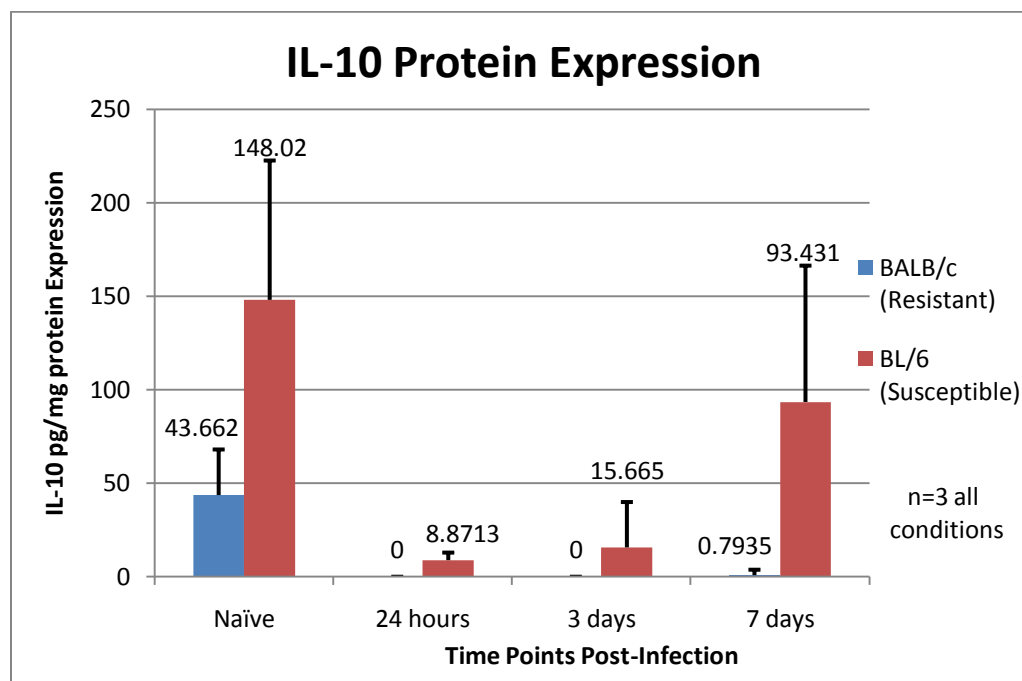


Figure 22. IL-10 protein expression differs significantly between strains in the spleens of naïve and MuLV-infected BALB/c and BL/6 mice. The x-axis shows the condition of the animals; the y-axis shows the average IL-10 expression in pg/mL normalized by total protein concentration in mg/mL. Three animals composed each averaged group (n=3). The standard deviation within each group is indicated by the error bars. Based on p-values calculated by ANOVA, there is a highly significant difference in IL-10 expression across time ($p < 0.001$) and a highly significant difference in expression between strains ($p < 0.001$).

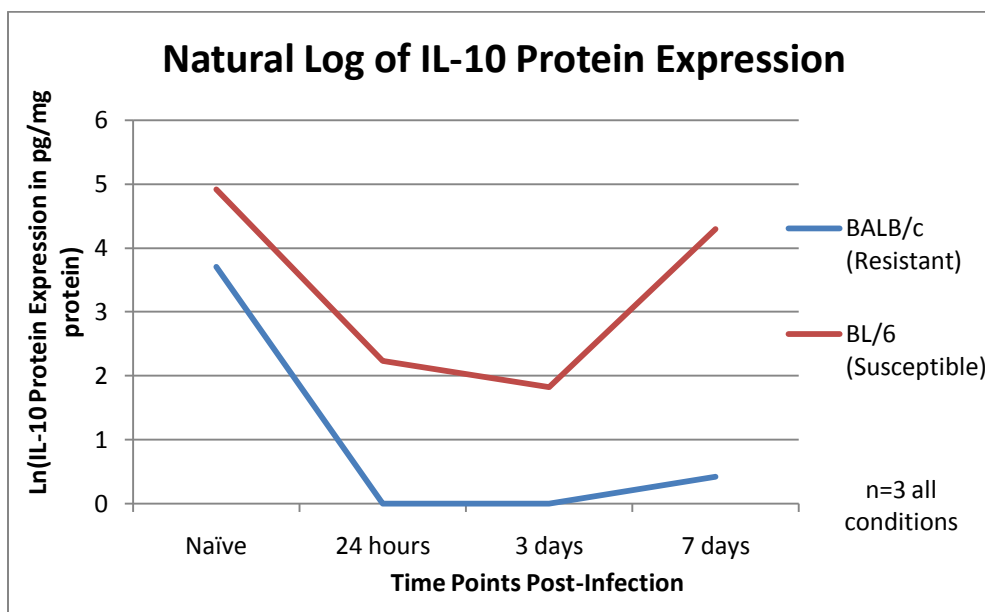


Figure 23. Natural log of IL-10 protein expression differs significantly across time in the spleens of naïve and MuLV-infected BALB/c and BL/6 mice. At every time point tested BL/6 mice express more IL-10 than their BALB/c cohorts ($p < 0.001$). In both strains, IL-10 is most highly expressed in naïve animals, a somewhat unusual finding for an anti-inflammatory cytokine. IL-10 expression declines substantially between 24 hours and 3 days post-MuLV infection, becoming undetectable in BALB/c mice. By 7 days post-infection, IL-10 expression increases in BL/6 mice and again becomes detectable in BALB/c mice. IL-10 makes a far stronger recovery in post-infection expression in BL/6 mice than in the BALB/c strain. IL-10 protein expression in both strains is highly significantly affected by time post-infection ($p < 0.001$).

When analyzed by a statistical ANOVA test, the IL-10 ELISA results (transformed to natural log scores) indicated highly significant differences in IL-10 expression across time and between strain of mouse. Much like the IDO qPCR results, BL/6 animals expressed more IL-10 at all time points ($p < 0.001$). While the expression patterns of both BALB/c and BL/6 mice look similar, expression is substantially lower in BALB/c than BL/6. BL/6 mice showed a decrease in IL-10 expression between naïve mice and 24 hours p.i., then expression began to recover by 3 days and had substantially recovered by 7 days. In contrast, BALB/c animals showed IL-10 expression in naïve animals, lost all detectable expression at 24 hours and 3 days p.i., and made only a minimal recovery to pre-infection IL-10 levels by 7 days. Difference in IL-10 expression across time points following infection was found to be highly significant ($p < 0.001$).

DISCUSSION

In immunity, balance between immune activation and regulation is key. An immune response must be strong enough to overcome the invading pathogen, but cannot be so strong that it risks injuring the host in the process of defeating the pathogen. While many decades of research have addressed the topic of how an immune response is activated and strengthened, only recently has the importance of signals opposing activation – those that turn off or damp down an immune response throughout an infection – come to the attention of the scientific community. These negative regulators are crucial for their role in returning the immune system to a basal state after an antigen has been cleared, and in maintaining unresponsiveness, or tolerance, to self-antigens. This recent research has yielded breakthrough ideas that may solve current problems in medical science, including autoimmunity, and immune system exhaustion or nonresponsiveness seen during some chronic infections. Identifying and utilizing molecules that can selectively limit an immune response may also benefit other areas of practical immunology, including transplantation, autoimmune diseases, and tumor immunology.

Many types of cells and molecules exist that can negatively regulate an immune response. One of the earliest inhibitory molecules discovered was the receptor CTLA-4 expressed on T cells. CTLA-4 was found to bind to the costimulatory molecule B7 on antigen presenting cells, thereby damping down activation and limiting T cell proliferation. This is in direct contrast to the other

B7 ligand found on T cells, known as CD28, which is constitutively expressed and is responsible for providing an activating signal to T cells. CTLA-4 is structurally similar to CD28, but is upregulated only during an immune response and functions as an antagonist (Parham, 2009). CTLA-4 also binds B7 twenty-fold more strongly than does CD28, providing an extremely sensitive form of ‘brakes’ for the immune system. Other receptor-ligand pairs, such as PD-1 and PD-L1, can also negatively inhibit immune responses in a fashion similar to CTLA-4. These surface receptors have also been linked to key control points in an immune response.

The positive identification of a suppressive T cell population known as regulatory T cells (Tregs) has hugely advanced the study of negative immune regulators. Tregs, often characterized by their expression of the transcription factor FOXP3, are notable for their ability to shut down an immune response after it has successfully tackled an invading organism, as well as their ability to limit immune responses that could attack self tissues (autoimmunity). Humans and mice expressing FOXP3 mutations do not make Tregs and suffer from widespread autoimmunity (Bacchetta *et al.*, 2006). However, the genes and proteins involved with this down regulation of immune control have only recently been discovered, and remain an active area of research. Anti-inflammatory cytokines produced by these Tregs, as well as by other cell types, provide part of the mechanism by which inflammation is controlled. IL-10, the most notable example of an anti-inflammatory cytokine, is marked for its ability to deactivate macrophages and T

cells, as well as to limit the production of cytokines like IL-2 and IFN- γ , which are pro-inflammatory and encourage T cell-biased immune responses.

Finally, molecules not previously connected to the immune response at all have also been shown to play immunomodulatory roles. One example of a physiological molecule with negative immunological effects is indoleamine 2,3-dioxygenase (IDO), an enzyme of the tryptophan degradation pathway. IDO's involvement in tolerogenic responses occurring during pregnancy has long been demonstrated (Mellor *et al.*, 2002). IDO has also been suggested to play a role in tumor immune escape and pathogen immune evasion, mainly through the generation of a tolerogenic environment that limits effective immune responses (Zamanakou *et al.*, 2007; Zelante *et al.*, 2008).

Chronic infections exemplify a situation where striking an appropriate balance between persistent immune activation (which can cause tissue pathology or damage) and immune regulation becomes especially important. The very nature of a chronic infection such as HIV, with its lengthy period of immune activation and continuous presence of pathogen, can result in high systemic levels of cytokines and a cytokine imbalance that is just as harmful as the pathogen itself. While incessant presence of pathogen constantly provokes the immune system to produce inflammatory cytokines, already high levels of inflammatory cytokines and immune cells provide contradictory negative feedback signals suggesting that it is time to begin shutting the immune system off. Chronic viral infections are often characterized by gradual functional impairment of virus-

specific T-cell responses, with this defect being a principal reason for the host's inability to eliminate the persisting pathogen (Barber *et al.*, 2006). This phenomenon of initial T cell functionality followed by gradual loss of function is referred to as 'immune exhaustion'. The mechanisms that result in immune system exhaustion are still under investigation, but the inadvertent effects of immunomodulation are considered plausible triggers for this self-defeating trend.

The pathology of a chronic infection may also be worsened when the wrong type of immune response is shut off in favor of another, less effective response. In example, chronic HIV infection is marked by a transition from cytokines that promote a T cell-mediated response (Th1 cytokines) to those more efficient at promoting a B cell-mediated response (Th2 cytokines). As infections by viruses and intracellular pathogens are typically better controlled by T cell-mediated killing of infected cells than by the neutralizing antibodies produced by B cells, it is thought that this Th1- to Th2- transition may be a fundamental failure of the immune system that prevents it from ever defeating HIV. Identifying the negative signals that turn off production of Th1 cytokines in favor of Th2 cytokines is a topic of primary importance.

The MAIDS model provides an ideal system in which to examine the role played by natural immunosuppressors during a chronic retroviral infection. The model used in the Stranford laboratory allows direct comparison between the disease-resistant strain's immune response, which is successful at subduing MuLV infection, and the disease susceptible strain's immune response that fails to

control the virus, allowing the mice to eventually develop MAIDS. This project attempted to discern if a clear difference exists in how the two strains express immunosuppressive molecules - especially early in the immune response, where the 'direction taken' matters for the future development of the more specific adaptive immune response. Immunosuppressive, anti-inflammatory molecule quantities may be compared to levels of activating inflammatory molecules to gain a general sense of the 'direction' of the immune response at a particular time point. Should significant differences in the levels of suppressive molecules exist, the levels in MAIDS-resistant BALB/c mice may be taken as the 'correct' amount and compared to the 'incorrect' levels expressed by C57BL/6 mice. Far more research would be necessary to ascertain whether differing expression levels of immunosuppressors actually resulted in a physiologically better or worse immune response. However, a consistent trend in immunosuppressor expression may hint at the balance between activation and regulation that prevents the development of MAIDS, and could therefore present potentially fruitful areas of investigation for HIV-induced AIDS.

The experiments described in this thesis continue the work of other scientists who have examined Type I interferons, IL-10, and IDO within models of murine retroviral immunity. The original intent of this thesis was to confirm the work of Heng *et al.* (Heng *et al.*, 1996) in the Stranford Laboratory's MAIDS model. Heng and colleagues showed that increased expression of Type I (α/β) interferons increased host resistance to murine AIDS. The group noted that an

IFN- α/β response was detected in the first nine hours after LP-BM5 infection in resistant mice, but not in susceptible mice. This suggested that the ability to produce IFN- α/β in response to LP-BM5 infection may contribute to host resistance to MAIDS (Heng *et al.*, 1996).

As interferon experiments to corroborate these findings were underway, a paper was published linking the absence of IDO to the upregulation of Type I interferons in a retrovirus-infected mouse (Hoshi *et al.*, 2010). The comparison between levels of inflammatory versus suppressive molecules seemed a worthwhile one, and experiments analyzing IDO mRNA expression were initiated. The suppressive anti-inflammatory cytokine IL-10 was later added to this study, after finding reports supporting IL-10's role in moderating the effects of MuLV-induced disease in MAIDS-susceptible mice (Green *et al.*, 2008).

In its totality, this thesis attempts to compare the magnitude of key early pro- and anti-inflammatory mediators in the MAIDS model while trying to identify possible relationships and trends between the two opposing responses. While exploration of IFN- α/β , IL-10, and IDO expression has taken place in other laboratories, none have studied the relative levels of these molecules in the first week after infection: most groups wait until later in the disease course, once susceptible mice have begun to exhibit symptoms of MAIDS. In contrast, we were interested in the pro- and anti-inflammatory instigators of the *early* anti-MuLV response in this model system. Other groups also fail to test responses in

disease-resistant strains, limiting their ability to compare expression differences playing a role in resistance to MAIDS.

Type I interferon expression does not differ between BALB/c and C57BL/6 mice

A variety of techniques were used to assess the presence of Type I interferons in both BALB/c and C57BL/6 mice. Both ELISA and qPCR experiments demonstrated very low expression levels of Type I interferons, making it difficult to quantify IFN- α/β much less to find expression differences between MAIDS-resistant and –susceptible strains. These results raised questions about the importance of Type I interferon expression in defining a successful versus an unsuccessful immune response against MuLV at this early stage of infection.

Expression of IFN- β at various time points and in multiple organs (lymph node, spleen, liver, and thymus) was compared qualitatively between strains using conventional PCR. Although IFN- β was reported as showing detectable expression levels at a wide variety of time points in previously published works (Heng *et al.*, 1996; Gerlach *et al.*, 2005), only two conditions exhibited detectable bands when conventional PCR products were analyzed by gel electrophoresis: 8 and 18 hour MuLV-infected BALB/c spleen. This was initially thought to be the result of faulty primer design, but newly ordered primers used in a previously published study (Linenklaus *et al.*, 2009) did not improve the faint band strength seen for these conditions. qPCR was then used to see if IFN- β was more easily

detectable by this highly sensitive technique. cDNA made from 18 hour MuLV-infected BALB/c spleens was used to test IFN- β primers for qPCR. The qPCR IFN- β trial showed high Ct values (around 34 cycles) for IFN- β reactions, as contrasted to typical Ct values seen for the TBP housekeeping gene (around 22 cycles). This indicates that very low levels of IFN- β mRNA were present in the initial template, requiring many cycles of amplification to obtain a detectable level of fluorescence. Taken together, both the conventional PCR and qPCR results suggest very limited levels of IFN- β mRNA in both BALB/c and C57BL/6 mice, making it difficult to quantify the differences between strains.

Low IFN- β expression may have been caused by several factors. Although a significant amount of time was spent testing appropriate time points and conditions in which to analyze IFN- β expression, it is possible that the peak of IFN- β expression occurs at an even earlier time point. IFN- β production is known to induce IFN- α production (Theofilopoulos *et al.*, 2005), so the greatest levels of IFN- β production might be present at the very onset of innate immunity, within hours after the initial act of infection. Heng *et al.* (1996) examined IFN- α/β expression at 3, 6, and 9 hours post-MuLV infection. While a limited number of conventional PCR experiments were pursued using mice sacrificed at 8 hours post-infection, it is possible that wider use of these very early time points may have been better for assessing IFN- β mRNA expression. IFN- β may also be under tight levels of posttranscriptional control, meaning that very small changes in the amount of IFN- β mRNA from a very low baseline level might result in larger

changes in protein expression. In hindsight, the fact that Heng *et al.* could not detect IFN by bioassay and needed dot blot hybridization to amplify the signal observed from IFN- α/β qPCR products should have indicated that IFN- β might be a difficult target gene to study. In this respect, the IFN- β results described here do support previously published literature in the low levels of expression seen. The fact that signal was only detected in MuLV-infected MAIDS-resistant BALB/c mice does seem to indicate some level of virus-induced differential expression. However, it is impossible to statistically analyze this difference with the results obtained in these studies, and suggests that these levels may not be biologically relevant.

More success was had when analyzing expression levels of IFN- α by qPCR. Low levels of IFN- α expression were again seen with detectable fluorescence in qPCR assays typically arising after 30 cycles (as compared to the average Ct value of 22 cycles for TBP). Despite this, all samples yielded detectable levels of IFN- α . Other groups have also noted that more IFN- α is expressed than IFN- β in retrovirus-infected mice (Gerlach *et al.*, 2006), so it is comprehensible that IFN- α may be detectable while IFN- β is not. IFN- α quantities were normalized by TBP housekeeping gene quantities and calibrated against the sample used to generate the standard curve, producing a fold expression value. These fold expression values were transformed by natural log and compared quantitatively using a univariate ANOVA test between BALB/c and C57BL/6 mice as well as between time points. No significant difference was seen between

strains ($p = 0.563$), but a highly significant difference was seen across time in both strains ($p = 0.002$). More IFN- α was seen at 24 hours than at 7 days – a result that is not surprising, as IFN- α is a cytokine of innate, not adaptive, immunity. Because no strain-specific difference in IFN- α mRNA expression was seen by qPCR, these results further indicate that it is unlikely IFN- α expression is a major contributor to the differing success of the BALB/c and C57BL/6 immune responses against MuLV.

The IFN- α ELISA experiments also indicated no difference in IFN- α expression between BALB/c and BL/6 mice ($p = 0.103$). However, no difference in expression across time points was found at the protein level, unlike in previous qPCR experiments ($p = 0.072$). As in the conventional PCR and qPCR experiments, very low levels of IFN- α expression were seen by ELISA, with no animal yielding more than 4.5 pg IFN- α /mg protein. Nearly all sample OD readings fell at the bottom of or below the standard curve, requiring some extrapolation. Accordingly, it is important to understand these IFN- α concentrations in this light, with some doubt placed on the verity of ‘2 pg IFN- α /mg’ as compared to ‘4 mg IFN- α /mg’ or the biological relevance of values this low.

It is more important to read these results in the context that very little IFN- α protein is detectable in the spleens of MuLV-infected mice post-infection, and all the levels detected are below that which is physiologically relevant to virus resolution. As 14 subtypes of IFN- α exist, it is possible that this ELISA assay

may be designed for a subtype less prevalent in this strain of mouse.

Alternatively, the spleen may somehow underestimate systemic presence of Type I interferons, or may not be the key site for this anti-viral activity. As the compilation of IFN- α experiments from this work are considered, it is perhaps more likely that IFN- α is expressed in highly specific, local environments of infection, making it difficult to detect expression changes in a whole-organ lysates (spleen levels partially replicate expected blood levels). The consistently low Type I interferon levels seen in these experiments and lack of differential expression do not support Heng *et al.*'s suggestion that Type I interferon expression is increased in MAIDS-resistant mice.

IDO mRNA is differentially expressed by BALB/c and C57BL/6 mice

In contrast to Type I interferons, mRNA expression of the immunosuppressive tryptophan catabolic enzyme indoleamine 2,3-dioxygenase (IDO) does appear to differ between BALB/c and C57BL/6 mice when tested by qPCR. A significant strain-specific difference in IDO mRNA fold expression exists between BALB/c and C57BL/6 mice at all time points ($p < 0.001$), with MAIDS-susceptible C57BL/6 mice expressing more mRNA for this immunosuppressive enzyme at every single time point. IDO expression also differs significantly depending on time after infection ($p = 0.006$), suggesting that this may be induced by virus exposure and that these changes in expression may be directed towards the antiviral response.

Both BALB/c and C57BL/6 mice follow similar patterns of IDO expression, with the primary dissimilarity seen at 3 days post-infection. In both strains, IDO mRNA expression decreases at 24 hours post-MuLV infection compared to levels seen in naïve (uninfected) mice. However, IDO expression in C57BL/6 mice begins to recover by 3 days, while IDO expression in BALB/c mice continues to decline. Both animals show increased levels of IDO mRNA at 7 days post-infection compared to day 3. IDO mRNA levels are higher at 7 days than in naïve mice in both strains.

This differential trend of expression at 3 days may have significant implications on the ability of the two strains to ramp up an adaptive immune response against MuLV. At three days, an adaptive immune response against the retrovirus has just begun a critical phase of expansion marked by selection and proliferation of pathogen-specific T and B cells. BALB/c mice appear to strengthen this attempt at pro-inflammatory immunity by decreasing the presence of potentially suppressive IDO mRNA transcripts. This may aid in taking the 'brake' off of the immune system to allow for increased immune cell proliferation. In contrast, C57BL/6 mice continue to increase the levels of IDO mRNA at three days post-infection. Increased presence of IDO may limit T cell proliferation in the disease-susceptible C57BL/6 mice at a time where clonal expansion should be unrestricted, possibly allowing MuLV to replicate at levels much higher than in BALB/c. Poorly controlled viral replication early on in

MuLV infection may disadvantage MAIDS-susceptible mice from the very beginning, forcing them to overreact later against much larger quantities of virus. In support of this argument are data showing relative viral loads in the two strains. A plot comparing the viral load of BM5 *Def*, the replication-defective virus component causing MAIDS, with IDO mRNA expression levels can be seen in Figure 24 (viral mRNA real time expression data by Dr. Bakkour, unpublished results). It should be noted that at 3 days post-infection, where IDO expression is the lowest in BALB/c mice, viral load in BALB/c mice also begins to decrease. In fact, the peak of viral load occurs in the disease-resistant mice at 3 days post-infection, which is also the time point at which IDO mRNA levels are their lowest. In contrast, IDO expression in C57BL/6 mice continues to increase after 24 hours, as does the viral load.

The fact that MAIDS-susceptible C57BL/6 mice always express more IDO mRNA than MAIDS-resistant BALB/c mice in the week following MuLV infection suggests a generally suppressive immune environment that favors immune system control over activation. Even before infection, C57BL/6 mice possess more IDO mRNA transcripts available for translation into protein. This suggests that susceptible mice may always be more cautious during immune activation, keeping more immunosuppressive IDO on tap in naïve mice to prevent overactivation of immunity when infection actually does occur.

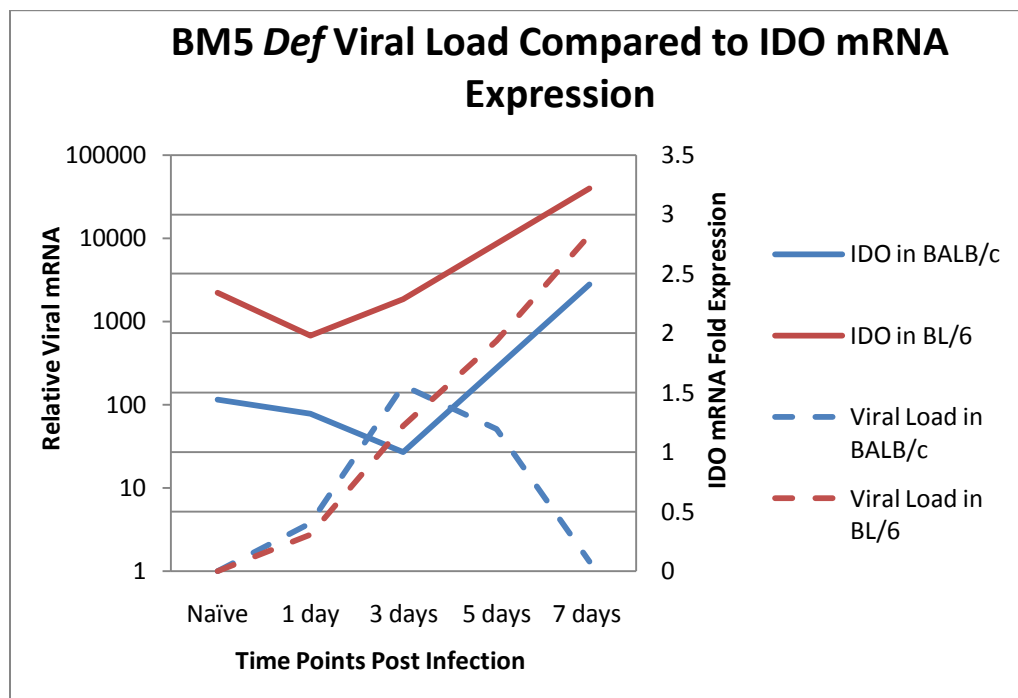


Figure 24. BM5 *Def* viral load as compared to IDO mRNA fold expression. Levels of replication-defective BM5 *Def* viral mRNA were measured by qPCR (Dr. Bakkour, unpublished data). Plotted on the opposing axis are IDO mRNA fold expression values as described previously. Naïve (uninfected) mice were defined as having a viral load of zero, while IDO mRNA expression at the 5 day time point was extrapolated by connecting the 3 day and 7 day post-infection data points. IDO expression is the lowest in BALB/c mice at 3 days, corresponding with the time point at which viral load begins to decrease in BALB/c. IDO expression and viral load in C57BL/6 mice continue to increase from 24 hours to 7 days p.i.

Suppression of an immune response to MuLV through IDO may occur via a variety of downstream effector mechanisms. IDO's primary mechanism of immune system inhibition is currently believed to be limitation of immune cell proliferation by degradation of an amino acid crucial for protein synthesis (Mellor and Munn, 1999). Although tryptophan is important for all dividing cells, T cells are especially prone to cell cycle arrest and subsequent apoptosis when deprived of tryptophan (Mellor and Munn, 2004). T cells may sense low tryptophan concentrations by either one of two amino-acid sensitive signaling pathways: the GCN2 stress-kinase pathway and the mTOR (mammalian target of rapamycin)-signaling pathway, both of which are inhibited by amino-acid withdrawal (Mellor and Munn, 2004). T cells seem particularly sensitive to inhibition of the mTOR pathway, as shown by the clinical use of rapamycin (an mTOR inhibitor) as a T-cell immunosuppressant (Mellor and Munn, 2004). By locally inhibiting the clonal expansion of T cells, IDO may prevent a strong T cell response from being initiated at draining lymph nodes.

Other effector mechanisms for IDO have also been studied. IDO may exert additional immunosuppressive effects through the downstream products of tryptophan degradation (Hoshi *et al.*, 2010). These kynurenine metabolites may bind directly to effector T lymphocytes, NK cells, and other cell types, thereby limiting their reactivity and activation. IDO expression may also preferentially encourage the expansion of inhibitory Treg cells, further encouraging an immunosuppressive environment.

The results described in these experiments do tend to support previously published work depicting IDO's potentially detrimental role in suppressing immune responses against retroviruses. Hoshi *et al.* (2010) noted that IDO *-/-* mice upregulated Type I interferon production and suppressed LP-BM5 (MuLV) better than wild type mice. In these experiments, MAIDS-susceptible mice upregulated IDO mRNA expression in comparison with MAIDS-resistant mice – also indicating that the presence of IDO is unfavorable to the ability of a mouse to suppress MuLV replication. In primate model systems, monkeys infected with simian/human immunodeficiency virus have been shown to have widely distributed IDO-expressing macrophages and other mononuclear cells in peripheral lymphoid tissues (Munn and Mellor, 2004). As in the results seen here, high IDO expression triggered by retroviral infection may suggest immunosuppression that eventually contributes to widespread immune dysregulation.

IL-10 protein is differentially expressed by BALB/c and C57BL/6 mice

Expression of the anti-inflammatory, tolerance-inducing cytokine IL-10 also differed between BALB/c and C57BL/6 mice when tested by ELISA. A significant strain-specific difference in IL-10 expression existed between BALB/c and C57BL/6 mice at all time points ($p < 0.001$), with susceptible mice expressing more IL-10 at all time points. IL-10 expression also differed across time points post-infection in both strains ($p < 0.001$), suggesting that this is a virus-induced

response and that the mice are modulating the levels of IL-10 for different stages in the antiviral immune response.

IL-10 expression is highest in both strains in naïve mice – a somewhat unusual finding for an anti-inflammatory cytokine. Typically, an infection is required to first produce inflammation, which is then eventually decreased by anti-inflammatory cytokines. It is unclear what produced this unusual pattern of expression in these experiments. While the immune system indeed seeks to maintain tolerance and homeostasis in ‘naïve’ times preceding infection, IL-10 is typically considered a mechanism of damping down an immune response post-infection, not as a way to maintain homeostasis on an everyday basis. Upon infection with MuLV, IL-10 expression decreases in both strains at 24 hours and 3 days post-infection (see Figure 22). While some IL-10 is still detectable in C57BL/6 mice, no IL-10 expression was seen in BALB/c mice (shown by negative OD readings). By 7 days, IL-10 expression has recovered substantially in MAIDS-susceptible C57BL/6 mice, but is only barely detectable in MAIDS-resistant BALB/c mice. It is hypothesized that this dip in expression at 24 hours and 3 days corresponds with the time at which the immune response is most pro-inflammatory. During times where inflammation is most necessary, anti-inflammatory cytokines are least welcome and production is accordingly low. By 7 days, a significant amount of inflammation has already been generated, and it becomes necessary to turn the immune response down to prevent harming self molecules (even though in C57BL/6 mice, the virus is not well-controlled). It is

possible that the MAIDS-susceptible C57BL/6 mice begin turning the immune response down too much and too early with tolerance-inducing IL-10, allowing the pathogen to escape immune control. A plot comparing viral load of the pathogenic BM5 *Def* virus to IL-10 expression levels can be seen in Figure 25 (viral mRNA expression data from Dr. Bakkour, unpublished results). IL-10 expression stays fairly low in BALB/c mice as the viral load first increases then decreases, but IL-10 expression in C57BL/6 mice increases correspondingly as viral load increases.

A significant amount of standard deviation exists within each group. As seen in Table 4, this is not the result of a single outlier within three animals, but is caused by a fairly wide range in IL-10 expression values across animals within single groups. Larger standard deviation values are seen for larger expression values, a trend noticed several times throughout this thesis. Despite these standard deviations seen within groups, statistical significance was still seen between strains ($p < 0.001$) and across time ($p < 0.001$). This indicates that while the exact amount of IL-10 expressed may differ considerably within animals, a significant trend is still seen where MAIDS-susceptible mice express significantly more IL-10 than MAIDS-resistant mice. Differential expression of this tolerance-inducing, immunoregulatory molecule may help to predispose C57BL/6 mice towards developing MAIDS.

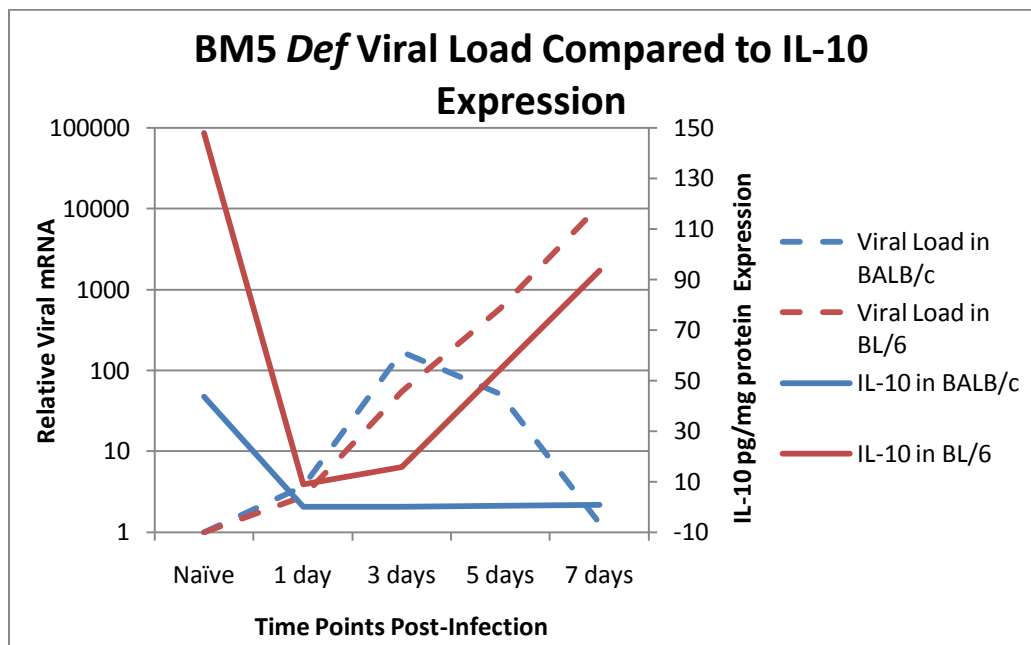


Figure 25. BM5 *Def* viral load as compared to IL-10 protein expression. Levels of replication-defective BM5 *Def* viral mRNA were measured by qPCR (Dr. Bakkour, unpublished results). Plotted on the opposing axis are IL-10 pg/mg total protein values as described previously. Naïve (uninfected) mice were defined as having a viral load of zero, while IL-10 expression at the 5 day time point was extrapolated by connecting the 3 day and 7 day post-infection data points. IL-10 expression in BALB/c mice remains low following infection as the viral load first increases, then decreases. In contrast, in BL/6 mice IL-10 expression increases steadily from 24 hours to 7 days p.i., as the viral load also increases.

These results are consistent with those from previously published experiments suggesting that Th2 cytokines, including IL-10, are upregulated throughout disease progression in MAIDS-susceptible mice (Gazzinelli *et al.*, 1992; Beilharz *et al.*, 2004). While Beilharz and colleagues showed a peak in IL-10 production between 12 to 16 days post-MuLV infection, Gazzinelli and associates saw a peak in IL-10 production much later on at 8 weeks post-MuLV infection. Neither group tested IL-10 expression within the first week post-infection. IL-10's ability to limit cytokine production by Th1 cells may contribute to the cytokine dysregulation seen in MAIDS. This cytokine imbalance has been implicated in biasing an immune response towards a B cell-mediated response less effective at combating viruses, instead of encouraging a T cell-mediated response more appropriate for viral infections.

Interestingly, these results show differential IL-10 expression at very early time points - beginning from even before the mice are infected to 7 days after infection. The majority of other studies have described IL-10 expression only in MAIDS-susceptible mice and far later in the disease course, after MAIDS pathology has already become apparent. The results described here support the idea that MAIDS-susceptible mice may be predisposed towards a more suppressive immune environment from the very onset of infection. This may give MAIDS-susceptible C57BL/6 mice an early disadvantage in their struggle to overpower MuLV before it causes widespread immune deficiency.

Sources of Error

The qPCR and ELISA techniques utilized in these experiments involved a variety of steps where error may have occurred, including tissue isolation, RNA and supernatant preparation, completion of the actual assays, and data analysis.

During tissue isolation, pairs of axillary, brachial, and inguinal lymph nodes were collected, as well as spleens. However, at times it was impossible to collect all six lymph nodes, potentially varying the concentrations and exact elements present in lymph node samples. Spleens collected were cut in half *longitudinally* prior to homogenization to attempt to collect even amounts of red and white pulp. Despite this, different amounts of red and white pulp – and therefore fluctuating quantities of immune cells – may have been placed in the spleen supernatants.

Measuring the concentration of supernatant samples for ELISA by Bradford assay may also have induced some error in the ELISA data collected. It was determined that the temperature of the Bradford reagent used as a blank greatly influenced the reading seen on the spectrophotometer (L. Lentz Marino, personal communication), which accordingly affected the subsequent samples calibrated. The Bradford blank may have been at a lower temperature for samples read early on, while later samples may have been calibrated against a Bradford blank closer to room temperature. As such, great effort was made to use the Bradford reagent at a consistent temperature instead of allowing temperature change to occur on the benchtop between readings. Spectrophotometer readings for the Bradford blank were kept as consistent as possible between samples.

However, some variation caused by temperature changes may have affected calculated sample concentrations depending on when in a sequence a sample was read on the spectrophotometer. For future experiments, blanks should be aliquoted prior to beginning the Bradford assay experiment and kept at 4 °C until it is absolutely necessary to bring them to the benchtop.

For the IL-10 ELISA assays, high OD readings were seen in control wells containing diluted (1:10) lysis buffer only. Further experiments determined that this signal was caused by the Triton-X contained in the lysis buffer reacting inappropriately with some reagent in the IL-10 kit. These extremely high readings disappeared when actual samples were included with the lysis buffer (OD readings close to zero were obtained for diluted sample wells). This indicated that any protein content prevented the reaction between the IL-10 kit reagents and the Triton-X, implying that this interaction did not significantly skew results in tissue homogenate samples. However, it is still a cause for concern to see such high signal in control wells, even if this signal disappears in low sample dilutions or wherever tissue homogenate is added. For future ELISA experiments, different samples should be prepared with a variety of lysis buffer detergents or with varying concentrations of Triton-X and tested prior to completing experiments to minimize any sort of false OD readings caused by lysis buffer reagents.

Calculation of RNA concentrations may have provided a source of error within the qPCR assays. Initial concentrations were obtained on the Nanodrop 3.1 spectrophotometer machine by a previous thesis student in the laboratory

(Gopinath, 2006). From these concentrations, sample RNAs were diluted to 125 ng/ μ L for storage at -80 °C, then made into cDNA at a final concentration of 50 ng/ μ L. Errors in any of these steps would have skewed the amount of cDNA added to a qPCR reaction. Housekeeping gene expression values from animal replicates should be very consistent between animals if the RNA samples are at the same concentration. However, several samples showed increased expression of both the housekeeping gene and the gene of interest, most likely indicating that these cDNAs were added at a higher concentration than the others; despite this error, normalizing the gene of interest (GOI) to TBP should have controlled for this. For future experiments, samples showing these dually high TBP and GOI expression values should have their RNA concentrations remeasured and qPCR experiments repeated.

A possible source of error in the qPCR data analysis involved calculation of standard deviations. Expression values for a gene of interest were divided by housekeeping gene expression values as a form of normalization, meaning that standard deviations should truly be calculated as the standard deviations of quotients (Applied Biosystems, 2008). To do this, one must first calculate the coefficient of variance ($cv = \text{standard deviation}/\text{mean value}$) for both the gene of interest and housekeeping gene. One must then find the coefficient of variance for the quotient ($cv_q = cv_1^2 + cv_2^2$), then find the standard deviation of the quotient ($cv_q = \text{standard deviation}_q/\text{mean value}_q$). However, this formula assumes that the housekeeping gene expression values are very consistent between samples, and

only the gene of interest varies. In my qPCR assays, some samples were seen expressing both high levels of the gene of interest and high levels of the housekeeping gene (most likely indicating that the initial sample RNA was added at a higher concentration than intended, or that this animal's sample was expressing high levels of mRNA in general). It is this sort of background variance and 'concentration check' that normalization attempts to address. However, calculating standard deviations as quotients seemed to 'double count' the deviation seen in these higher values, instead of accounting for the fact that high values were linked together and addressed by normalization. Standard deviations calculated as quotients were often two to three times higher than standard deviations calculated using the traditional formula ($\sqrt{\frac{\sum[(x-\bar{x})^2]}{(n-1)}}$). After much discussion, it was decided that calculating standard deviations as quotients was inappropriate because high housekeeping gene values were linked with high gene of interest values, and standard deviations were calculated using the traditional formula.

Future Studies

The results of these studies pose important questions regarding the balance of expression of immune activators and immunosuppressors following MuLV infection in MAIDS-resistant and -susceptible mice. Failure to regulate the immune response may be self-injurious, yet excessive immunosuppression may prevent mice from mounting an effective immune response, resulting in persistent

infection which directly or indirectly contributes to the development of MAIDS. Discerning the balance between immune activators and suppressors displayed by MAIDS-resistant mice may help to identify an immune balance most successful at preventing retrovirus-induced immunodeficiency– a finding that may have important applications to humans infected with HIV.

Prior to pursuing related experiments, the results of these studies should be confirmed by increasing the number of biological replicates at the hands of another scientist. While five mice per condition were used for the IDO qPCR experiments, all other experiments utilized only three mice per condition due to time constraints and reagent limitations. Increasing the number of animals to five per condition could decrease the impact of variability between mice and increase the confidence in the observed patterns of expression. A greater number of samples will also confirm the statistical significance of the findings. Completing these experiments at the hands of another scientist will also confirm that no experimenter-induced bias has been created throughout these experiments.

Future experiments should begin by examining IDO protein expression in the lymph nodes at a variety of time points. The levels of IDO mRNA expression seen here may not translate directly into the levels of IDO protein expression. Assays directly measuring IDO protein levels would confirm the hypothesis that actual IDO protein expression is upregulated in MAIDS-susceptible mice, not just IDO mRNA. Assembly of an IDO protein ELISA kit is a current project underway in the Stranford laboratory. Previously published work has studied IDO

protein expression by western blot; this assay provides an excellent alternative should the efforts to produce an IDO ELISA kit prove unsuccessful. As a secondary alternative, the concentration of IDO's kynurenine metabolites could be measured as a way to measure enzyme activity levels. Measuring IDO metabolite levels has successfully been used to show changes in IDO activity following MuLV infection, and would lend insight into the effects of viral activity on the enzyme's function instead of merely its concentration (Hoshi *et al.*, 2010).

Because of these promising results showing the increased expression of selected immunosuppressors by MAIDS- susceptible mice, future studies should involve treatments that mimic the effects of these immunosuppressors. Useful studies might involve supplying IL-10 to MAIDS-resistant mice and assessing its effects on disease resistance. BL/6 mice could also be infected concurrently with other pathogenic organisms inducing increased levels of immunosuppressors, and the effects on disease progression could be measured. Further work should also be devoted to identifying and testing other immunosuppressors in the MAIDS model. Viable candidates might include a variety of molecules and enzymes involved with maintaining immune homeostasis, inducing tolerance, and shutting off an immune response. It is worth investigating the expression of molecules such as CTLA-4 (the inhibitory receptor on T cells), the central tolerance-inducing transcription factor AIRE, suppressive Treg cells, and the immunosuppressive cytokine TGF- β , along with many others. If upregulation of these molecules is again seen in the early immune responses of MAIDS-susceptible mice, this may

provide more concrete evidence that susceptible mice are inadvertently suppressing an immune response against MuLV, predisposing them towards developing MAIDS.

If other immunosuppressors are also overexpressed in MAIDS-susceptible mice, future studies might also address the downstream effects of these immunosuppressors. Such questions might address the type of activating response turned down/off, whether the immunosuppressor target primarily B cell- or T cell-mediated responses, and potential pathways through which the immunosuppressors exert their functions. For example, IDO is known to decrease T cell proliferation by way of a tryptophan-sensitive checkpoint in the cell cycle of T cells. However, accumulation of the tryptophan derivatives kynurenines has also been implicated in providing an inhibitory signal for immune activation. Discerning the route through which kynurenines exert these negative effects on immune cells may indicate potential places for disease regulation when developing drugs for fighting HIV.

The ultimate goal of studies within the MAIDS model system is to provide new ideas and angles from which to address the immense area of HIV/AIDS research. Relatively little work has been completed studying the effects of natural immune regulation within the human immune response to HIV; immunosuppressors whose differential expression seems crucial to MAIDS resistance may provide new targets for research in HIV drug and vaccine development.

Conclusion

The field of immunology has long focused on the study of how immune responses are activated, while mostly ignoring the opposing suppressive factors that turn off or slow down an immune response at the conclusion of an infection. Only recently have these negative molecules controlling immune responses come under equal scrutiny as immune activators. Balance between immune activation and control is critical during an infection, as the immune system must be active enough to restrain the invading pathogen but controlled enough to prevent harming self molecules while clearing the infection. This balance becomes especially important in systemic infections such as those caused by retroviruses, where long-lasting immune responses can become dysregulated and cause as much harm as the pathogens themselves. Recent research has implicated overactive or upregulated expression of natural immunosuppressors such as IDO as preventing effective immune responses against the murine leukemia virus, thereby contributing to the development of MAIDS (Hoshi *et al.*, 2010).

The findings of increased immunosuppressor (IL-10 and IDO) expression in MAIDS-susceptible C57BL/6 mice in the first week post-MuLV infection may contribute to a dampened immune response that does not adequately control MuLV replication. Failure to control the virus early on in the infection may predispose disease-susceptible mice to irrecoverable immune dysregulation later in the infection's time course. This pattern of natural immunosuppressor expression may help to explain the more efficient eradication of pathogen by

BALB/c mice, whose immune responses are less hindered by presence of immunosuppressors. In contrast, the finding that Type I (α/β) interferons are not differentially expressed between strains may indicate that Type I interferons do not play a critical role in determining the success of an immune response against MuLV.

The differences in natural immunosuppressor expression seen here in the MAIDS model and their correlation with the efficiency of pathogen eradication may have similar relevance in HIV/AIDS. Overzealous immune system control mechanisms may handicap the human immune system in its effort to mount a rapid and effective adaptive response against HIV. Elevated IL-10 levels have been found consistently in the serum of late-stage AIDS patients (Clerici *et al.*, 1994); for obvious reasons little is known about IL-10 expression levels immediately following HIV infection. It is possible that some effects of immunosuppression in both the early and advanced stages of AIDS could come from increased production of IL-10. Others have found an accumulation of Tregs and their functional markers (indoleamine 2,3-dioxygenase, TGF- β , and CD80) in the lymphoid organs of patients with chronic HIV infection, whose immunosuppressive effects may influence the outcome of HIV infection (Andersson *et al.*, 2005). Long-term nonprogressors - those who are infected with HIV but who never progress to AIDS - may show lower expression of natural immunosuppressors as compared to other HIV-infected individuals. This is an area worth investigation in humans.

Further study of natural immunosuppressors may provide new targets for drug and vaccine development. Knowledge of immunosuppressor expression patterns and downstream effector mechanisms may be used to channel their function into useful therapeutics. By designing drugs or vaccine adjuvants that limit immunosuppressor function as induced by viral infection (possibly in the form of a 'day after' pill following potential exposure to HIV), it is possible that one may increase the immune system's natural efficacy at fighting HIV. Care must be taken when designing such a therapeutic that the immune system's ability to control itself is not wholly turned off, as such an action may result in devastating autoimmunity.

The role of natural immunosuppression in MAIDS and the factors that influence it commands further investigation, as it may offer important insights into the balance between immune system activation and control in human HIV/AIDS. The findings presented in this research paper characterizing increased expression of immunosuppressors in MAIDS-susceptible mice advocate the importance of natural immune modulation to an effective immune response, and may be relevant to human vulnerability to AIDS following infection with HIV.

APPENDIX

Bradford Assay Results

A Bradford assay was used to determine the protein concentrations of the lymph node and spleen supernatants used to test IL-10 and IFN- α protein expression by ELISA. Two Bradford assays were completed to test the entirety of the samples – 24 hour and 3 days post-infection samples were tested in the first Bradford assay, while naïve and 7 day post-infection samples were tested in the second Bradford. Please refer to Figure 26 for the respective standard curves from these assays. Please refer to Table 5 for the complete list of supernatant concentrations.

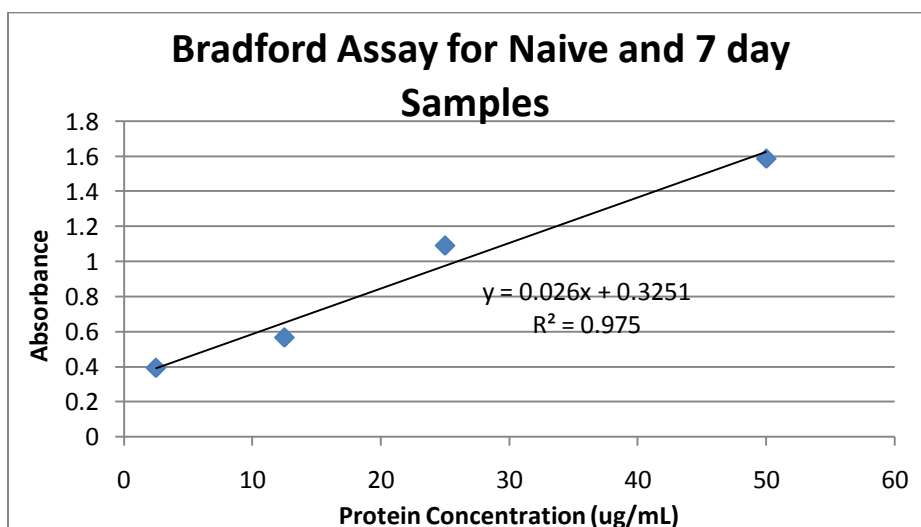
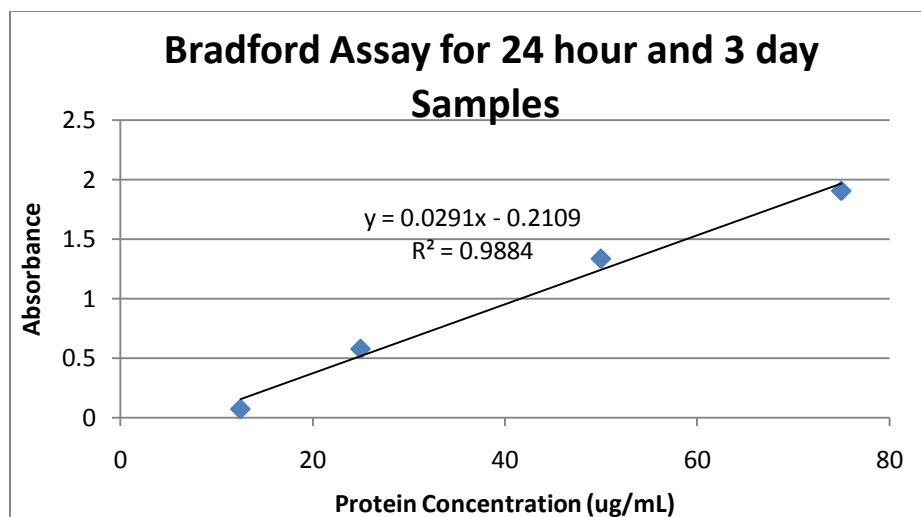


Figure 26. Standard curves for Bradford assays used to calculate total protein concentration ($\mu\text{g}/\text{mL}$) in spleen supernatants used for ELISA. Measured absorbance values are represented on the y-axis, while supernatant concentrations are shown on the x-axis ($\mu\text{g}/\text{mL}$). The standard curve obtained in the first Bradford assay was $y = 0.0291x - 0.2109$, with an r^2 value of 0.9884. The standard curve obtained in the second Bradford assay was $y = 0.026x + 0.3251$, with an r^2 value of 0.975.

Table 5. Spleen supernatant protein concentrations ($\mu\text{g/mL}$) obtained via Bradford Assay.

Condition	Individual	Total Protein Concentration ($\mu\text{g/mL}$)
Naïve BALB/c	#1	11.62385
	#2	9.15
	#3	10.63846
Naïve BL/6	#1	11.50962
	#2	6.671538
	#3	6.879231
24 hour BALB/c	#1	12.68247
	#2	10.3701
	#3	12.4433
24 hour BL/6	#1	8.724742
	#2	10.37113
	#3	9.160825
3 day BALB/c	#1	12.18454
	#2	9.18866
	#3	13.05155
3 day BL/6	#1	8.076289
	#2	13.04536
	#3	11.39794
7 day BALB/c	#1	9.726923
	#2	11.43577
	#3	13.80577
7 day BL/6	#1	10.26346
	#2	8.193462
	#3	13.37769

Statistical Analysis

Data was analyzed by univariate analysis of variance (ANOVA) tests using the SPSS statistical analysis software. Data was transformed using the natural log prior to conducting univariate ANOVA analysis, in order to meet the assumption of equal variances (standard deviations that are no different than approximately 3x within a species group). Residuals were assessed to ensure that they followed an acceptably random pattern. Significance values (p-values) less than 0.05 were considered to be statistically significant.

Table 6. Means, Standard Deviations, and Univariate ANOVA Tables from SPSS.

IFN-α qPCR: Means and Standard Deviations from SPSS				
<i>Species</i>	<i>Time</i>	<i>Natural Log (Mean Fold Expression)</i>	<i>N</i>	<i>Std. dev.</i>
BALB/c	24 hours	0.406	3	0.569
	7 days	-0.840	3	0.151
BL/6	24 hours	0.537	3	0.573
	7 days	-0.649	3	0.432

IFN-α qPCR: Univariate ANOVA Results from SPSS					
<i>Source</i>	<i>Type III Sum of Squares</i>	<i>df</i>	<i>Mean Square</i>	<i>F</i>	<i>Sig.</i>
Species	0.078	1	0.078	0.363	0.563
Time	4.43	1	4.43	20.6	0.002
Species*Time	0.003	1	0.003	0.013	0.913
Error	1.72	8	0.215	---	---
Total	6.24	11	---	---	---

IFN-α ELISA: Means and Standard Deviations from SPSS				
<i>Species</i>	<i>Times</i>	<i>Natural Log (Mean IFN-α pg/mg total protein)</i>	<i>N</i>	<i>Std. dev.</i>
BALB/c	Naïve	0.704	3	0.469

	24 hours	1.01	3	0.438
	3 days	0.019	2	0.657
	7 days	0.104	3	0.568
BL/6				
	Naïve	0.959	3	0.133
	24 hours	0.607	3	0.139
	3 days	0.758	3	0.145
	7 days	0.599	3	0.133

IFN-α ELISA: Univariate ANOVA Results from SPSS					
<i>Source</i>	<i>Type III Sum of Squares</i>	<i>df</i>	<i>Mean Square</i>	<i>F</i>	<i>Sig.</i>
Species	0.413	1	0.413	3.017	0.103
Time	1.171	3	0.390	2.853	0.072
Species*Time	1.026	3	0.342	2.500	0.099
Error	2.051	15	0.137	---	---
Total	4.463	22	---	---	---

IDO qPCR: Means and Standard Deviations from SPSS				
<i>Species</i>	<i>Time</i>	<i>Natural Log (Mean IDO Fold Expression)</i>	<i>N</i>	<i>Std. dev.</i>
BALB/c	Naïve	0.316	5	0.351
	24 hours	0.265	5	0.205
	3 days	-0.012	5	0.163
	7 days	0.782	5	0.487

BL/6	Naive	0.822	5	0.261
	24 hours	0.660	5	0.239
	3 days	0.749	5	0.433
	7 days	1.07	5	0.470

IDO qPCR: Univariate ANOVA Results from SPSS					
<i>Source</i>	<i>Type III Sum of Squares</i>	<i>df</i>	<i>Mean Square</i>	<i>F</i>	<i>Sig.</i>
Species	2.39	1	2.39	19.9	0.000
Time	1.80	3	0.599	4.98	0.006
Species*Time	0.305	3	0.102	0.845	0.480
Error	3.85	32	0.120	---	---
Total	8.34	39	---	---	---

IL-10 ELISA Results: Means and Standard Deviations from SPSS				
<i>Species</i>	<i>Times</i>	<i>Natural Log (Mean IL-10 pg/mg total protein) + 1</i>	<i>N</i>	<i>Std. dev.</i>
BALB/c	Naive	3.73	3	0.500
	24 hours	0.693	3	0.000
	3 days	0.693	3	0.000
	7 days	0.962	3	0.429
BL/6	Naive	4.92	3	0.518
	24	2.34	3	0.349

	hours			
	3 days	2.11	3	1.57
	7 days	4.31	3	0.919

IL-10 ELISA: Univariate ANOVA Results from SPSS					
<i>Source</i>	<i>Type III Sum of Squares</i>	<i>df</i>	<i>Mean Square</i>	<i>F</i>	<i>Sig.</i>
Species	21.7	1	21.7	42.1	0.000
Time	33.1	3	11.0	21.4	0.000
Species*Time	4.34	3	1.45	2.80	0.073
Error	8.26	16	0.516	---	---
Total	67.5	23	---	---	---

REFERENCES

- Akira, S., S. Uematsu, O. Takeuchi. 2006. Pathogen Recognition and Innate Immunity. *Cell*. 124: 783–801.
- Andersson, J., A. Boasso, J. Nilsson, R. Zhang, N.J. Shire, S. Lindback, G.M. Shearer, C.A. Chougnat. 2005. Cutting Edge: The Prevalence of Regulatory T Cells in Lymphoid Tissue Is Correlated with Viral Load in HIV-Infected Patients. *J. Immunol.* 174(6):3143-3147.
- Applied Biosystems. 2008. Guide to Performing Relative Quantification of Gene Expression Using Real-Time Quantitative PCR. < http://www3.appliedbiosystems.com/cms/groups/mcb_support/documents/generaldocuments/cms_042380.pdf >. Accessed 28 April 2011.
- Baccheta, R., L. Passerini, E. Gambineri, M. Dai, S.E. Allan, L. Perroni, F. Dagna-Bricarelli, C. Sartirana, S. Matthes-Martin, A. Lawitschka, C. Azzari, S.F. Ziegler, M.K. Levings, M.G. Roncarolo. 2006. Defective regulatory and effector T cell functions in patients with FOXP3 mutations. *J Clin Invest.* 116(6): 1713–1722.
- Barber, D.L., E.J. Wherry, D. Masopust, B. Zhu, J.P. Allison, A.H. Sharpe, G.J. Freeman, and R. Ahmed. 2006. Restoring function in exhausted CD8 T cells during chronic viral infection. *Nature.* 439: 682-687.
- Beilharz, M.W., L.M. Sammels, A. Paun, K. Shaw, P. van Eeden, M.W. Watson, M.L. Ashdown. 2004. Timed Ablation of Regulatory CD4+ T Cells Can Prevent Murine AIDS Progression. *J. Immunol.* 172: 4917–4925.
- Boehm, U., T. Klamp, M. Groot, J. C. Howard. 1997. Cellular Responses to Interferon-Gamma. *Annu. Rev. Immunol.* 15:749–95.
- Borovikova, L.S., S. Ivanova, M. Zhang, H. Yang, G.I. Botchkina, L.R. Watkins, H. Wang, N. Abumrad, J.W. Eaton, and K.J. Tracey. 2000. Vagus nerve stimulation attenuates the systemic inflammatory response to endotoxin. *Nature* 405:458-462.

Chattopadhyay, S.K., H.C. Morse, M. Makino, S.K. Ruscetti, J.W. Hartley. 1989. Defective virus is associated with induction of murine retrovirus-induced immunodeficiency syndrome. *Proc. Natl. Acad. Sci.* 86: 3862-3866.

Clerici, M., T.A. Wynn, J.A. Berzofsky, S.P. Blatt, C.W. Hendrix, A. Sher, R.L. Coffman, G.M. Shearer. 1994. Role of interleukin-10 in T helper cell dysfunction in asymptomatic individuals infected with the human immunodeficiency virus. *J. Clin. Invest.* 93: 768-775.

Coffin, J.M., S.H. Hughes, and H.E. Varmus (Eds.). 1997. Retrovirus-Induced Immunodeficiencies. *Retroviruses*. New York: Cold Spring Harbor Laboratory Press.

Constant, S.L., K. Bottomly. 1997. Induction of Th1 and Th2 CD4+ T Cell Responses: The Alternate Approaches. *Annu. Rev. Immunol.* 15:297-322

Couper, K.N, D.G. Blount, E.M. Riley. 2008. IL-10: The Master Regulator of Immunity to Infection. *J. Immunol.* 180: 5771-5777.

Espey, M.G., M.A. Namboodiri. 2000. Selective metabolism of kynurenine in the spleen in the absence of indoleamine 2,3-dioxygenase induction. *Immunology Letters.* 71: 67-72.

Fauci, A.S., G. Pantaleo, S. Stanley, D. Weissman. 1996. Immunopathogenic Mechanisms of HIV Infection. *Annals of Internal Medicine.* 124(7): 654-663.

Fehérvári, Z., S. Sakaguchi. 2004. CD4+ Tregs and immune control. *J. Clin. Invest.* 114(9): 1209-1217.

Gallo, R.C., P.S. Sarin, E.P. Gelmann, M. Robert-Guroff, E. Richardson, V.S. Kalyanaraman, D. Mann, G.D. Sidhu, R.E. Stahl, S. Zolla-Pazner, J. Leibowitch, M Popovic. 1983. Isolation of human T-cell leukemia virus in acquired immune deficiency syndrome (AIDS). *Science.* 220 (4599): 865-867.

Gazzinelli, R.T., M. Makino, S.K. Chattopadhyay, C.M. Snapper, A. Sher, A.W. Hugin, H.C. Morse III. 1992. CD4+ Subset Regulation in Viral Infection: Preferential Activation of Th2 Cells during Progression of Retrovirus-Induced Immunodeficiency in Mice. *J. Immunol.* 148(1): 182-188.

- Gerlach, N., S. Schimmer, S. Weiss, U. Kalinke, U. Dittmer. (2006). Effects of Type I Interferons on Friend Retrovirus Infection. *J. Virol.*, 80(7), 3438-44.
- Gopinath, S. 2006. Real Time PCR Analysis of Select Immune Response Genes in Murine Leukemia Infected BALB/c and BL/6 Mice. Honors Thesis, Mount Holyoke College.
- Green, K.A., T. Okazaki, T. Honjo, W.J. Cook, W.R. Green. 2008. The Programmed Death-1 and Interleukin-10 Pathways Play a Down-Modulatory Role in LP-BM5 Retrovirus-Induced Murine Immunodeficiency Syndrome. *J. Virol.* 82(5): 2456–2469.
- Heng, J.K., P. Price, C.M. Lai, M.W. Beilharz. 1996. Alpha/Beta Interferons Increase Host Resistance to Murine AIDS. *J. Virol.*, 70(7), 4517-22.
- Hoshi, M., K. Saito, A. Hara, A. Taguchi, H. Ohtaki, R. Tanaka, H. Fujigaki, Y. Osawa, M. Takemura, H. Matsunami, H. Ito, M. Seishima. 2010. The Absence of IDO Upregulates Type I IFN Production, Resulting in Suppression of Viral Replication in the Retrovirus-Infected Mouse. *J. Immunol.* 185: 3305-3312.
- Hutchison, J.F. 2001. The Biology and Evolution of HIV. *Annu. Rev. Anthropol.* 30:85–108.
- Jolicoeur, P. 1991. Murine acquired immunodeficiency syndrome (MAIDS): an animal model to study the AIDS pathogenesis. *FASEB Journal.* 5: 2398-2405.
- Krummel, M. F., J.P. Allison. 1995. CD28 and CTLA-4 Have Opposing Effects on the Response of T cells to Stimulation. *J. Exp. Med.* 182: 459-465.
- Li, W., W.R. Green. 2006. The Role of CD4 T Cells in the Pathogenesis of Murine AIDS. *J. Virol.* 80(12): 5777–5789.
- Liang, B., J.Y. Wang, R.R. Watson. 1996. Murine AIDS, a Key to Understanding Retrovirus-Induced Immunodeficiency. *Viral Immunology.* 9(4): 225-239.
- Linenklaus, S. M. Cornitescu, N. Ziętara, M. Lyszkiewicz, N. Gekara, J. Jabłońska, F. Edenhofer, K. Rajewsky, D. Bruder, M. Hafner, P. Staeheli, S.

Weiss 2009. Novel Reporter Mouse Reveals Constitutive and Inflammatory Expression of IFN- β In Vivo. *J. Immunol.* 183: 3229-36.

Mellor, A.L., D.H. Munn. 1999. Tryptophan catabolism and T-cell tolerance: immunosuppression by starvation?. *Immunology Today.* 20(10): 469-473.

Mellor, A.L., D.H. Munn. 2004. IDO Expression by Dendritic Cells: Tolerance and Tryptophan Catabolism. *Nature Rev. Immunol.* 4:762-774.

Mellor, A.L., P. Chandler, G.K. Lee, T. Johnson, D.B. Keskin, J. Lee, D.H. Munn. 2002. Indoleamine 2,3-dioxygenase, immunosuppression and pregnancy. *Journal of Reproductive Immunology.* 57:143–150.

Morse, H.C., N. Giese, R. Morawetz, Y. Tang, R. Gazzinelli, W.K. Kim, S. Chattopadhyay, J.W. Hartley. 1995. Cells and cytokines in the pathogenesis of MAIDS, a retrovirus-induced immunodeficiency syndrome of mice. *Springer Semin Immunopathol.* 17:231-245.

Mosier, D.E. 1996. Small Animal Models for Acquired Immune Deficiency Syndrome (AIDS) Research. *Laboratory Animal Science.* 46(3):257-264.

Mosmann, T.R., S. Sad. 1996. The expanding universe of T-cell subsets: Th1, Th2 and more. *Immunology Today.* 17(3): 138-146.

Munn, D.H., A.L. Mellor. 2004. IDO and tolerance to tumors. *Trends in Molecular Medicine.* 10(1): 15-18.

National Institute for Allergy and Infectious Diseases (NIAID). 2010. HIV Replication Cycle. < <http://www.niaid.nih.gov/topics/HIVAIDS/Understanding/Biology/Pages/hivReplicationCycle.aspx>>. Accessed 13 January 2011.

Norkin, L.C. 2010. *Virology: Molecular Biology and Pathogenesis*. Washington (DC): ASM Press.

O'Garra, A., P.L. Vieira, P. Vieira, A.E. Goldfeld. 2004. IL-10-producing and naturally occurring CD4⁺ Tregs: limiting collateral damage. *J. Clin. Invest.* 114(10):1372–1378.

Parham, P. 2009. *The Immune System*. 5th ed. New York: Garland Science, Taylor & Francis Group.

Paul, W. 2003. *Fundamental Immunology*. 5th ed. Philadelphia: Lippincott Williams & Wilkins.

Pestka, S., J.A. Langer. 1987. Interferons and Their Actions. *Ann. Rev. Biochem.* 56:727-77

Pitha, P.M., D. Biegel, R.A. Yetter, H.C. Morse. 1988. Abnormal Regulation of IFN- α , - β , and - γ Expression in MAIDS, a Murine Retrovirus-Induced Immunodeficiency Syndrome. *J. Immunol.* 141(10): 3611-3616.

Potula, R., L. Poluektova, B. Knipe, J. Chrastil, D. Heilman, H.D. Osamu Takikawa, D.H. Munn, H.E. Gendelman, Y. Persidsky. 2005. Inhibition of indoleamine 2,3-dioxygenase (IDO) enhances elimination of virus-infected macrophages in an animal model of HIV-1 encephalitis. *Blood.* 106: 2382-2390.

Sharon, J. 1998. *Basic Immunology*. Baltimore: William & Wilkins.

Schröcksnadel, K., B. Wirleitner, C. Winkler, D. Fuchs. 2005. Monitoring tryptophan metabolism in chronic immune activation. *Clinica Chimica Acta.* 364:82-90.

Tepsuporn, S. 2005. Differential Immune Response Gene Expression in a Mouse Model of AIDS. Honors Thesis, Mount Holyoke College.

Theofilopoulos, A.N., R. Baccala, B. Beutler, D.H. Kono. 2005. Type I Interferons (α/β) in Immunity and Autoimmunity. *Annu. Rev. Immunol.* 23:307-36

UNAIDS. 2010. UNAIDS Report on the Global AIDS Epidemic. <<http://www.unaids.org/globalreport/default.htm>>. Accessed 1 January 2011.

USAID. 2010. Botswana: HIV/AIDS Health Profile. United States Agency for International Development. <http://www.usaid.gov/our_work/global_health/aids/Countries/africa/botswana_profile.pdf>. Accessed 1 January 2011.

Vandesompele, J., K. De Preter, F. Pattyn, B. Poppe, N. Van Roy, A. De Paepe, F. Speleman. 2002. Accurate normalization of real-time quantitative RT-PCR data by geometric averaging of multiple internal control genes. *Genome Biology*. 3(7):1-12.

WHO/UNAIDS. 2010. Fast Facts on HIV/AIDS. World Health Organization. <http://www.who.int/hiv/data/fast_facts/en/index.html>. Accessed 1 January 2011.

Zamanakou, M., A.E. Germanis, V. Karanikas. 2007. Tumor immune escape mediated by indoleamine 2,3-dioxygenase. *Immunology Letters*. 111: 69–75.

Zelante, T., F. Fallarino, F. Bistoni, P. Puccetti, L. Romani. 2008. Indoleamine 2,3-dioxygenase in infection: the paradox of an evasive strategy that benefits the host. *Microbes and Infection* 11: 133-141.